Addis Ababa University

Addis Ababa Institute of Technology

School of Electrical and Computer Engineering

Doubly Fed Induction Generator (DFIG) Modeling and Control of Active and Reactive Power flow

By:

Estibel Abeje Alemayehu

A thesis submitted to Addis Ababa Institute of Technology in partial fulfillment of the requirement for the Degree of Master of Science in Electrical and Computer Engineering (**Control Engineering)**

Advisor:

Dr. Mengesha. Mamo

ADDIS ABABA ETHIOPIA 2021

Addis Ababa University

Addis Ababa Institute of Technology

Department of Electrical and Computer Engineering

Doubly Fed Induction Generator (DFIG) Modeling and Control of Active and Reactive Power flow

By

Estibel Abeje Alemayehu

A thesis submitted to Addis Ababa Institute of Technology in partial fulfillment of the requirement for the Degree of Master of Science in Electrical and Computer Engineering (**Control Engineering)**

APPROVED BY BOARD OF EXAMINERS

_____	_____
Chairman, Department of Graduate Committee	Signature
Dr. Mengesha Mamo	_____
Advisor	Signature
_____	_____
Name of Internal examiner	Signature
_____	_____
Name of External Examiner	Signature

DECLARATION

I, the undersigned declare that this thesis is my original work, and has not been presented for a degree in this or any other university, and all sources of materials used for the thesis have been fully acknowledged.

Name: Estibel Abeje Alemayehu

Signature _____

Place: Addis Ababa, Ethiopia

Date of submission _____

This thesis has been submitted with my approval as a university advisor

Name: Dr. Mengesha Mamo

Signature _____

ACKNOWLEDGMENTS

First of all, I would like to thank the Almighty God for providing me everything I have and smoothening of all aspects regarding my study.

Secondly, I would like to express my deepest thanks and gratitude to my advisor Dr. Mengesha Mamo for his invaluable advices, comments, encouragement, continuous guidance, supervision and a remarkable patience support during my graduate studies.

Last but not least, I am always indebted to my wife, my colleagues and my family members for their endless support and love throughout the year. They gave me additional motivation and determination during my graduate study.

Abstract

Recently, with a view to supplementing electricity obtained from traditional energy sources, the generation of energy from renewable energy sources has become increasingly important around the world. From the renewable energy sources, wind energy conversion system is the largest contributor to power generation system. It is one of the fastest growing renewable energy sources due to increasingly severe global environmental or climate problems, as well as rapidly growing fuel costs and electricity demand. Wind energy conversion systems using doubly-fed induction generators (DFIGs) are one of the most important types of generator, including grid-connected systems. Due to intermittent wind speed, the production of wind farms fluctuates. In energy conversation system using DFIG which directly connected to the grid, the changes in wind speed results the violation of voltage and frequency. This violation causes a system stability problem.

This research work presents with the application of field-oriented control system for a decoupled control of the active and reactive powers flow by using fuzzy self- tuning PID controller. Controlling of power is essential to the stable operation of the power system through rotor side converter and grid side converter. The power control of the system due to vector control of dq- axis rotor currents result constant output stator voltage and frequency. The grid-side converter control provides a constant dc_ link voltage which used for source of generator rotor winding current.

The simulation of power control DFIG was done on MATLAB/Simulink software and the result shows an improved performance in terms of settling time, overshoot and frequency deviation. The design of fuzzy tuning PID controller gives a transient response of with settling time 0.167 sec and overshoot 8.21%, and PID control also has settling time 0.204 sec and overshoot 27.3%. Then fuzzy-PID controller have improved time domain transient performance with respect to convectional PID controller for active and reactive power control.

Keywords: Rotor side converter, Grid side converter, DC-link voltage and Fuzzy self-tuning PID control

Table of content

Content's page

List of Tables

List of Figures

List of Abbreviations

WECS	Wind Energy Conversion System
Rs	Stator resistance
Ls	Stator leakage inductance
Lr	Rotor leakage inductance
Lm	Magnetizing inductance
Lls	Stator self-inductance
Llr	Rotor self-inductance
J	Inertia
Wm	Turbine angular speed
Tem	Electromagnetic Torque
V	Wind speed
C_p	Power coefficient
DFIG	Double fed Induction Generator
PLL	Phase Locked Loop
GSC	Grid Side Converter
RSC	Rotor Side Converter
PID	Proportional Integral derivative
PWM	Pulse Width Modulation
FLC	Fuzzy Logic Controller
FPID	Fuzzy Proportional Integral Derivative
WRIG	Wound rotor induction generator
IGBT	Insulated-gate bipolar transistors

CHAPTER ONE

1 Introduction

1.1 Background of the study

Energy supply plays an important role in the social and economic development of nations. With increases in energy consumption, scarcity and cost of basic energy resources have become a worldwide challenge. While coal remains apparently an abundant resource, oil and natural gas supply have concerns of declining in the long run. Further, using conventional carbon-based energy resources will have harmful environmental impacts including global warming and climate change. As a result, to develop an ecologically sustainable energy supply, much attention is focused on utilizing renewable energy resources such as wind, photovoltaic, small hydro, wave, tidal, biomass and geothermal. Wind energy one of the most important and promising renewable energy source in the world, because of its non-polluting and economical viability. The variable wind turbine has been used for several reasons such as ability to get the maximum active power of the wind speed and possibility to control the reactive power independently. But Unbalanced penetration of wind power into power system concerns such as voltage control and stability, power quality, reliability and control issues will affect the performance of the overall power system.

Researchers are now able to control the speed of wind, power of the generator, torque and frequency with different approaches. There is lot of research going on around the world in this area and technology is being developed that offers great deal of capability. It requires an understanding of power systems, machines and applications of power electronic converters and control schemes put together on a common platform. Modelling wind farms will facilitate the understanding of their operation and impacts on the overall power system. Various approaches have been used to model the wind turbine, generator, transformers and control and protection systems

[1]- [2].

The generators used for the wind energy conversion system mostly are of either doubly fed induction generator (DFIG) or permanent magnet synchronous generator (PMSG) type. Nowadays double fed induction machine (DFIG) is widely used generator specially in variables wind speed energy application

DFIG have windings on both stationary and rotating parts, where both windings transfer significant power between shaft and grid. Majority of wind turbine manufacturers utilize DFIG for their WECS due to the advantages in terms of cost, weight and size. Furthermore, advantage of DFIG is that the power electronic converters have to handle only a fraction (20-30%) of the total system power (i.e power losses in power electronic converters of a DFIG are much lesser than the direct connected synchronous generator [3]. The doubly fed induction generator (DFIG) is a special variable speed induction machine and is widely use as

modern large wind turbine generators. This wounds rotor induction machine directly connected to the grid with its stator terminal and rotor windings connected through an AC/DC/AC converter. The AC/DC/AC converter normally consists of a rotor side converter (RSC) and a grid-side converter (GSC). Depending on the operating condition of the drive, the power is fed in or out of the rotor through this converter. To achieve independent control active and reactive power using these converters, synchronously reference frame is used [4] [5].

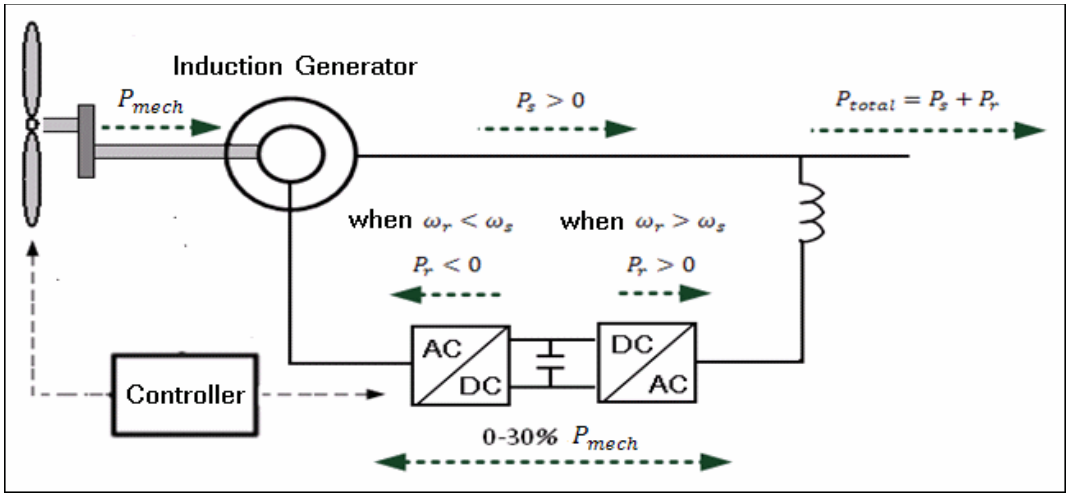

Fig. 1.1, Basic configuration of DFIG wind turbine

1.2 Motivation

Wind power is the most reliable and quick developing among the various renewable energy sources in Ethiopia. Wind turbines can operate both in fixed as well as variable speed operation mode. Double fed induction generator plays a vital role by operating in grid system as well as in standalone mode for different purpose as we need. It has attracted more attention due to its variable speed, reduced converter cost, less switching losses, higher energy efficiency and also for improved power quality.

1.3 Statement of the problem

Wind energy is one of the most important and promising sources of renewable energy all over the world, mainly because it reduces the environmental pollution caused by traditional power plants as well as the dependence on fossil fuel, which have limited reserves. The wind turbine is subjected to seasonal as well as the stochastic behavior of wind. Because of intermittent property of wind speed usually results violation of voltage and frequency of system in grid connected generator. This fluctuating nature of wind speed can cause instability in the power system delivered to the grid. This variable speed turbine based DFIG can store some of the power fluctuations due to turbulence by increasing rotor speed, pitching the rotor blade turbine can control the power output at any given wind speed. The control system in this thesis proposed

that arrangement of DFIG with converter and controlling of active and reactive power of generators are able to maintain power fluctuation. In order to control decouple active and reactive power generated by generators, vector control scheme is used. Besides the analysis and modeling, control over the active and reactive power fed by the doubly fed induction generator, the grid side controller has been simulated in order to get constant dc link voltage. In addition, a fuzzy-PID controller is used in the vector control scheme to improve DFIG's transient performance, and the results are analyzed using Simscape MATLAB/Simulink simulation.

1.4 Objectives

1.4.1 General objective

The overall goal of this thesis is to model double feed induction generator and to regulate its active and reactive power flow in order to extract maximum power from a wind energy source while supplying power to the grid at a consistent voltage and frequency.

1.4.2 Specific Objectives

- To model double fed induction generator (DFIG) in a rotating reference frame.
- Design PID controller for DFIG with rotor side and grid side converter.
- Design fuzzy-PID controller for DFIG with rotor side converter control using MATLAB.
- Simulate and compare system response performance with PID and F_PID controllers of a decoupled control of active and reactive power.
- Simulate and compare system usage of DFIG in mathematical modeled and directly from simscape/ MATLAB.

1.5 Significance of the Research

In this work, the proposed system can extract maximum power and power flow control in fluctuating wind speed by controlling of magnetizing feeder rotor winding current at a constant frequency and voltage of grid system. The simulations are proving with studying maximum power capability as function of wind speed. The model includes aerodynamic wind speed fluctuations, double feed induction machine, and grid side filter enabling control of DC link voltage. Based on results, the proposed vector control of DFIG is capable of simultaneous capturing maximum power of wind energy with fluctuating wind speed. It also provides design of Machine side and grid side conversion control model in the Simulink environment.

1.6 Organization of the Study

This thesis is organized into five chapters. The first chapter presents the overview of doubly fed induction generator control mechanism, a statement of the problem, relevance and objectives of the study. In chapter two, different literatures, related to control of wind energy conversion systems and their DFIG control

system, are reviewed. Besides this, basic of fuzzy and PID controllers are also reviewed. Description of basic concepts and mathematical modeling of mechanical system and electrical system of the thesis are presented in chapter II. Chapter three dedicated to the modeling generator with simplified mathematical expression controllers of the system. MATLAB/SIMULINK simulation results are presented and discussed in chapter four. Finally, chapter five presents conclusions and recommendations.

CHAPTER TWO

2 Double Fed Induction Generator (DfIG) and Literature Review

2.1 Introduction

Doubly fed induction generator (DFIG) is one of the most popular asynchronous generators, which includes an induction generator with slip ring. Wind power is the most rapidly growing one since the 20th century due to its reproducible, resourceful, and pollution-free characteristics. Wind energy has a significant impact on dynamic behavior of power system during normal operations and transient faults with larger penetration in the grid. This brings new challenges in the stability issues and, therefore, the study of influence of wind power on power system transient stability has become a very important issue nowadays. Depending of the speed, there are two types of variable-speed wind turbines. First one, full variable-speed concept in which generator can be synchronous (WRSG, PMSG) or induction generator (WRIG) connected to grid through the full-scale frequency converter. This type of WT can be connected to the generator without speed increasing gearbox; hence, it is now as direct drive wind turbine. Secondly limited variable speed concept in which the generator stator is connected to grid so that the rotor frequency and speed is controlled. The generator is wound rotor induction generator (WRIG). This type is classified in two classes of variable generator rotor resistance (variable-slip) and doubly fed induction generator (DFIG) [6].

With the recent progress in modern power electronics, a wind turbine with doubly fed induction generator (DFIG) has drawn increasing attention. In the DFIG, the induction generator is grid connected at the stator terminals as well as at the rotor mains via a partially rated variable frequency AC/DC/AC converter. The frequency AC/DC/AC converter takes a full control of the generator, like decoupled control of active and reactive power, faster dynamic response with low harmonic distortion [7]. Figure (2.1) shows the overall block diagram of the wind energy conversion system (WECS). Here, $V\omega$ represents wind speed, Pω, Pm and Pe represent wind power, mechanical power and electrical power respectively.

Fig. 2.1, DFIG based wind turbine power conversion

2.2 Wind turbine

Wind turbines are mechanical devices specifically designed to convert part of the kinetic energy of the wind into mechanical energy. The wind turbine captures the wind ‘s kinetic energy of air mass by a rotor consisting of two or more blades which is mechanically coupled to an electrical generator. Most of the time the turbine is mounted on a tall tower to enhance the wind energy capture. Wind turbines convert the aerodynamic power into electrical energy. In a wind turbine two conversion processes take place. The aerodynamic power (available in the wind) is first converted into mechanical power. Next, that mechanical power is converted into electrical power.

A modern wind turbine comprises of the principal components such as the tower, the yaw, the rotor and the nacelle, which houses the gear box and the generator. The tower holds the main part of the wind turbine and keeps the rotating blades at a height to capture sufficient wind power. The yaw mechanism is used to turn the wind turbine rotor blades in the direction of the wind. The gearbox transforms the slower rotational speeds of the wind turbine to higher rotational speeds on the electrical generator side. Electrical generator will generate electricity when its shaft is driven by the wind turbine, whose output is maintained as per specifications, by employing suitable control and supervising techniques. The block diagram of a typical wind energy conversion system is shown in Figure (2-2) below [8].

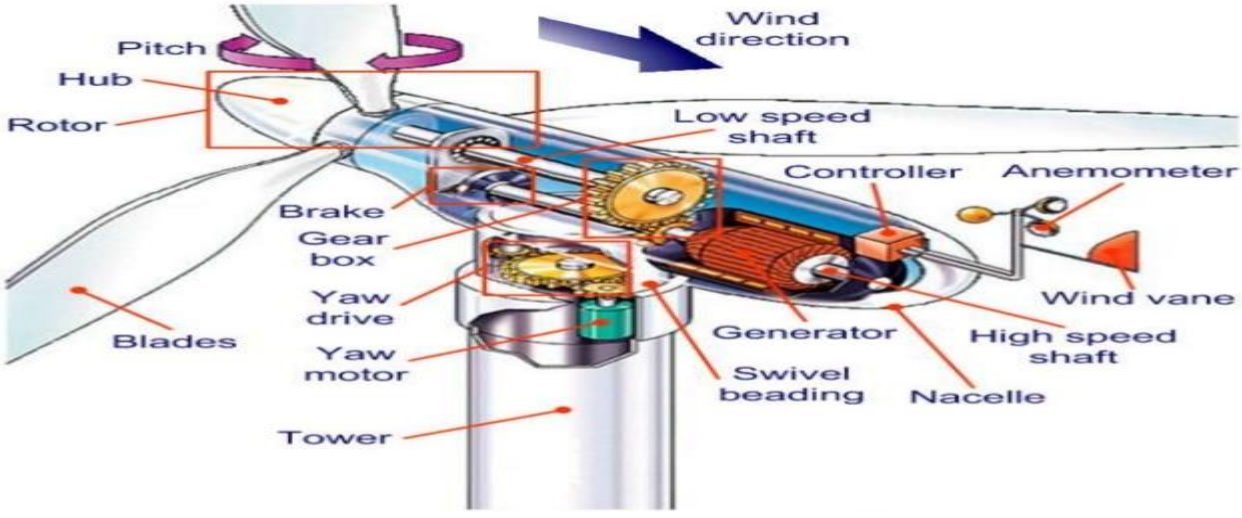

Fig. 2.2, components of wind tirbine-generator energy conversion system

2.2.1 Wind Turbine (Aerodynamic) Modeling

The aerodynamic theory that justifies the benefit of the variable speed operation has been well described in a number of independent sources. In short, the aerodynamics of the blades are such that for a particular wind speed, there is a particular rotational speed that captures the largest amount of power passing through

the swept area. The wind is characterized by its speed and direction, which are affected by several factors, *e.g.*, geographic location, climate characteristics, height above ground, and surface topography [9].

$$P_w = {}^1/_2\,\rho r^2 V_w{}^3 \quad (2.1)$$

Here ρ is the air density, r is the area radius (blade-length) and V_w is the wind speed. Not all of this power can be captured by the wind turbine. The theoretical limit set by Betz's law, states that the maximum amount of wind power Pw that can be captured by the turbine in theoretical limit is 0.59 percent. This fraction of actual power developed by the rotor to the theoretical power available in the turbine is called coefficient of power (Cp) [26] [10].

Wind turbines interact with the wind, capturing part of its kinetic energy and converting it into usable energy. The kinetic energy in air of an object of mass m moving with speed v is equal to:

$$KE = 1/2\, mv\text{^}2 \quad (2.2)$$

The power in the moving air, if we assume constant wind velocity, is:

$$P_{wind} = \frac{dK_E}{dt} = {}^1_2\dot{m}\, v^2 \quad (2.3)$$

Where: $\dot{m}$ is the mass flow rate per second. For a stream flowing through a transversal area A the mass flow rate is.

$$\dot{m} = \rho A v \quad (2.4)$$

The relation between mechanical power and the wind speed passing through turbine rotor expressed as [26] [28]:

$$P_m = P_w \times Cp = {}^1/_2\,\rho A V^3 \times C_P(\lambda, \beta) \quad (2.5)$$

Where: Pm is the mechanical power, P_w is the power contained in wind, β is blade pitch angle, λ is tip speed ratio ρ is the air density and v is the wind speed.

The power coefficient is not a static value as defined in the main question (2.6); it varies with the tip speed ratio of the turbine. The basic formula of power coefficient Cp used for simulation purpose can be defined as a function of the tip-speed ratio and the blade pitch angle as follows [9] [11]:

$$C_P(\lambda, \beta) = c_1\left(\frac{c_2}{\lambda_i} - c_3\beta - c_4\right)e^{\frac{-c_5}{\lambda_i}} + c_6\lambda \quad (2.6)$$

$$\frac{1}{\lambda_i} = \frac{1}{\lambda - 0.08\beta} - \frac{0.035}{\beta^3 + 1} \quad (2.7)$$

It is also conventional to define a tip speed ratio λ

$$\lambda = \frac{\omega R}{v} \qquad 2.8$$

Where ω is rotational speed of rotor (in rpm), R is the radius of the swept area (in meter). The tip speed ratio **λ** and the power coefficient Cp are the dimensionless and so can be used to describe the performance of any size of wind turbine rotor [12].

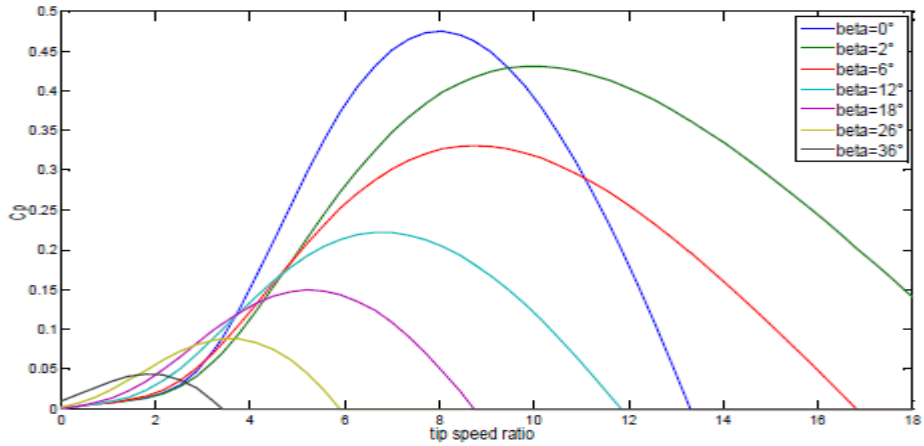

Fig. 2.3, Power coefficient Cp versus tip speed ration

Here it can be clearly seen that for a given pitch angle, there exists a nominal tip speed ratio (λnom), that maximizes C_P (λ, β) and hence maximizes the power output of the turbine for a given wind speed. Therefore, it is highly desirable to be able to change the speed of the turbine as the wind speed changes, such that the turbine maintains the nominal tip speed ratio [16] [13].

2.3 Double Fed Induction Generator

A large variable wind turbine equipped with doubly fed induction generator (DFIG) is considered as the most effective and popular configuration for electricity generation due to its advantages. Double fed electric machines are basically electric machine that are fed ac currents into both the stator and the rotor windings. Most induction generators in the world are cage-type machines. Special classes of induction generators with a three phase wound rotor, called doubly fed induction generators (DFIG), have become very popular for use as wind generators. A cage-type induction generator draws a fixed amount of reactive power, which will cause the power factor to be lagging overall operating conditions [26]. doubly fed electric machines in industry today are three phase wound rotor induction machines. Although their principles of operation have been known for decades, double fed electric machines have only recently entered into a common use. This is due almost exclusively to the advent of wind power technologies for electricity generation [3] [14].

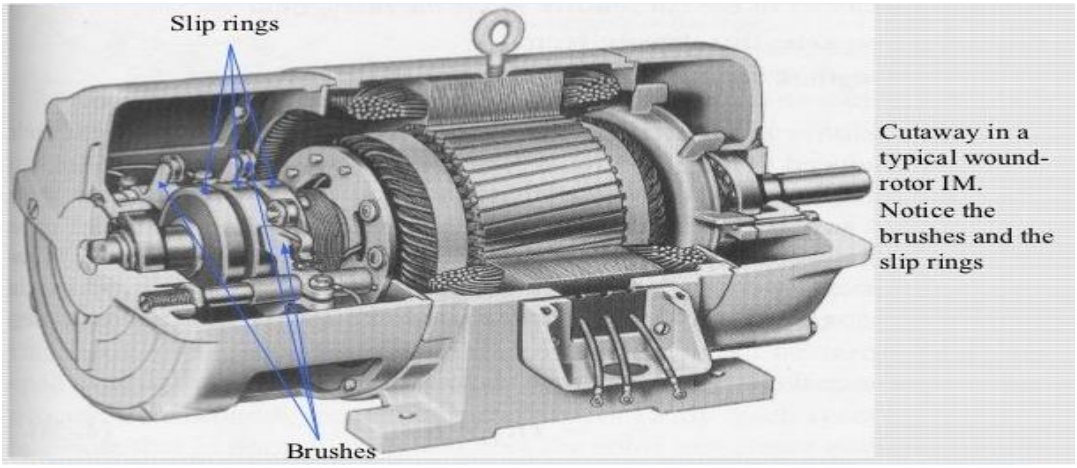

Fig. 2.4, Cut view of Induction machine [15]

The variable speed wind turbine with doubly-fed induction generator (DFIG) as shown in Figure (2.2) and (2.4), the power captured by turbine from wind is converted into electrical power by a wound rotor induction generator as a kind of induction generator running at super synchronous speed and then, it is transmitted to the grid via two way (so-called doubly fed); from the stator windings directly connected to the three-phase grid and also with the rotor windings connected to a back-to-back (AC/DC/AC) frequency converter via slip rings and brushless to allow current into or out of the rotating secondary windings [6].

In DFIG, variable speed operation over a large, but restricted range has become possible due to the presence of power converters that compensating the difference between the variable mechanical frequency and fixed electrical frequency by injecting a rotor current with a variable frequency according to the shaft speed [6]. Through collector rings, the power converter supplied thus rotor windings with a voltage with variable magnitude and frequency. Hence, the behavior of generator is governed by the power converter and its controllers during both normal and fault condition. In other words, to keep constant frequency (fs) of stator voltage of DFIG, rotor frequency (fr) of AC excited generator fed by the bi-directional power converter should be adjusted according to the relations to accommodate varying rotational speed of wind turbine. Large size wind turbines are basically divided into two types which determine the behavior of the wind turbine during wind speed variations: fixed-speed wind turbines and variable-speed wind turbines [6].

In fixed-speed wind turbines, three phase asynchronous generators are generally used. Because the generator output is tied directly to the grid the rotation speed of the generator is fixed and so is the rotation speed of the wind turbine. Any fluctuation in wind speed naturally causes the mechanical power of the

wind turbine rotor to vary and, because the rotation speed is fixed, this causes the torque at the wind turbine rotor to vary accordingly.

In other words, the frequency is adjusted so that the speed of the rotating magnetic field passing through the stator windings remains constant. The frequency of the AC voltages produced at the stator of a DFIG is proportional to the speed of the rotating magnetic field at the stator. When a DFIG is used to produce power at the AC power network voltage and frequency, any deviation of the generator rotor speed from the synchronous speed is compensated by adjusting the frequency of the AC currents fed into the generator rotor windings so that the frequency of the voltage produced at the stator remains equal to the AC power network frequency [26] [27].

In variable-speed wind turbines, the rotation speed of the wind turbine rotor is allowed to vary as the wind speed varies. This precludes the use of asynchronous generators in such wind turbines as the rotation speed of the generator is quasi-constant when its output is tied directly to the grid.

2.3.1 DFIG Working Principle

A three phase wound rotor induction machine can be setup as a doubly fed induction generator; mechanical power at the machine shaft is converted into electrical power supplied to the AC power network via both the stator and rotor windings. Furthermore, the machine operates like a synchronous generator whose synchronous speed (speed at which the generator shaft must rotate to generate power at the AC power network frequency) can be varied by adjusting the frequency of the AC currents fed into the rotor windings. Mechanical power applied to the generator shaft by the prime mover is thus converted to electrical power that is available at the stator windings. In conventional (singly-fed) induction generators, the relationship between the frequency of the ac voltages induced across the stator windings of the generator and the rotor speed is expressed using the Equation.

$$\boldsymbol{fs = \frac{\omega * p}{120}} \tag{2.9}$$

Where,

f_s - Frequency of the ac voltages induced across the stator windings

ω- Speed of rotor in rps

p– Number of poles in the DFIM per phase

From the above Equation, it is very clear that, when the speed of the generator rotor is equal to the generator synchronous speed, the frequency of the AC voltages induced across the stator windings of the generator is equal to the frequency of the power network. The same operating principles apply in a doubly-fed induction generator as in a conventional induction generator. The only difference is that the magnetic field

created in the rotor is not static (not static means, it is created using three-phase current instead of DC current), but rather rotates at a speed proportional to the frequency of the AC currents fed into the generator rotor windings. This means that the rotating magnetic field passing through the generator stator windings not only rotates due to the rotation of the generator rotor, but also due to the rotational effect produced by the AC currents fed into the generator rotor windings. Therefore, in a DFIG both the rotation speed of the rotor and the frequency of the AC currents fed into the rotor windings determine the speed of the rotating magnetic field passing through the stator windings, and thus, the frequency of the alternating voltage is induced across the stator windings [27].

Taking into account the principles of operation of doubly-fed induction generators, it can thus be determined that, when the magnetic field in the rotor rotates in the same direction as the generator rotor, the rotor speed and the speed of the rotor magnetic field add up. The frequency of the voltages induced across the stator windings of the generator can thus be calculated using the Equation below.

$$\boldsymbol{fs = \frac{\omega * p}{120} + fr} \tag{2.10}$$

Where

f_r - Frequency of rotor current fed into the rotor of DFIG

Conversely, when the magnetic field at the rotor rotates in the direction opposite to that of the generator rotor, the rotor speed and the speed of the rotor magnetic field are subtracted from each other. The frequency of the voltages induced across the stator windings of the generator can thus be calculated using the Equation.

$$\boldsymbol{fs = \frac{\omega * p}{120} - fr} \tag{2.11}$$

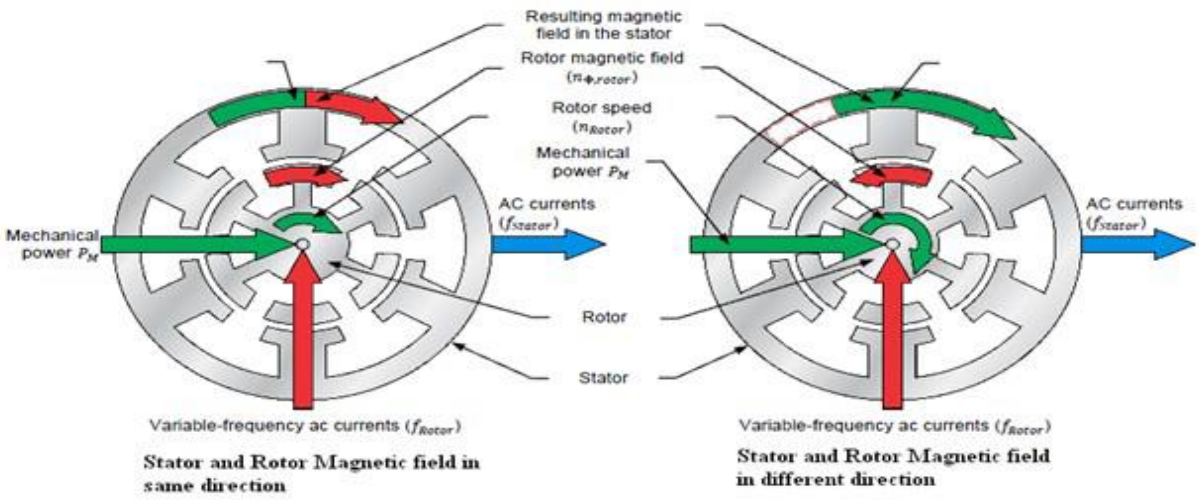

Fig. 2.5, Double fed induction machine [17].

2.3.2 DFIG for Variable Speed Application

DFIG's come into play for wind power conversion, as they allow the generator output voltage and frequency to be maintained at constant values. This is achieved by feeding AC currents of variable frequency and amplitude into the generator rotor windings. By adjusting the amplitude and frequency of the AC currents fed into the generator rotor windings. It is possible to keep the amplitude and frequency of the voltages (at stator) produced by the generator constant, despite variations in the wind turbine rotor speed caused by fluctuations in wind speed [6].

By doing so, this also allows operation without sudden torque variations at the wind turbine rotor, thereby decreasing the stress imposed on the mechanical components of the wind turbine and smoothing variations in the amount of electrical power produced by the generator. Using the same means, it is also possible to adjust the amount of reactive power exchanged between the generator and the AC power network. This allows the power factor of the system to be controlled. Finally, a doubly fed induction generator in variable-speed wind turbines allows electrical power generation at lower wind speeds than with fixed-speed wind turbines using an asynchronous generator [21] [27].

Generally, using a DFIG in wind turbines has the following advantages:

1. Operation at variable rotor speed while the amplitude and frequency of the generated voltages remain constant.
2. Optimization of the amount of power generated as a function of the wind available up to the nominal output power of the wind turbine generator.
3. Virtual elimination of sudden variations in the rotor torque and generator output power.
4. Generation of electrical power at lower wind speeds.
5. Control of the power factor.

2.3.3 Mode of DFIG

For a doubly-fed induction machine, four operating modes can be achieved, as schematized in Figure 2.6. The machine functions as motor if the stator absorbs power, the mode is sub synchronous ($\omega rotor < \omega stator$) if the rotor provides power and super synchronous ($\omega rotor > \omega stator$) if the rotor absorbs power. The machine operates as generator if the stator provides power, the mode is sub synchronous ($\omega rotor < \omega stator$) if the rotor absorbs power and super synchronous ($\omega rotor > \omega stator$) if the rotor provides power. In this study, an interest will be accorded to the sub and super synchronous modes of a DFIG (see later). For ensuring its magnetizing energy, the stator absorbs a reactive power from the utility, and then it generates only an active power. Thus, reactive power flows from utility to stator, and active power flows from stator

to loads. The absorbed power has a positive algebraic sign and the provided power is distinguished by a negative sign [18].

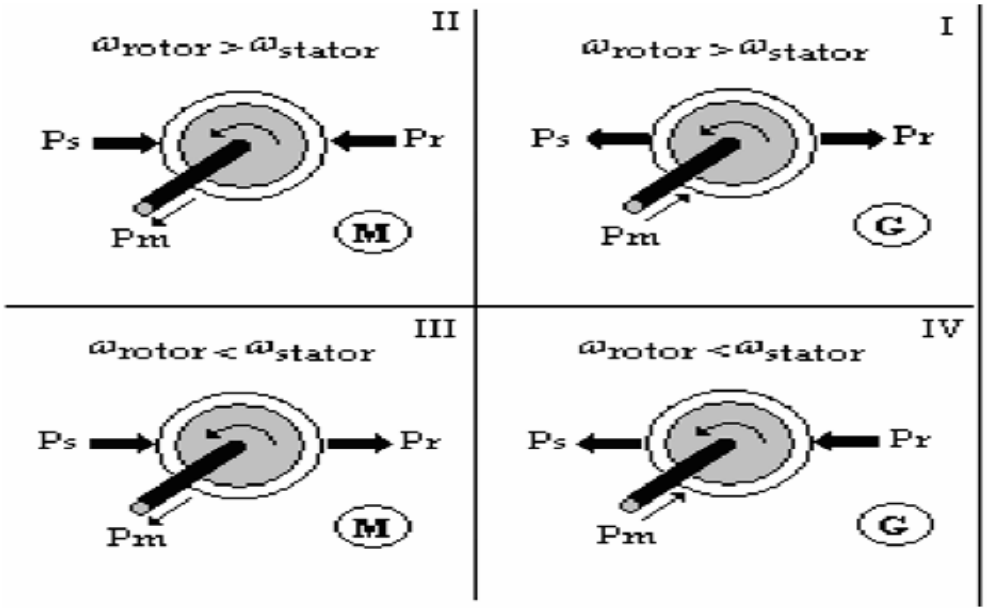

Fig. 2.6, Operation mode of double fed induction machine

2.4 Dynamic Model

The time domain voltage, current, and flux linkages equations for a doubly fed machine are quite complicated. There are three stator windings and three rotor windings, all linking each other. In particular, the interaction between the stator and rotor windings is complicated by the linkage being dependent on the angular position of the rotor.

It has been found that some of the induction machine inductances are functions of the rotor speed, where upon the coefficients of the differential equations (voltage equations) that describe the behavior of these machines is time varying except when the rotor is stalled. A change of variables is often used to reduce the complexity of these differential equations. The general transformation refers machine variables to a reference that rotates at an arbitrary angular velocity. All known real transformations are obtained from the axis transformation by simply assigning the speed of the rotation reference frame [19] [20].

2.4.1 Dq Transformations (park and Clark transformation)

This transformation converts balanced three-phase quantities into balanced two-phase quadrature quantities. Park transformation converts vectors in balanced two-phase orthogonal stationary system into orthogonal rotating reference frame. The three reference frames considered in this implementation are:

1. three-phase reference frame, in which I_a, I_b, and I_c are co-planar three-phase quantities at an angle of 120 degrees to each other.

2. Orthogonal stationary reference frame, in which I_α (along α axis) and I_β (along β axis) are perpendicular to each other, but in the same plane as the three-phase reference frame.
3. Orthogonal rotating reference frame, in which I_d is at an angle θ (rotation angle) to theα-axis and I_q is perpendicular to I_d along the q axis.

The stator voltage field-oriented techniques for double fed induction machine modeling using the park transformation with synchronous rotating frame as shown figure 2.7 [4].

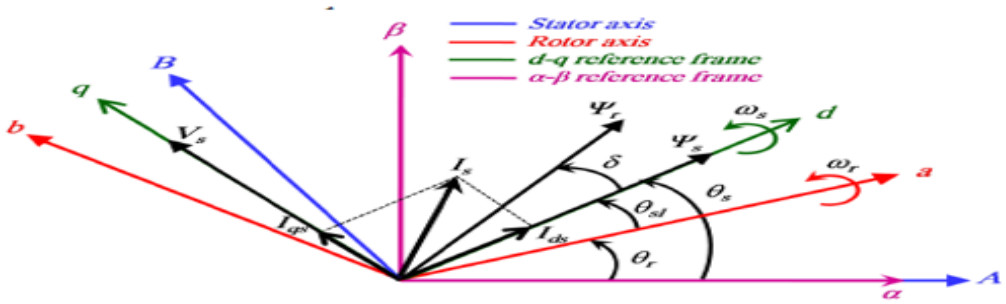

Fig. 2.7, Stator field-oriented phasor diagram

Forward transformation

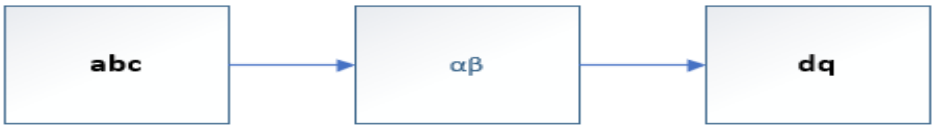

$$\begin{bmatrix} f\alpha \\ f\beta \end{bmatrix} = \frac{3}{2}\begin{bmatrix} 1 & \frac{-1}{2} & \frac{-1}{2} \\ 0 & \frac{\sqrt{3}}{2} & -\frac{\sqrt{3}}{2} \end{bmatrix} \times \begin{bmatrix} fa \\ fb \\ fc \end{bmatrix} \begin{bmatrix} fd \\ fq \end{bmatrix} = \begin{bmatrix} \cos\emptyset & \sin\emptyset \\ -\sin\emptyset & \cos\emptyset \end{bmatrix} \times \begin{bmatrix} f\alpha \\ f\beta \end{bmatrix}$$

$$\begin{bmatrix} fd \\ fq \end{bmatrix} = \frac{3}{2}\begin{bmatrix} cos\,\emptyset & cos(\emptyset-\gamma) & cos(\emptyset+\gamma) \\ -sin\,\emptyset & -sin(\emptyset-\gamma) & -sin(\emptyset+\gamma) \end{bmatrix} \times \begin{bmatrix} fa \\ fb \\ fc \end{bmatrix}$$

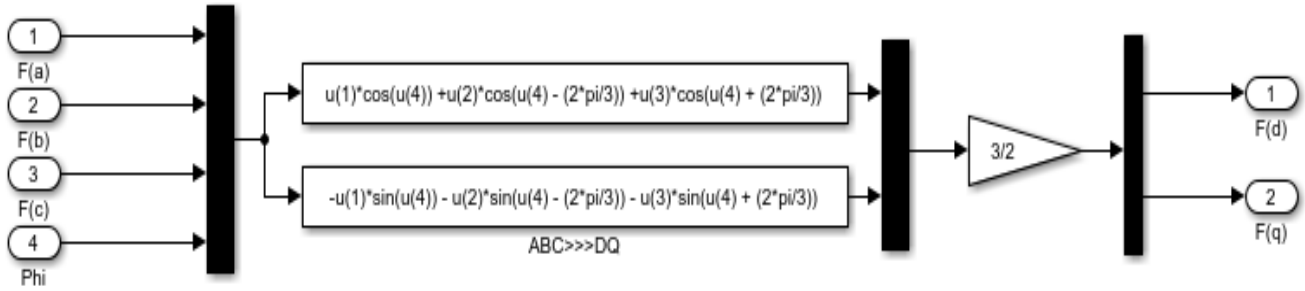

Fig. 2.8, Simulink abc to dq conversion

Inverse d-q transformation

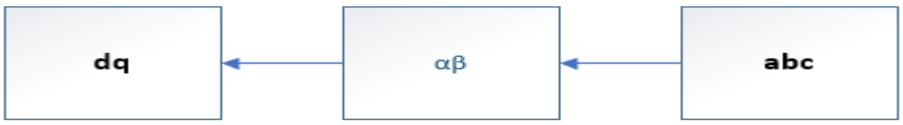

$$\begin{bmatrix} f\alpha \\ f\beta \end{bmatrix} = \begin{bmatrix} \cos\emptyset & -\sin\emptyset \\ \sin\emptyset & \cos\emptyset \end{bmatrix} \times \begin{bmatrix} fd \\ fq \end{bmatrix} \quad \text{And} \quad \begin{bmatrix} fa \\ fb \\ fc \end{bmatrix} = \begin{bmatrix} 1 & 0 \\ \frac{-1}{2} & \frac{\sqrt{3}}{2} \\ \frac{-1}{2} & -\frac{\sqrt{3}}{2} \end{bmatrix} \times \begin{bmatrix} f\alpha \\ f\beta \end{bmatrix}$$

$$\begin{bmatrix} fa \\ fb \\ fc \end{bmatrix} = \begin{bmatrix} cos\,\emptyset & -sin\,\emptyset \\ cos(\emptyset-\gamma) & -sin(\emptyset-\gamma) \\ cos(\emptyset+\gamma) & -sin(\emptyset+\gamma) \end{bmatrix} \times \begin{bmatrix} fd \\ fq \end{bmatrix}$$

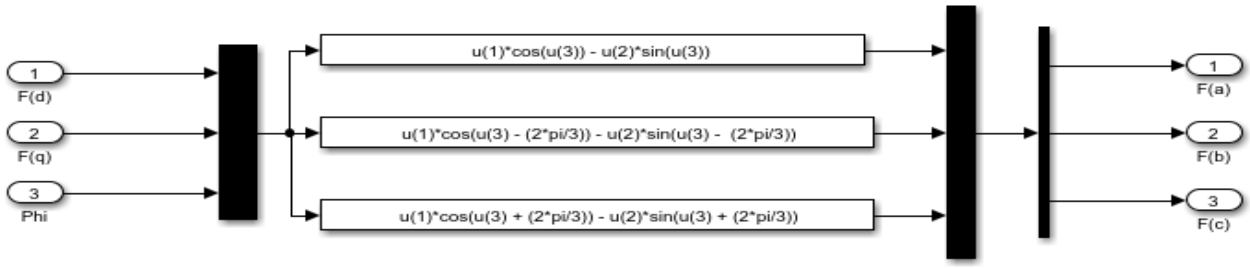

Fig. 2.9, Simulink Inverse (dq to abc) transformation

Where $\boldsymbol{\gamma = \frac{2\pi}{3}}$ and $\emptyset$= angle between dq and αβ reference frame

2.5 General block diagram representation of the system

DFIG machine the stator winding is directly connected to the grid and the rotor winding connects to the grid through the rotor side converter and grid side converter. The rotor winding is connected to the rotor side converter (RSC) by slip ring and brushes.

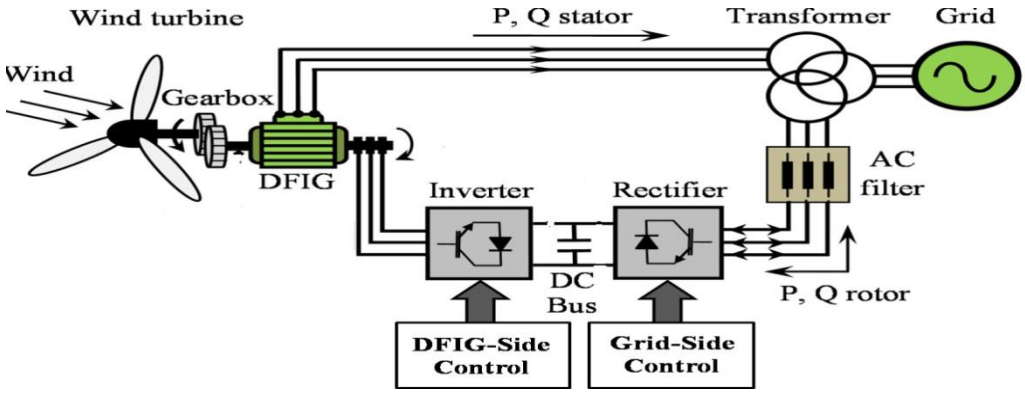

Fig. 2.10, Power flow and, RSC and GSC control system of DFIG

In normal operation the aim of the rotor side converter is to control independently the active and reactive power on the grid, while the grid side converter has to keep the DC-link capacitor voltage at a set value

regardless of the magnitude and the direction of the rotor power and to guarantee a converter operation with unity power factor (zero reactive power). This double fed induction generator is equipped with two identical converters and two different control algorithms (i.e., rotor side control and grid side control). The converter allows a wide range of variable speed operation of the Wound Rotor Induction Machine. Wide range of variable speed operating mode can be achieved by Appling a controllable voltage across the rotor terminal. This is can be done through the rotor side converter (RSC). Appling rotor voltages can be varying in both magnitude and phase by converter controller, which control the rotor currents and hence decoupled control of active and reactive power can be achieve [21].

2.6 Back-to-back converter operation

The back to back converter is including of four main parts: including of two inverters, that each of them besides switching control have another control as well, which rotor side converter is responsible for voltage control or reactive power and extraction of the optimal power from the wind, network side converter is responsible for control of the dc bus voltage amount, which is interface of the two converter and transformer or series reactors which connects the converter to the network [22].Its rotor-side ensures the rotational speed being adjusted within a large range, whereas its grid-side transfers the active power to the grid and attempts to cancel the reactive power consumption. The back-to-back converter consists of two converters, i.e., machine-side converter and grid-side converter that are connected back-to-back. Between the two converters a dc-link capacitor is placed, as energy storage, in order to keep the voltage variations (or ripple) in the DC-link [9].

The main task of rotor side converter (RSC) is to control output power and terminal voltage of the DFIG by adjusting the rotor current fed into rotor winding. Converter controls were modeled based on the rotor-controlled voltage source, so the rotor's d and q axial current should be controlled. RSC converter operation of back-to-back converter is three-phase, six-pulse, and full-wave rectification. A full-wave rectifier converts the whole of the input waveform to one of constant polarity at its output. Six-pulse refers to the number of DC pulses for every 360° of electrical rotation, in other words a complete period [23].

Since DFIG base of the wind system is sensitive to the voltage changes, disturbed grid voltage conditions should be considered in the quality design of GSC. As noted, the most important task of grid side converter (GSC)is regulating bus voltage regardless of the rotor power flow side, so should be compared with its reference amount and applies to a controller to take the amount of the flow at the grid side converter [27].

2.7 PWM (switching)

Sinusoidal pulse width modulation (PWM) is the most straightforward method used to vary the inverters output voltage and frequency. The average value of voltage fed to the load is controlled by turning the switch between supply and load on and off at a fast pace. The duty cycle describes the portion of "on" time of the regular period, and the higher the duty cycle, the higher the power delivered to the load. Switching must be done fast enough as not to disturb the load. The main advantage of PWM is that power loss in the switching devices is very low (practically no current during off-mode and hardly any voltage drops during on mode). With a sufficiently high switching frequency and, when necessary, using additional passive electronic filters, the output waveform can be smoothed [23] [24].

There are several PWM techniques each has its own ad-vantages and also disadvantages. The basic PWM techniques are described briefly in the following subsections. The considered PWM techniques are [25]:

1) Sinusoidal PWM (most common)

2) Space-Vector PWM

A). Sinusoidal Pulse width modulation (SPWM)

A sinusoidal output voltage waveform produces at a desired frequency, three sinusoidal control signals that are 120 angle shifts are compared with a triangular waveform, as shown in figure 2.12. It should be noted that an identical amount of average dc component is present in the output voltages of V_{AN} and V_{BN}, which are measured with respect to the negative DC bus. In the inverter, the switches are controlled based on the comparison of $\mathbf{V}_{con}$ and $\mathbf{V}_{tri}$, and the following output voltage results [23]. The modulation signal for phase-a can be defined as follows:

$$v_{ma} = V_{ma}\cos(\omega t - \gamma) \qquad 2.12$$

where, V_m and I_m , are the magnitudes of the AC side input voltages to the power neutral point 0.

Then the fundamental component of the AC side voltage of converter output, V_{a1} (t) can be expressed as [23] [24].

$$Va1(t) = \frac{1}{2}\frac{V_{ma}}{V_T}Vdc\cos(\omega t - \gamma) \qquad 2.13$$

Where V_{ma}, is the magnitude of the modulation signal, and V_T, is the magnitude of the carrier signal, while Va1, where, is the fundamental component of V (a ,0), which is the voltage from the AC side of the converter output to the power neutral point (i.e point 0).

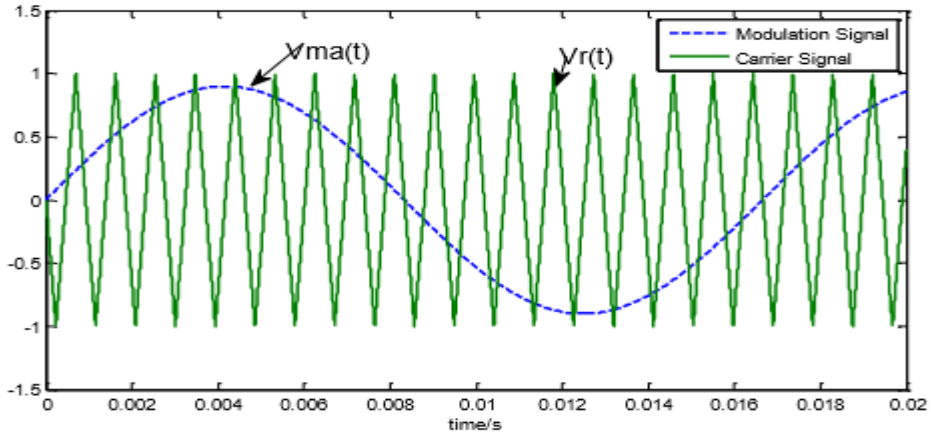

Fig. 2.11, SPWM modulation waveform

So, the modulated signal for phase a can be derived as follows:

$$v_{ma} = V_{ma}\cos(\omega t - \gamma) = \frac{2V_{a1}(t)V_T}{V_{dc}} \qquad 2.14$$

Since the voltage, V_{a1}, is the fundament component of the voltage (a, 0), therefore, it would be convenient to obtain the modulation signal by using the voltage, V (a, 0), according to equation (2.14). Through comparing the PWM converter models expressed in the ABC reference frame and the dq synchronous reference frame, it can be seen that the control signals, Vd and Vq, are the transformed voltages expressed in the dq synchronous reference frame for the AC side voltages, V (a ,0), V(b,0) and V (c,0). Therefore, in order to obtain the modulation signals, it is necessary to transform the voltages, Vd and Vq, back to the ABC reference frame [24].

B). Space vector pulse width modulation (Svpwm)

There are eight possible states (on and off patterns) for the two-level converter ($n^3 = 2^3 = 8$) which produce the voltage vectors as shown in figure. The phase voltages corresponding to the eight combinations of switching patterns can be calculated and then converted into the stator two phase (αβ) reference frames. This transformation results in six of these vectors have equal lengths and are located every sixty degree (100, 110,010,011,101) which are non-zero voltage vectors and the other two vectors are in the origin because of their null lengths (000,111).

The angle between any adjacent two non-zero vectors is 60 electrical degrees. The zero vectors are at the origin and apply a zero voltage vector to the machine. The envelope of the hexagon formed by the non-zero vectors is the locus of the maximum output voltage. SVPWM consists of controlling the stator currents represented by a vector. This control is based on projections which transform a three phase time and speed dependent system into a two coordinate (d and q co-ordinates) time invariant system. Field

orientated controlled machines need two constants as input references: the torque component (aligned with the q co-ordinate) and the flux component (aligned with d co-ordinate).

A typical schematic diagram of a two-level voltage source inverter is shown in Figure.2.13. Six switches (S1 to S6) are the power switches that make the output shape. The upper switches and lower switches are complimentary to each other [25].

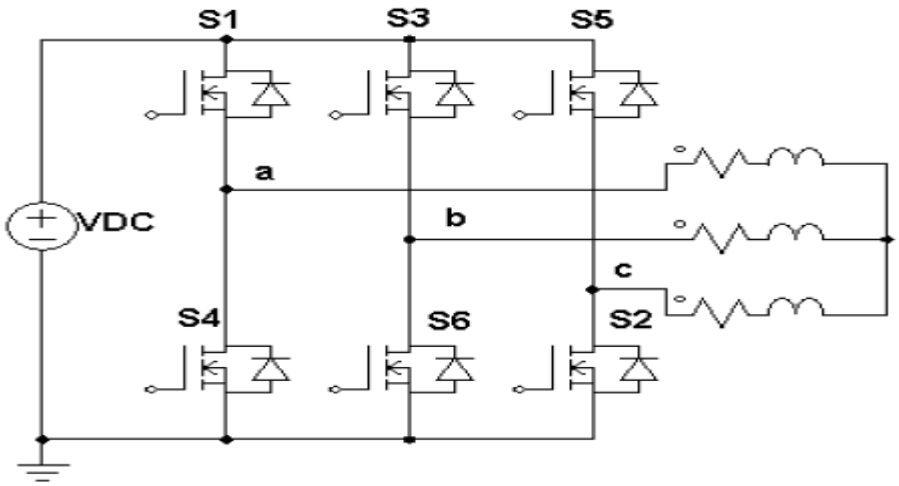

Fig. 2.12, Schematic two level voltage source inverter

As shown figure 2.13, there is a possibility for eight structures of switching status can be configured in the two-level VSI as inserted in Table 2-1. Status (1) means one of the upper switches is conduct, and status (0) means one of the lower switches is conduct. The three digits in the status correspond to the legs (a, b, & c) in inverter respectively. For example, the switching status [100], means in leg (a) one of the upper switches (S1) is conduct, and in legs (b & c) there are two of the lower switches (S6& S1) are conducted in the inverter respectively. There are two statuses, [111] and [000] gives zero in the output called zero conditions, and the others are active conditions.

The active and zero switching conditions can be represented by active and zero space vectors, respectively. The six vectors V_1 to V_6 shapes a symmetric hexagon with similar sectors (1 to 6). Each sector is separated by 60 degrees to each other. From Figure 2.14, Vref is the reference voltage vector which used to control the magnitude and frequency of fundamental voltage [25].

Space vector		Switching conditions	On- status switches
Zero Vector	Vo	111	S1, S93, S5
		000	S4, S6, S2
Active Vector	V_1	100	S1.S6, S2

	V_2	110	S1, S3, S2
	V_3	010	S4, S3, S2
	V_4	011	S4, S3, S5
	V_5	001	S4, S6, S5
	V_6	101	S1, S6, S5

Table 2-1 switching conditions and on-status switches

Space vector Calculation

When these 3-phase voltages in equations (1), (2) & (3) are applied to the AC machine, they produce a revolving magnetic flux in the air gap of the machine. This revolving flux component can be represented as a single revolving vector. The magnitude and angle of the revolving vector can be found by {α, β} or Clark's Transformation. The SVPWM can be achieved by, let three-phase sinusoidal voltage quantities be [25]:

$$v_a = V_m \sin(\omega t)$$
$$v_b = V_m \sin\left(\omega t - \frac{2\pi}{3}\right) \qquad 2.15$$
$$v_c = V_m \sin\left(\omega t - \frac{4\pi}{3}\right)$$

$\vec{V}$ref and α through clark transformation can be determined as

$$\vec{V}_{erf} = \boldsymbol{V_\alpha} + \boldsymbol{jV_\beta}$$
$$= \frac{2}{3}(\boldsymbol{V_\alpha} + \boldsymbol{V_b}\, \boldsymbol{e}^{j\frac{2\pi}{3}} + \boldsymbol{V_c}\, \boldsymbol{e}^{j\frac{4\pi}{3}} \qquad 2.16$$

$$|\vec{V}_{erf}| = \sqrt{\boldsymbol{V_\alpha}^2 + \boldsymbol{V_\beta}^2} \qquad 2.17$$

$$\boldsymbol{\alpha} = \mathbf{tan^{-1}}\left(\frac{\boldsymbol{V_\beta}}{\boldsymbol{V_\alpha}}\right) \qquad 2.18$$

Using forward park transformation, the real and imaginary parts are:

$$V_a = \frac{2}{3}(V_a + V_b \cos\frac{2\pi}{3} + V_c \cos\frac{2\pi}{3}) \qquad 2.19$$

$$V_\beta = \frac{2}{3}(V_b \sin\frac{2\pi}{3} - V_c \sin\frac{2\pi}{3}) \qquad 2.20$$

The switching time duration, T_0, T_1, and T_2 are calculated for sector one by using the volt -sec method as follow:

$$V_{ref}\, T_S = V_1 T_1 + V_2 T_2 + V_0 T_0 \qquad 2.21$$

$$T_1 = T_S\alpha\,[\sin(\frac{n\pi}{3} - \theta)] \quad 2.22$$

$$T_2 = T_S\alpha\,\sin(\theta - \frac{n-1}{3}\pi) \quad 2.23$$

$$T_O = T_S - T_2 - T_1 \quad 2.24$$

Where , $\alpha = \frac{\sqrt{3}\,V_{ref}}{V_d}$ is the modulation index and n = 1 to 6

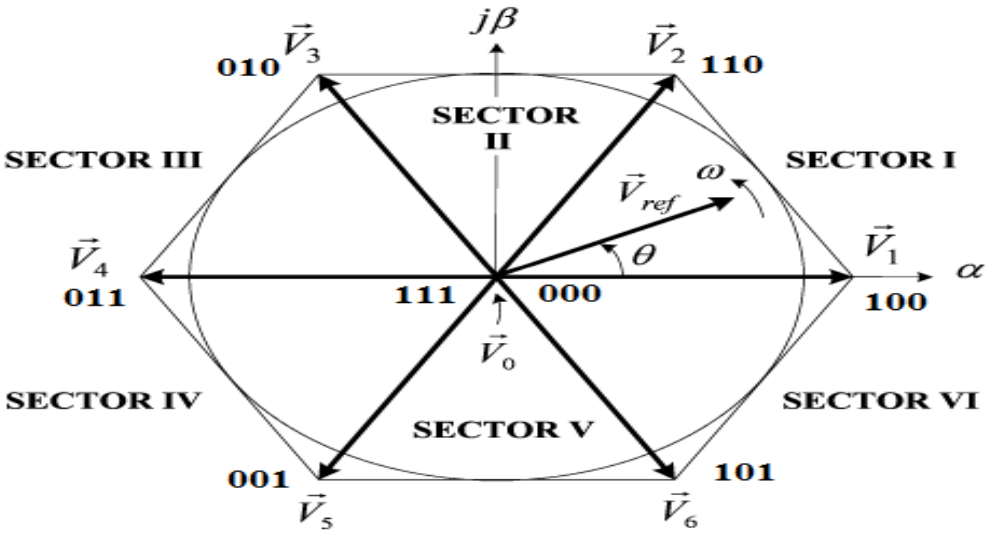

Fig. 2.13, Phasor representation of Space vector

2.8 PID Controller

A proportional-integral-derivative controller (PID controller) is a generic control loop feedback mechanism widely used in industrial control systems. The success of the PID controller depends on its accuracy in determining PID constant (reinforcement). Practically the determination process PID constants are based on human expertise based on rules called rules of thumb. If the right result has been obtained, then this PID constant used for further control. This of course has weaknesses because this constant is the same for every error value that occurs and requires tuning reset if there are changes in plant parameters in the PID constant. For To overcome this, a method is needed to determine the PID constant exactly according to the plant. It is hoped that the performance of the PID control can be improved [26].

A PID controller calculates an "error" value as the difference between a measured process variable and a desired set point. The controller attempts to minimize the error by adjusting the process control inputs. Many processes can be controlled using PID controllers providing that controller parameters have been tuned well. In spite their simplicity, they can be used to solve even very complex control problems. While proportional and integrative modes are also used as single control modes, a derivative mode is rarely used in control systems. The values can be interpreted in terms of time where P depends on the present error, I on the accumulation of past errors, and D is a prediction of future errors, based on current rate of change.

The PID control scheme is named after its three correcting terms, whose sum constitutes the manipulated variable. The controller output signal u (t) algorithm can be to calculated as [9] [27]:

$$U(t)=K_P\times e(t)+\int Kt\times e(t)\,dt+Kd\times\frac{de(t)}{dt} \quad (2.25)$$

Where, k_p: Proportional gain, depend on the present error

k_i: Integral gain, accumulation of past error

k_d: Derivative gain, prediction of future errors

e: Error

t: Time or instantaneous time (the present)

τ: Variable of integration, takes on values from time 0 to the present t.

Proportional term*:* accounts for present values of the error. Because a non-zero error is required to drive it, a proportional controller generally operates with a so-called steady-state error. Steady state error may be mitigated by adding a compensating bias term to the set point or output, or corrected dynamically by adding an integral term [27]. The proportion gain is given by

$$P_{out}=K_P \quad (2.26)$$

Integral term*:* accounts for past values of the error. The contribution of the integral term is proportional to both the magnitude of the error and the duration of the error. The accumulated error is then multiplied by the integral gain and added to the controller output [27]. The integral term is given by:

$$I_{out}=\int Ki\times e(t)dt \quad (2.27)$$

The integral term accelerates the movement of the process towards set point and eliminates the residual steady-state error that occurs with a pure proportional controller [27].

Derivative term: accounts for possible future values of the error, based on its current rate of change. Derivative action predicts system behavior and thus improves settling time and stability of the system. The derivative of the process error is calculated by determining the slope of the error over time and multiplying this rate of change by the derivative gain. The magnitude of the contribution of the derivative term to the overall control action is termed the derivative gain, Kd. The derivative term is given by:

$$D_{out}=K_d\times\frac{de(t)}{dt} \quad (2.28)$$

A PID controller relies only on the measured process variable, not on knowledge of the underlying process, it is broadly applicable. By tuning the three parameters of the model, a PID controller can deal with specific process requirements. The response of the controller can be described in terms of its responsiveness to an

error, the degree to which the system overshoot set point, and the degree of any system oscillation. The use of the PID algorithm does not guarantee optimal control of the system or even its stability [9] [27].

Parameter	Rise Time	Overshoot	Settling Time	Steady-State Error	Stability
Kp	Decrease	increase	Small change	Decrease	Decrease
Ki	Small decrease	Increase	Increase	Eliminate	Decrease
Kd	Minor change	Decrease	Decrease	Minor change	Improve if k_d small

Table 2-2effect of independent P, I and D tuning on closed-loop system

Discrete PID as function of sampling time

The way to discretize PID controller is convert the integral and derivative terms to their discrete time counterpart. There are commonly three ways to do so, by means of forward euler, backward euler and trapezoidal methods. For sampling time 'Ts' the integral term $\frac{K_i}{s}$ can be represented in desecrate form by:

Forward Euler : $\frac{K_i \ T_s}{z-1}$

Backward Euler : $\frac{K_i \ T_s \ z}{z-1}$

Trapezoidal : $\frac{K_i \ T_s}{z} * \frac{z+1}{z-1}$

The derivative term $k_{ds}$is commonly changed to a lowpass filter to make it less noise, and which can be described as

Forward Euler : $\frac{N(z-1)}{z-1+NT_s}$

Backward Euler : $\frac{N(z-1)}{(z-1)(1+NT_s)}$

Trapezoidal : $\frac{N(z-1)}{z\left(1+\frac{NT_s}{2}\right)+\frac{NT_s}{2}-1}$

Where K_p is proportional gain, K_i is derivative gain,K_d is T_s is sampling time and N is filter coefficient

2.9 Fuzzy logic controller

The PID controllers always have a very vital role concerning the constancy of the power system. However, the performance of the double fed induction generator greatly depends on the suitable choice of the controller gain parameters of the PID. The difficulty regarding the PID controller gain is the fine tuning of the controller so as to achieve the optimal operation of the task. The major drawback of the PID controller is faced when the process is nonlinear and also when the system is having oscillations. Considering all these facts, a fuzzy logic controller was designed to control linear as well as in nonlinear design parameters [27].

Fuzzy logic starts with the concept of a fuzzy set. A fuzzy set is a set without a crisp, clearly defined boundary. It can contain elements with only a partial degree of membership. To understand a fuzzy set, first consider the definition of a classical set. A classical set is a container that wholly includes or wholly excludes any given element. Fuzzy set theory first introduced by Zadeh was used to describe inexact information, but after Mamdani ‘s pioneer work on its application to a steam engine control, many applications of fuzzy control in industry processes have been developed. It has a hierarchical structure which consists of two rule bases. The first one is the general rule base of an FLC. The second one is, constructed by meta-rules, which exhibit human like learning ability to create and modify. The fuzzy controller consists of a set of linguistic rules that describe the operator ‘s control strategies. These rules are based, on the experiences of a human operator, because the detailed dynamics of the controlled process is not needed in the design process. Fuzzy control processes an inherent robust property. A typically fuzzy controller as illustrates in Fig 2-14, consists of three major parts: a fuzzification, decision making logic (fuzzy inference system), and defuzzification. The key to successful design of a fuzzy controller relies on the suitable selection of fuzzy variable and linguistic rules, obtained practical experiences and intuitive tries [28] [27].

Currently, many research efforts are focused on emulating human learning, mainly on the ability to create fuzzy control rules and to modify them or tune based on experience. The tuning process of FLC, through trial-and-error approach will continue until satisfactory results are obtained. If the results are not as desired, changes are made either to the number of the fuzzy partitions or the mapping of the membership function and then the system can be tested again. Definitely it is usually a tedious and time-consuming task. The derivation of the rule based basically follows these four approaches:

i) Expert experiences and control engineering knowledge

ii) Based on operator ‘s control actions

iii) Based on fuzzy model of a process

iv) Based on learning.

From these four methods, only two will be used in this case which is based on learning and from the expert experiences and control engineering knowledge. An expert experience is the least structured of the four methods and yet it is one of the most widely used today [9] [27].

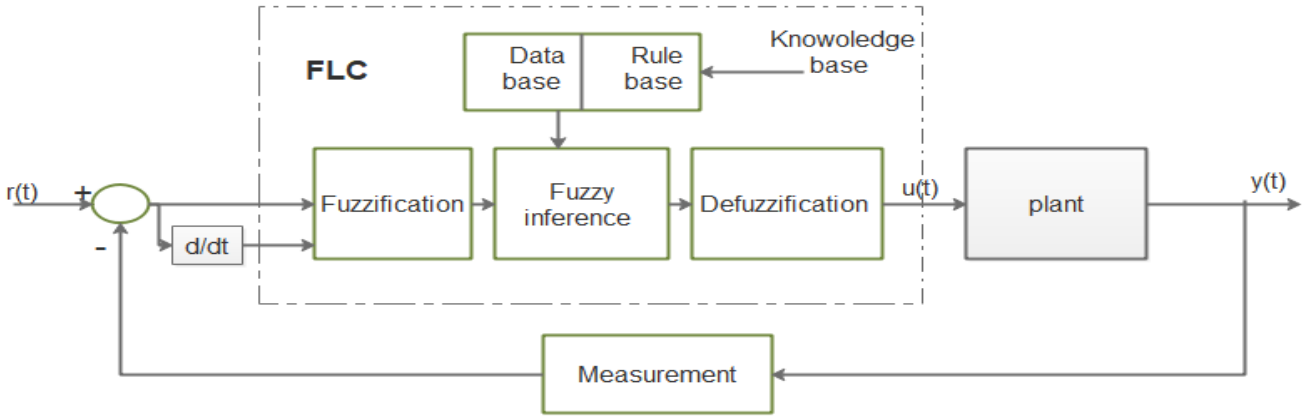

Fig. 2.14, Design of fuzzy controller

Fuzzification:

The term fuzzification means to fuzzify the data. This is done by converting the classical set to fuzzy set. For this process we need different fuzzifiers such as Triangular, Trapezoidal, Singleton and Gaussian. With the help of these fuzzifiers we assign some membership function to each and every input and convert it into fuzzy set [27].

In fuzzy logic, the truth of any statement becomes a matter of degree. A formal definition of a fuzzy set is, if X is a collection of objects denoted generically by x then a fuzzy set A in X is a set of ordered pairs: [23]

$$A= (\frac{x,\mu_x(x)}{x})\varepsilon X$$

Where μA(x) is called the grade of membership or membership function of x in A. An often used method for denoting a fuzzy set is

$$A= \Sigma x_1 \varepsilon \frac{\int x\mu_A(X)}{x} \text{ if X is continuous}$$

$$A= \Sigma x_1 \varepsilon \frac{X\mu_A(x_i)}{X_i} \text{ if X is discrete}$$

Fuzzy Inference system:

It consists of a knowledge base, in which the rules are framed. Fuzzy inference engine can be broadly categorized into two types of methods [29]: first one is mamdani method; it is a fuzzy inferencing method in which the linguistic logic is used to make the rules. It is easy to implement, user friendly and widely accepted method of fuzzy inference. Second, sugeno method is based on mathematical analysis and calculations. It is more complex compared to the Mamdani method. Sugeno method works well with the linear systems. A so-called rule-based fuzzy inference system (FIS) consists of a number of if-then rules. These rules are based on the linguistic variables. The inference system uses the experience embodied in fuzzy relations [30].

Defuzzification:

It is a process of converting a fuzzy set into classical set. It is inverse process of fuzzification. It is of much importance as by defuzzification process we convert the fuzzy values back into the classical or crisp values. There are different methods for defuzzification such as the centroid method, bisector method, largest of maximum, middle of maximum and finally the smallest of maximum. Among all of this the most efficiently used method is centroid [9] [27].

Rule Base

Rules form the basis for the fuzzy logic to obtain the fuzzy output. The rule-based form uses linguistic variables as its antecedents and consequents. The antecedents express an inference or the inequality, which should be satisfied. The consequents are those, which we can infer, and is the output if the antecedent inequality is satisfied. The fuzzy rule-based system uses if–then rule based system given by, IF antecedent, THEN consequent [9] [27].

2.10 Literature review

Zhi and L. Xu, [31] have proposed the principle of direct power control developed after direct torque control of doubly fed induction generator control system. The development of this control strategy is due to the relationship of torque and flux. Direct power control (DPC) is an alternative approach, based on what inverter switching vectors were selected from optimal switching table using the estimated rotor or stator flux position, and the errors in the active power and reactive powers. Thus, high performances, robustness and low sensitivity to the system parameter variations can be considered as the main advantages of the DPC method. However, these desirable characteristics have a penalty of high ripple in developed torque or power and also a non-constant switching frequency, which is a source of non-linear behavior, especially in the power hysteresis comparators. It is shown that the rotor side converter's switching frequency is highly influenced by the shaft speed, which is mainly due to the power slope that depends on

speed. The variable switching frequency degrades the stator side AC filter's efficiency by increasing the size and power loss.

The experimental test bed consists of a DFIG, induction machine, variable speed driver and a bi-directional back-to-back converter. Also, TMS320F2812 microcontroller has been used to control the system. According to the analysis above, it needs to find the relationship between stator powers and the rotor voltages. But DPC responses fast and have good performance, which has a dependency to the machine parameters and operation conditions **[9]**.

Adel Mehdi, AbdellatifReama and Hocine Benalla [32] **have proposed** sensorless direct active and reactive power control (DPC) of grid connected DFIG using back-to-back PWM voltage source converters in the rotor circuit, the sensor less DPC has been proposed to overcome the drawbacks of large power ripple and variable switching frequency in c1assieal DPC. The stator active and reactive powers are made to track references using hysteresis controllers without including any synchronous coordinate transformations. A switching table and hysteresis comparator are used to directly determine the first active vector, and to improve the system robustness with constant switching frequency a second null vector is also chosen, exhibits lower power ripples and better harmonic performance of stator and rotor currents. A sensor less method is implemented for detection of the rotor position based on the comparison between actual and estimated rotor currents. A sensor less operation is desirable because the use of a position encoder has several drawbacks in term of robust, cost, cabling, and maintenance.

By Ivan Villanueva, Antonio Rosales perdo ponce and Arturo Molina [33] a stator flux oriented sliding mode control, which regulates torque and reactive power in DFIG, was proposed. The controller is not dependent on electric machine parameters and do not require modulation, injecting the desired voltage vector directly to a two-level power converter. Despite the proposed SMC controller has a variable switching frequency, which is not desired in practical applications, the switching frequency is limited by a hysteresis loop in the torque and reactive power controllers. when compared with classical control techniques as DTC, the presented SMC does not require the modification of the control loop. However, it requires infinite switching frequency, which is not possible in real physical systems; therefore, the most common solution for this issue is to include a hysteresis loop to the ideal sign function. This scheme is affected by generator parameter variations and introduces delay in the control system. It is well known that the relationship between maximum power from wind and wind speed is nonlinear. So, it is not possible therefore to design a controller to operate satisfactorily at one operating state.

Azzouz TAMAARAT, Abdelhamid BENAKCHA [35]The modeling and control strategy of a grid connected wind power generation scheme using a doubly fed induction generator (DFIG) driven by the

rotor. This paper presents the complete modeling and simulation of a wind turbine driven DFIG in the second mode of operating (the wind turbine pitch control is deactivated). It will introduce the vector control, which makes it possible to control independently the active and reactive power exchanged between the stator of the generator and the grid, based on vector control concept (with stator flux or voltage orientation) with classical PI controllers. In this vector-controlled DFIG is the possibility to achieve decoupled control of the stator side active and reactive power in both motor and generator applications. The quadratic component of the rotor u_{rq} controls the active power and the direct component U_{rd} controls the reactive power exchanged between the stator and the network. The modeling and control strategy of DFIG using conventional PI controller in MATLAB simulation. The control strategy of Generator allows a perfect decoupling between the active and reactive stator power and also keep the active and reactive power to their desired values. Disadvantage of this approach is slow response to changes in system parameter due to uncertainty and to reference change.

Matrix converter (MC) based Wind Energy Conversion System (WECS) at different wind speeds is useful for estimating the available reactive power support to the grid from the DFIG. To maximize the active power injected into the grid at any wind speed the wind turbine should be operated in the Maximum Power Point Tracking (MPPT) mode and the power losses occurring in different components of the generating system (i.e., generator, converters, filters, etc.) should be minimized. It uses control algorithm to calculate the DFIG Rotor Side Converter (RSC) current component references to achieve the control objective. This algorithm, however, does not consider the losses occurring in the power converters. Rotor side converter's active power is controlled by the d-axis component of the rotor current in outer control layer. Rotor side converter's reactive power is controlled by q-axis component of the rotor current. The control method of the rotor side converter is based on SFOC. For the grid side converter, it is a vector control strategy with the grid voltage orientation. The d-axis voltage component is along with the position of grid voltage space vector, and the q-axis voltage component is regarded as zero. So, the grid side converter's active power and reactive power can be manipulated by using d-axis and q-axis components of grid side converter's line current respectively.in the calculation of active and reactive power in terms of dq current not correct or interchanged [38].

The aim of this thesis is to extract maximum power from wind energy conversion system and control of power flow using self tuning Fuzzy-PID controller. When controlling of rotor ejected current, the rotor speed of DFIG was controlled to get the maximum power. To overcoming almost all the above mentioned research gaps, in thesis a well-organized, fuzzy tuning F_PID based active and reactive power control of double fed induction generator can be designed to replaces the traditional PI controller. Under the work

performance of proposed control is checked using varying of wind turbine speed. During the checkup time, fuzzy logic controller adjusts control parameters gain of the proportional-integral -derivative (PID), so the parameter gains of PID not fixed. These advantages of F_PID makes it have good performance and, hence, found to be a suitable replacement of the PI controller for the high-performance in variable wind turbine conversion systems. In order to evaluate the proposed method, simulations are performed in MATLAB/SIMULIN.

CHAPTER THREE

3 Systems modeling and Controller design

3.1 Control Strategies for a Wind Turbine-Generator System

Wind turbines produce electricity by using the power of the wind to drive an electrical generator. The wind passes over the blades, generating lift and exerting a turning force. The rotating blades turn a shaft inside the nacelle, which goes into a gearbox. The gearbox increases the rotational speed that is appropriate for the generator, which uses magnetic fields to convert the rotational energy into electrical energy. The control schemes for a wind turbine generator system include the pitch angle control, maximum power point tracking control and traditional control techniques and advanced control techniques for wind turbine generator systems are reviewed in this section [13].

3.1.1 Pitch Angle Control

The pitch angle control is a mechanical method of controlling the blade angle of the turbine when the captured wind power exceeds its rated value or wind speed exceeds its rated value. Pitch angle control is enabled to limit the maximum output power to be equal to rated power, and thus project the generator when the wind speed experiences gust. The pitch angle controller is only activated at high wind speed [9]. This method is implemented to control the mechanical power in at the nominal value. Whenever the velocity of wind exceeds the rated value of power, a mechanical method is implemented so as to control the blade angle of the wind turbine from being damaged [21]. At low wind speed, a control system technique is applied so that highest amount of power can be extracted from the wind. In this case, the blades are turned back for the extraction of the maximum amount of energy. While during the gusty wind condition the pitch, angle is adjusted to limit the power extraction. This is done by turning the blades away from the wind. A pitch controller is used to regulate the blade angle by using proper technique for capturing the wind [9].

3.1.2 Maximum Power Point Tracking

The maximum power point tracking scheme is used to extract the highest amount of available energy from the wind, while it is operating over a large range of wind speed. According to maximum power tracking the generator speed is adjusted according to the variability of wind speed. The convectional control schemes included the control mode of operation which used to depend on the setting of reference value. But in intelligent controller (i.e., fuzzy logic, neural network etc.), which has some advantages like speed control against wind gusts and superior dynamic and steady state performances [21].

3.1.3 Conventional Control Schemes

Conventional control is an important ingredient of a distributed control system and also found in all areas where control is used. The PID controller is the most common form of convectional control scheme feedback. It refers to the first letters of the names of the individual terms that make up the standard three-term controller. These are P for the proportional term, I for the integral term and D for the derivative term. Three-term or PID controllers are probably the most widely used industrial controller. The values of these three parameters interpreted in terms of time, where, 'P' depends on the present error, 'I' on the accumulation of past errors and 'D' is a prediction of future errors, based on current rate of change. By tuning the three parameters in the algorithm of PID controller, the controller can provide control action designed for specific process requirements [39]. Practically all PID controllers made today are based on microprocessors.

3.2 Mathematical representation of Double Fed Induction Generator

Modeling is a basic tool for analysis, such as optimization, project, design and control. Wind energy conversion systems are very different in nature from conversion generators, and therefore dynamic studies must be addressed in order to integrate wind power into the power system. Dynamic modeling is needed for various types of analysis related to system dynamics: stability, control system and optimization [9].
DFIG scheme is basically consists of standard wound rotor induction generator with its stator windings directly connected to the grid and its rotor windings through the power frequency converters built by two self-commutated PWM converters with an intermediate DC voltage link. The behavior of the generator is controlled by these converters and their controllers in normal.

The DFIG has two sets of three-phase windings that display self and mutual inductances. Mutual inductances change as the machine turns and the angle between stator and rotor circuits varies with time, which ultimately leads to a time-varying mathematical model of the machine. This angle dependency in DFIG's model and the associated complexities can be surmounted by making a transformation from three-phase magnitudes to two axis magnitudes (Clark's transformation) and transforming the magnitudes into direct and quadrature components referred to a synchronously rotating reference frame (Park's transformation) [40].

3.2.1 DFIG in actual variables

The actual variables over here are the voltages and current. Due to the presence of three current in stator we have three currents in rotor as well. The simulation is going to be complex if there are six variables,

but if we transform these variables into dq model the complexity is greatly reduced with the reduction of the number of variables [30].

Equation of stator voltage

$$\boldsymbol{V\_abcs} = \begin{vmatrix} \boldsymbol{V_{as}} \\ \boldsymbol{V_{bs}} \\ \boldsymbol{V_{cs}} \end{vmatrix} = [\boldsymbol{r_s}]\boldsymbol{i_{-abcs}} + \boldsymbol{p\varphi\_abcs} \tag{3.1}$$

$[\boldsymbol{r_s}]\boldsymbol{i_{-abcs}}$ denotes the resistance drop and $\boldsymbol{p\varphi\_abcs}$ denotes the rate of change of flux linkages.

Equation of rotor voltage

$$\boldsymbol{V_{-abcr}} = \begin{bmatrix} \boldsymbol{V_{ar}} \\ \boldsymbol{V_{br}} \\ \boldsymbol{V_{cr}} \end{bmatrix} = [\boldsymbol{r_r}]\boldsymbol{i_{-abcr}} + \boldsymbol{p\varphi\_abcr} \tag{3.2}$$

Where stator and rotor currents are given by:

$$\boldsymbol{i_{-abcs}} = \begin{bmatrix} \boldsymbol{i_{as}} \\ \boldsymbol{i_{bs}} \\ \boldsymbol{i_{cs}} \end{bmatrix} \quad , \boldsymbol{i_{-abcr}} = \begin{bmatrix} \boldsymbol{i_{ar}} \\ \boldsymbol{i_{br}} \\ \boldsymbol{i_{cr}} \end{bmatrix} \tag{3.3}$$

3.2.2 DFIG in (α, β) Reference Frame

In order to describe the alpha-beta reference frame it must be considered that it resembles the dq0 but it is stationary [41] [20].

Stator voltage and fluxes in the (α, β) reference frame:

$$V_{\alpha s} = R_s i_{\alpha s} + \frac{d}{dt}\lambda_{\alpha s} \tag{3.4}$$

$$V_{\beta s} = R_s i_{\beta s} + \frac{d}{dt}\lambda_{\beta s} \tag{3.5}$$

$$\lambda_{\alpha s} = \int (V_{\alpha s} - R_s i_{\alpha s}) \tag{3.6}$$

$$\lambda_{\beta s} = \int (V_{\beta s} - R_s i_{\beta s}) \tag{3.7}$$

The stator currents are:

$$i_{\alpha s} = \frac{L_{lr} + L_m}{L_{lr}L_{ls} + L_m(L_{lr} + L_{ls})}\lambda_{\alpha s} - \frac{L_m}{L_{lr}L_{ls} + L_m(L_{lr} + L_{ls})}\lambda_{\alpha r} \tag{3.8}$$

$$i_{\beta s} = \frac{L_{lr} + L_m}{L_{lr}L_{ls} + L_m(L_{lr} + L_{ls})}\lambda_{\beta s} - \frac{L_m}{L_{lr}L_{ls} + L_m(L_{lr} + L_{ls})}\lambda_{\beta r} \tag{3.9}$$

The equation of the (α, β) frame of the rotor's voltage and current are:

$$V_{\alpha r} = R_r i_{\alpha r} + \frac{d}{dt}\lambda_{\alpha r} + \omega_r \lambda_{\beta r} \quad (3.10)$$

$$V_{\beta r} = R_r i_{\beta r} + \frac{d}{dt}\lambda_{\beta r} - \omega_r \lambda_{\alpha r} \quad (3.11)$$

$$\lambda_{\alpha r} = \int (V_{\alpha s} - R_r i_{\alpha r} - \omega_r \lambda_{\beta r}) \quad (3.12)$$

$$\lambda_{\beta r} = \int (V_{\beta r} - R_r i_{\beta r} + \omega_r \lambda_{\alpha r}) \quad (3.13)$$

$$i_{\alpha r} = \frac{L_{lr} + L_m}{L_{lr}L_{ls} + L_m(L_{lr} + L_{ls})}\lambda_{\alpha r} - \frac{L_m}{L_{lr}L_{ls} + L_m(L_{lr} + L_{ls})}\lambda_{\alpha s} \quad (3.14)$$

$$i_{\beta r} = \frac{L_{lr} + L_m}{L_{lr}L_{ls} + L_m(L_{lr} + L_{ls})}\lambda_{\beta r} - \frac{L_m}{L_{lr}L_{ls} + L_m(L_{lr} + L_{ls})}\lambda_{\beta s} \quad (3.15)$$

The electromagnetic torque can be written as follows:

$$T_e = \frac{3}{2} p (\lambda_{\alpha r} i_{\beta r} - \lambda_{\beta r} i_{\alpha r}) \quad (3.16)$$

3.2.3 DFIG in dq variable

Over here the three phase actual variables, namely the abc (stationary) variables are transformed into two phase variables, that are the direct axes(d) and quadrature axes(q). The two axes, d and q axes are in a position of perpendicular to each other. The angle θs gives the instantaneous location of the stator rotating magnetic field. The rotor itself is rotating and is instantaneously located at angle θ_r. Thus, with a reference frame attached to the rotor, the stator's magnetic field vector is at the location (θ_s- θ_r,) which is referred to as the 'slip angle'.

In doubly fed induction generator, flux linkage is chosen a basic variable representing the d-q axis used for simulation. This representation is based on two axis full-order known as the Park model. There is an equivalent two-axis representation of three axes. In that stator direct axis is represented as ds and quadrature axis is represented as qs, and Rotor direct axis is represented as dr and rotor quadrature axis is represented as qr. Here a synchronously rotating reference frame chosen as d-q reference frame which is rotating at synchronous speed. There by interaction between power and electromagnetic torque with current in the rotor is observed. In this model three-phase quantities are changed to the two-phase quantities. The generator model of DFIG can be expressed by voltage equations, power and electromagnetic torque equations under the d-q coordinate system [21] [41].

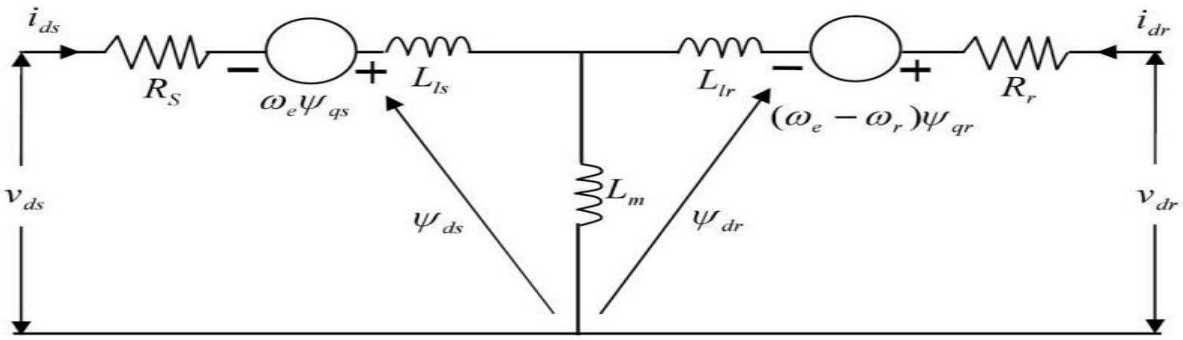

Fig. 3.1, The equivalent circuit of d-axis

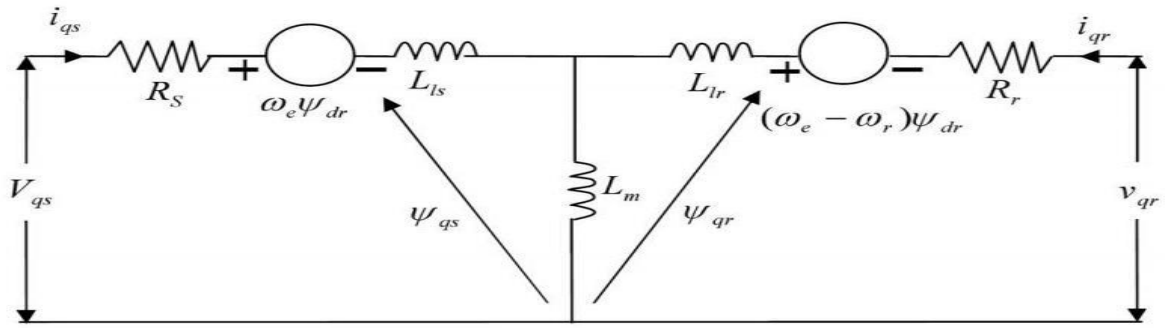

Fig. 3.2, The equivalent circuit of q-axis

The dynamic modeling of doubly-fed induction generator in synchronously rotating reference frame d–q involves the following equations [5] [42] [41].

Stator voltage component

$$V_{ds} = R_s I_{ds} + \frac{d}{dt}\varphi_{ds} - \omega_s \varphi_{qs} \tag{3.17}$$

$$V_{qs} = R_s I_{qs} + \frac{d}{dt}\varphi_{qs} + \omega_s \varphi_{ds} \tag{3.18}$$

Rotor components:

$$V_{dr} = R_r I_{dr} + \frac{d}{dt}\varphi_{dr} - (\omega_s - \omega_r)\varphi_{qr} \tag{3.19}$$

$$V_{qr} = R_r I_{qr} + \frac{d}{dt}\varphi_{qr} + (\omega_s - \omega_r)\varphi_{dr} \tag{3.20}$$

The flux linkages can be calculated in terms of currents as shown from equations (3.21) to (3.24) as:

Stator flux components:

$$\varphi_{qs} = L_s I_{qs} + L_m I_{qr} \tag{3.21}$$

$$\varphi_{ds} = L_s I_{ds} + L_m I_{dr} \tag{3.22}$$

Rotor flux components:

$$\varphi_{qr} = L_r I_{qr} + L_m I_{qs} \quad (3.23)$$

$$\varphi_{dr} = L_r I_{dr} + L_m I_{ds} \quad (3.24)$$

DFIG electromagnetic torque:

$$T_e = -\frac{3}{2}\frac{p}{2}\frac{L_m}{L_r}(\varphi_{ds} I_{qr} - \varphi_{qs} I_{dr}) \quad (3.25)$$

A doubly-fed induction generator is as a standard wound rotor induction generator with its stator windings directly connected to the power grid and rotor connected to the power grid through a frequency converter [6] [41]. It is important to administer the generator active power transmitted through the stator and the rotor as following equation:

$$P_t = p_s + p_r \quad (3.26)$$

Where

$$P_s = \frac{3}{2} R_e(V_{dqs.} I_{dqs}) \quad (3.27)$$

$$P_r = \frac{3}{2} R_e(V_{dqr.} I_{dqr}) \quad (3.28)$$

The amount of reactive power can be found from following equation

$$Q_t = Q_s + Q_r \quad (3.29)$$

Where

$$Q_s = \frac{3}{2} I_m(V_{dqs.} I_{dqs}) \quad (3.30)$$

$$Q_r = \frac{3}{2} I_m(V_{dqr.} I_{dqr}) \quad (3.31)$$

Neglecting the power losses associated with the stator and rotor resistances, the active and reactive stator powers are:

$$P_s = \frac{3}{2}(V_{ds} I_{ds} + V_{qs} I_{qs}) \quad (3.32)$$

$$Q_s = \frac{3}{2}(V_{qs} I_{ds} - V_{ds} I_{qs}) \quad (3.33)$$

And the active and reactive rotor powers are given by

$$P_r = \frac{3}{2}(V_{dr} I_{dr} + V_{qr} I_{qr} \quad (3.34)$$

$$Q_r = \frac{3}{2}(V_{qr} I_{dr} - V_{dr} I_{qr}) \quad (3.35)$$

3.2.4 The Simplified model of DFIG

The rotor side converter is controlled in synchronously rotating d-q axis frame with d-axis oriented along the stator flux vector position so to achieve decoupled control of stator active and reactive power. The stator voltage in DFIG, which is a variable-speed constant-frequency generator, remains constant. Moreover, the three phase sinusoidal voltage is transformed into d-q synchronous reference frame. This gives the relation as shown in equation bellow's. Model can be simplified by neglecting stator resistance

and keeping stator flux constant as the stator is connected to the grid [11]. The phase difference between stator flux and stator voltage is just 90 degree. In the stator-flux oriented reference frame, the *d*-axis is aligned with the stator flux linkage vector ψs, namely, $\psi ds = \psi s$ and $\psi qs = 0$.

$$V_{ds} = 0 = L_s I_{qs} + L_m I_{dr} \quad (3.36)$$

$$V_{qs} = V_s = \omega_s \psi_s \quad (3.37)$$

$$\psi_s = L_s I_{ds} + L_m I_{dr} \quad (3.38)$$

Then the stator d-q current in terms of rotor current can be calculated as follow

$$I_{ds} = \frac{\psi_s}{L_s} - \frac{L_m}{L_r} I_{dr} \quad (3.39)$$

$$I_{qs} = -\frac{L_m}{L_s} I_{qr} \quad (3.40)$$

Since $\psi_s = \frac{V_{qs}}{\omega_s} = \frac{V_s}{\omega_s}$ from the above equation, d-axis stator current further expressed as

$$I_{ds} = \frac{V_s}{\omega_s L_s} - \frac{L_m}{Ls} Idr \quad (3.41)$$

From equation (3.39) and (3.40), d-q rotor current in terms of stator current also be calculated.

$$I_{dr} = \frac{V_s}{\omega_s L_m} - \frac{L_s}{L_m} I_{ds} \quad (3.42)$$

Stator power as function of stator voltage and current at synchronously rotating reference frame

$$(P_s = f(V_s, I_s) = Q_s) \quad (3.43)$$

$$P_s = \frac{3}{2} V_s I_{qs} \quad (3.44)$$

$$Q_s = \frac{3}{2} V_s I_{ds} \quad (3.45)$$

Replacing the stator currents by their expressions given in (3.40) and (3.41), the equations below are expressed:

$$P_s \& Q_s = f(V_s, I_r) \quad (3.46)$$

$$P_s = -\frac{3}{2}\frac{L_m}{L_s} V_s I_{qr} \quad (3.47)$$

$$Q_s = \frac{3}{2} V_s \left(\frac{\varphi_s}{L_s} - \frac{L_m}{L_r} I_{dr}\right) = \frac{3}{2} V_s \left(\frac{V_s}{\omega_s L_s} - \frac{L_m}{L_s} I_{dr}\right) \quad (3.48)$$

Simplified DFIG electromagnetic torque expressed as

$$\boldsymbol{T_e = \frac{3}{2}\frac{p}{2}\frac{L_m}{L_r} \varphi_{ds} I_{qr} = \frac{3}{2}\frac{p}{2}\frac{L_s}{L_r}\frac{V_s}{\omega_s} I_{qs}} \quad (3.49)$$

In order for the rotor mmf to be in synchronism with the stator mmf, the frequency of the rotor current, ω*rf*, must satisfy the slip frequency constraint.

For any induction machine, cage or doubly fed type, the steady state frequency of the rotor currents and voltages will be the slip frequency. Therefore

$\omega_{\text{mech}} = \omega_{\text{syn}} - \omega_{\text{slip}} = \omega_{\text{syn}} - 2\pi f_r$ or $\omega_{fr} = \omega_s - \omega_r = g\omega_s$

In equation above, $\boldsymbol{\omega}_{\text{mech}}$ is the rotor rotational speed $\boldsymbol{\omega}_{\text{syn}}$ is the synchronous speed and f_r is the electrical frequency of the rotor currents and voltages. Here it can be clearly seen that, since the synchronous speed is fixed by the grid, the rotational speed can be controlled directly by using the rotor side converter to force the rotor currents to a desired frequency.

Rotor voltages can be expressed by:

$$V_{dr} = R_r I_{dr} + \sigma L_r \frac{dI_{dr}}{dt} - g\omega_s \sigma I_{qr} \tag{3.50}$$

$$V_{qr} = R_r I_{qr} + \sigma L_r \frac{dI_{qr}}{dt} + g\omega_s \sigma I_{dr} + g\frac{L_m V_s}{L_s} \tag{3.51}$$

Finally, the stator power as function of both stator voltage, rotor current and voltage also described by the following equation (i.e. Ps &Qs =*f* (vs, vr, ir))

$$P_s = -\frac{3}{2}\frac{L_m}{L_s} V_s \frac{(V_{qr} - g\, L_m/L_s V_s - g\omega_s (L_r - \llbracket L_m \rrbracket\, \hat{}2\,)/L_s) I_{dr}}{\left(L_r - \frac{L_m^2}{L_s}\right)\boldsymbol{s} + \boldsymbol{R_r}} \tag{3.52}$$

$$Q_s = -\frac{3}{2}\frac{L_m}{L_s} V_s + \frac{V_s^2}{L_s \omega_s}\left(\frac{g\omega_s \left(L_r - \frac{L_m^2}{L_s}\right) I_{qr} + V_{dr}}{\left(L_r - \frac{L_m^2}{L_s}\right)\boldsymbol{s} + \boldsymbol{R_r}}\right) \tag{3.53}$$

The DFIG dynamic torque equation

$$T_t = j\frac{d\Omega_r}{dt} + B\Omega_r + T_{em} \tag{3.54}$$

$$T_{em} = \frac{3}{2}\frac{L_s}{L_r}\frac{L_m}{\omega_s} I_{qs} = -\frac{3}{2}\frac{L_m}{L_r}\frac{Vs}{\omega s} I_{qr} \tag{3.55}$$

Then, total torque

$$T_t = (J_s + B)\Omega_r - \frac{3}{2}\frac{Lm}{Lr}\frac{Vs}{\omega s} I_{qr} \tag{3.56}$$

From the equation rotor speed can be calculated as

$$\boldsymbol{\Omega_r} = \frac{\boldsymbol{T_t} + \frac{3}{2}\frac{\boldsymbol{L_m}}{\boldsymbol{Lr}}\frac{\boldsymbol{V_s}}{\boldsymbol{\omega_s}} \boldsymbol{I_{qr}}}{(J_s + B)} \tag{3.57}$$

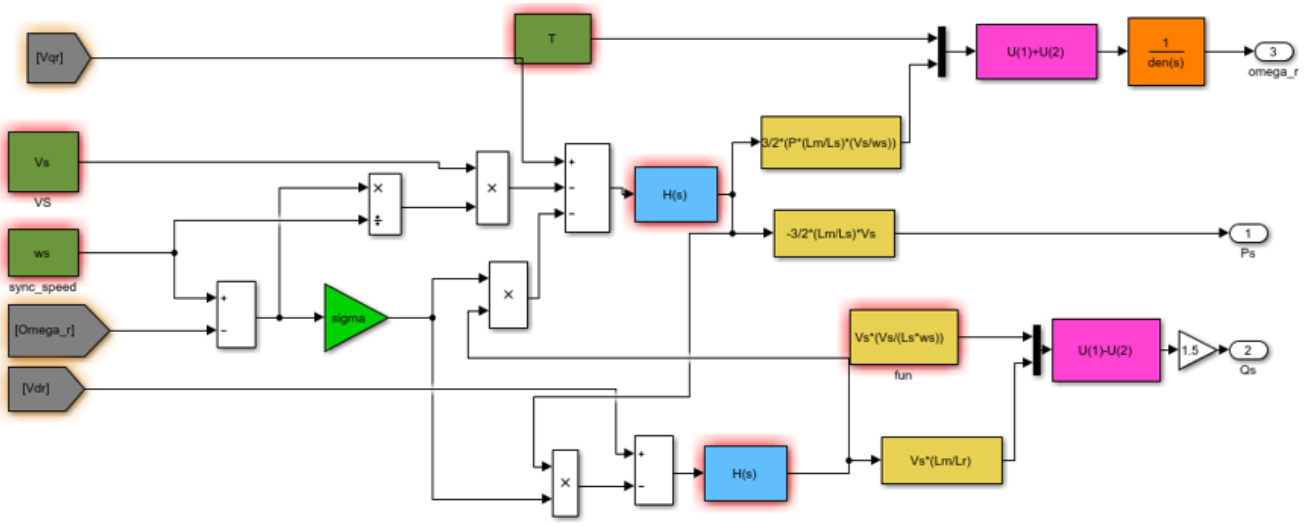

Fig. 3.3, Model of double fed induction generator

Where, **Ωr** is rotor speed, V is the voltage, I is the current, R is the resistance; subscripts r and s stand for stator and rotor, respectively and the subscripts d and q for direct and quadrature axis, respectively.

$\sigma = (L_r - \frac{{L_m}^2}{L_s})$,

g=*slip*

$L_s = L_{ls} + L_m$

$L_r = L_{lr} + L_m$

L_{ls}, $L_{lr}$and $L_m$are the stator leakage, rotor leakage and mutual inductances, respectively and B is viscous friction, j is inertia and $\boldsymbol{\Omega_r}$is rotor speed

3.3 Grid Side Converter Control

The main aim of grid side converter (GSC) is to maintain constant DC-link voltage across the common coupling between the back to back converters and to maintain the power factor at unity by controlling the reactive power flow injected into the grid. The dc link voltage has to be controlled independently of the direction of the slip power and to maintain a constant value; balance of power is of equal importance between the rotor and the grid side. To achieve this, vector control method is implemented in the grid side by decoupling of dq axis currents. Power flow is adjusted using the phase shift angle among the difference of the input voltage and source voltage. The regulation of the PWM converter is based on the current flowing through it. The direct axis current is used to regulate the DC-link voltage and to regulate the reactive power quadrature axis current is used. The basic of the vector control is d-q theory or reference frame theory which is used to overcome the problem of time varying parameters with the AC machines, essentially by transforming the stator variables to a synchronously rotating reference frame fixed in the rotor. With such transformation (Park's transformation) all the time varying inductances that occur due to

an electric circuit in relative motion and electric circuit with varying magnetic reluctances can be eliminated [9] [30] [43].

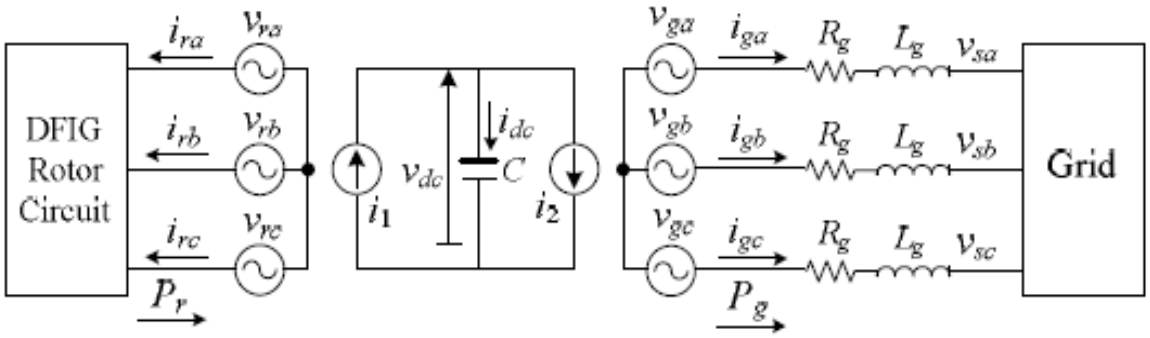

Fig. 3.4, Grid side converter system

The GSC voltages in its d-q reference frame, the components are obtained by the typical configuration of control strategy and the voltage balance across the grid filter is given by based on Kirchhoff's current and voltage laws, the following equation in matrix form can be defined as GSC of DFIG [43] [44].

$$\begin{bmatrix} V_a \\ V_b \\ V_c \end{bmatrix} = \begin{bmatrix} V_{sa} \\ V_{sb} \\ V_{sc} \end{bmatrix} - R^* \begin{bmatrix} I_a \\ I_b \\ I_c \end{bmatrix} - L \frac{d}{dt} \begin{bmatrix} I_a \\ I_b \\ I_c \end{bmatrix}$$

The dynamic model of balanced Grid side converter can be represented by the following equations using synchronous rotating reference frame [16]:

$$\begin{bmatrix} V_{dg} \\ V_{qg} \end{bmatrix} = Rg \begin{bmatrix} I_{dg} \\ I_{qg} \end{bmatrix} + L_g \frac{d}{dt} \begin{bmatrix} I_{dg} \\ I_{qg} \end{bmatrix} + \omega_s L_g \begin{bmatrix} -i_{qg} \\ i_{dg} \end{bmatrix} + \begin{bmatrix} V_{ds} \\ V_{qs} \end{bmatrix} \quad (3.58)$$

Or in linear mathematical equation

$$\begin{aligned} V_{qg} &= R_g I_{qg} + L_g \frac{dI_{qg}}{dt} + \omega_s L_g I_{dg} + V_{qg} \\ V_{dg} &= R_g I_{dg} + L_g \frac{dI_{dg}}{dt} - \omega_s L_g I_{qg} + V_{dg} \end{aligned} \quad (3.59)$$

Under balanced operating condition the three-phase output voltage of grid side converter are identical with magnitude and frequency. in such cases the dq components after the transformation of v_d and v_q are consider as constants values. The q axis component vq is then set as zero when d-axis oriented along output voltage position. It follows as the GSC active and reactive power can be simplified as follow.

$$P = \frac{3}{2}(V_d I_d + V_q I_q) = \frac{3}{2} V_d I_d \quad (3.58)$$

$$Q = \frac{3}{2}(V_d I_q + V_q I_d) = \frac{3}{2} V_d I_q \quad (3.63)$$

Since the GSC balances and delivers the power between three phase GSC and DC-link capacitor. The dc-link power should be equal to the grid side converter output power. it follows the grid side converter active power can be manipulated by d-axis component of line current Id which can be expressed as below.

$$V_{dc}I_{dc} = \frac{3}{2}V_d I_d \tag{3.59}$$

Also, the reactive power in GSC in equation above can be set as an injected reference based on the demand of back to back converter and grid operating condition. In such cases the q-axis component line current I_q will be control. WhereR_g and $L_g$are line resistance and inductance in the GSC; V_a, V_b and V_c are the output voltage of GSC; V_{sa}, V_{sb} and V_{sc} are the IGBT bridge output voltages; I_a, I_b and I_c are the line current of GSC. The grid side converter balance and delivers power between three phase grid and DC-link capacitor. Also, the DC-link voltage needs to be controlled and maintain as constant value under balanced operating conditions [29].

The control of dc link capacitor voltage to be in constant and it supply a source for rotor winding through rotor side converter. The amount of dc voltage stored in capacitor which comes from rectifier or grid side converter. The control of phase angle that triggers the gate of the IGBT through PWM by controlling of the reference input voltage V_abcs. The figure 3.5, illustrates structure of grid side converter block with the derivation of gate signals.

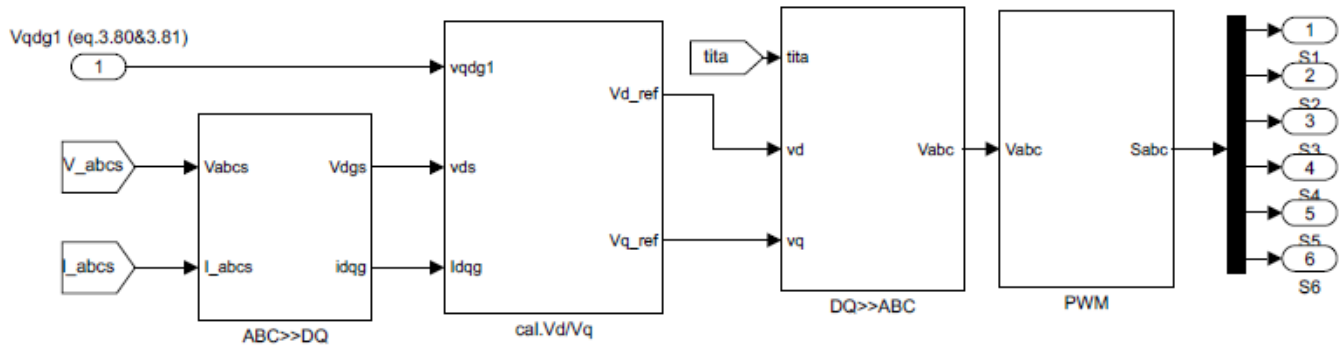

Fig. 3.5, Gate signal generation of grid side converter

3.4 Design of PID controller

The PID controller algorithm that operates as a position algorithm is shown in the following Figure (3.6) Where, *G*(*s*) and *E* (*s*) in 's 'domain denotes the control and error signals of the system are the proportion, integral and derivative gain values. The corresponding PID controller transfer function Gc (*s*) is given as

$$\mathrm{G_c(s)} = \left(K_p + \frac{Ki}{s} + K_d \mathrm{s}\right) E\,(\mathrm{s}) \tag{3.65}$$

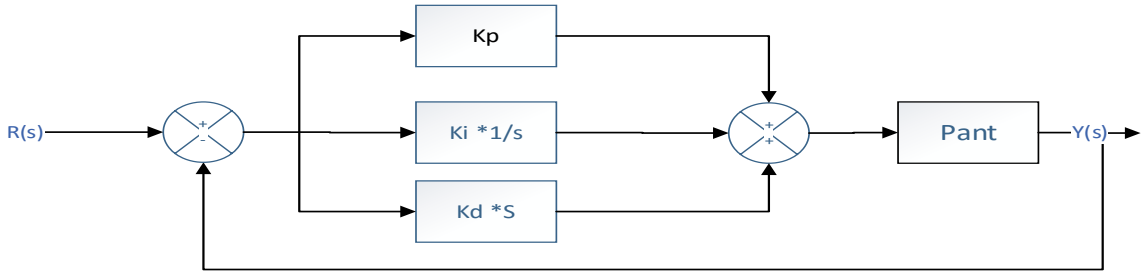

Fig. 3.6, General Block diagram of PID controller

We have a mechanism to continue to discrete that is using bilinear transformation formula which is given with $s = \frac{2}{T_s} * \frac{1- z^{-1}}{1+z^{-1}}$

And from the three commonly used variations of Euler methods which is described in section (2.8) for both integral and derivative terms to discretized the PID controller, using the backward Euler method.

$$G(z) = (K_p + \frac{K_i T_s z}{z-1} + \frac{K_d N(z-1)}{(1+NT_s)z-1})*E(Z)$$

Using tuning mechanism try and error we have the values , k_p= 8.92, $k_i = 15.2$, $k_d = 0.025T_s = 0.01$ *much with the sampling time and filter coefficent* N=120, substitute the value the discrete controller *G (z)* becomes,

$$G(z)=8.92 + \frac{0.152 z}{z-1} + \frac{3(z-1)}{2.2z-1})*E(Z)$$

3.5 Fuzzy controller design

In this study, a Mamdani fuzzy controller was chosen and designed with linguistic term if-then rule. The linguistic variables for the rule base were selected as, positive big (PB), positive medium (PM), positive small (PS), negative big (NB), negative medium (NM), negative small (NS)and zero (Z). As it was defined for the linguistic rule variables, Fig.3-9 shows the if-then rules for the five membership functions selected for each of the input error (E) and the change of error (ΔE). For the two inputs, only forty-nine possible rules are possible based on (7x7) = 49 if - then combinations.

In a fuzzy logic controller design, the following basic assumptions are considered [45]; the plant is observable and controllable, the controller will be designed within an acceptable range of precision and problems of optimality and stability are not addressable explicitly, etc.

Generally, in fuzzy controller design, the rule base is constructed from a priori knowledge from the following sources.

1. The physical law that governs the system dynamics

2. Data from existing (PID) controller

3. Expert knowledge about the plant

The expert knowledge about the system is obtained as follows

From the general conventional control, the error is given by e(t)=r(t)−c(t), and assuming a constant set point one can arrive at $\frac{de(t)}{dt} = -\frac{dC(t)}{dt}$

Where r(t) =reference/ desired output signal

e(t) = error signal

c(t)= actual output signal

e(t)= negative, Means the DFIG output power is greater than the reference power so that the DFIG needs to decrease its output.

e(t)= positive, Means the DFIG output power is less than the reference power so that the DFIG needs to increase output power until it reaches the desired value or until error is zero.

$\frac{dC(t)}{dt}$ = negative, means power is decreasing this implies $\frac{de(t)}{dt}$ = positive. Therefore, a positive change in the error rate indicates the power is decreasing.

$\frac{dC(t)}{dt}$ = positive, means output power is increasing this means $\frac{de(t)}{dt}$ = negative. Therefore, a negative change in the error rate indicates the power is increasing

For design the inference system, first we defined on E in the domain of e linguistic variables and defined on the EC in the domain of 'ec' linguistic variables. Set the deviation *'e'* basic domain in {-3, 3}, error change rate '*ec*' basic domain in {-2,2}, kp basic domain {-0.3,0.3}, ki basic domain {-0.05,0.05}and kd basic domain {-0.1,0.1}.

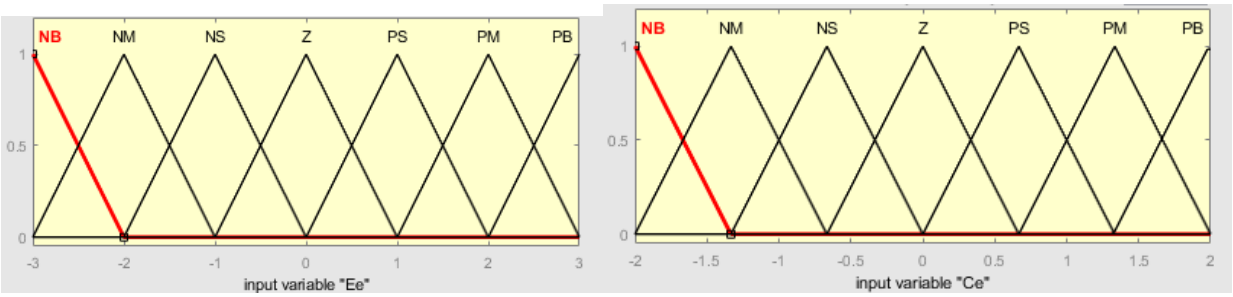

Fig. 3.7, Triangular membership functions for inputs; error and change in error

The typical FIS inputs are the signals of error E and change of error CE in DFIG power. The FIS output is the control action inferred from the fuzzy rules. The configuration of FIS for our fuzzy controller is given in the following figure 3.8.

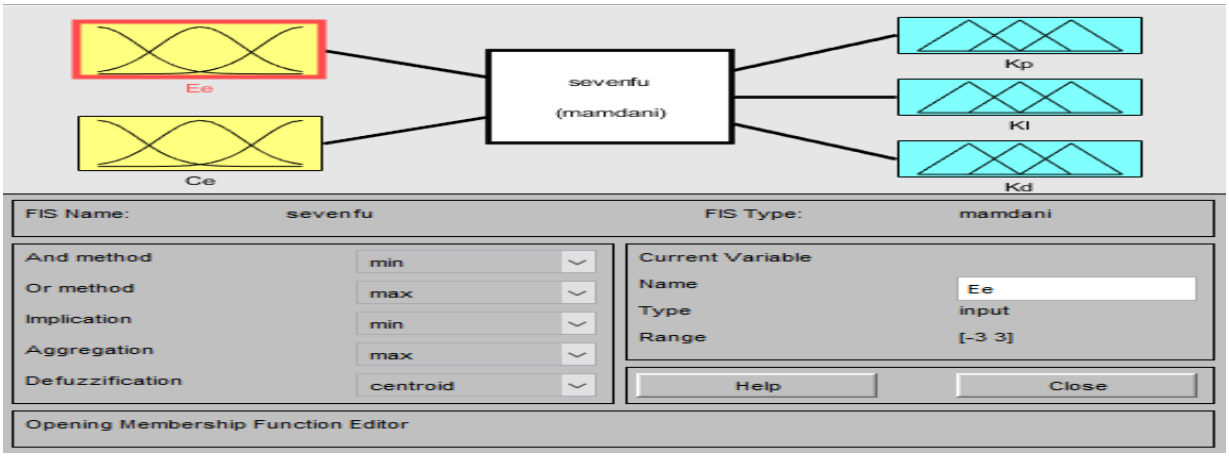

Fig. 3.8, Fuzzy inference block

Fuzzy inference system (FIS) consists of a number of if-then rules. These rules are based on the linguistic variables. The inference system uses error and rate of change of error for seven linguistic variables in the relation as follow.

Example: if error is NL AND rate of change of error PS then the control signal U is NM

	E							
ΔE		NL	NM	NS	ZE	PS	PM	PL
	NL	NL	NL	NL	NL	NM	NS	NL
	NM	NL	NL	NL	NM	NS	ZE	NM
	NS	NL	NL	NM	NS	ZE	PS	NS
	ZE	NL	NM	NS	ZE	PS	PM	ZE
	PS	NM	NS	ZE	PS	PM	PL	PS
	PM	NS	ZE	PS	PM	PL	PL	PM
	PL	ZE	PS	PM	PL	PL	PL	PL

Table 3-1Table of fuzzy rule base

The Centroid method is used to convert from the inference mechanism into the crisp values applied to the actual system. In the design inference system, as defined on E in the domain of e linguistic variables and defined on the EC in the domain of ‘ec’ linguistic variables and also U (kp, ki and kd) is output variable which set the deviation kp basic domain {-8,8}, ki basic domain {-5,5}and kd basic domain {-3,3}. The

Figures 3.9(a), (b) and 3.10 are shows output defuzzification membership functions for kp ,ki and kd respectively .

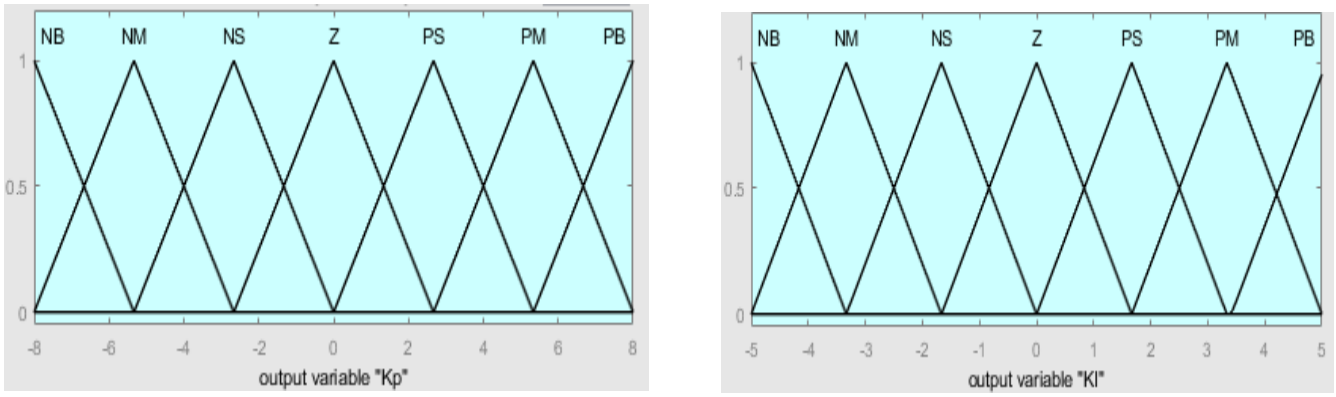

a b

Fig. 3.9, (a), Output membership function of Kp (b), Output membership function of Ki

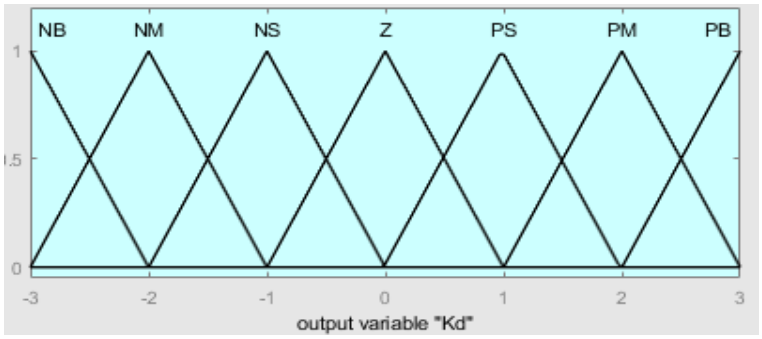

Fig. 3.10, Output membership function of Kd

In fig 3.11, the linguistic values found in the top row represents the premises for the input error e, the linguistic values in the left-most column represents the input premises change in error rate ce, and the linguistic values representing the consequents u (which is PID parameters kp, ki and kd), for each of the 49 rules are found in the intersection of the rows and columns of the appropriate premises.

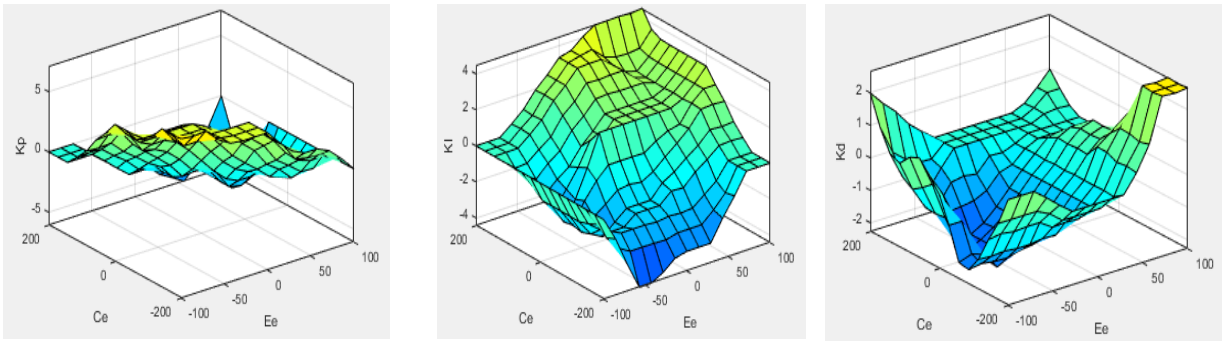

(a) (b) (c)

Fig. 3.11, Surface viewers of kp, ki and kd

3.6 Fuzzy-PID control Design

A fuzzy PID controller is a controller which is based on fuzzy logic with conventional PID controller structure. This fuzzy logic controller deals with many valued logic and reasoning instead of fixed and exact values that has the truth function varying from one point to another point as discussed in section (3.5). This very helpful in controlling the systems specially if the exact model of the system is not available.

Atypical structure of fuzzy logic controller, Mamdani type controller is used, which has two inputs namely," error" and "*change of* error "and single output. Input and output contain seven triangular membership functions. These seven membership functions are labeled as, *NL, NM, NS, Z, PS, PM, PL* which are same for inputs and output variables. The ranges for these inputs are dependent on the system and input value. The error input is nothing but difference between calculated power and set point power, and change of error is nothing but the difference between current power and previous power. To make the fuzzy logic controller function as a PID controller the following structure in figure (3.12) is adopted. The designing structure of fuzzy PID controller a set of membership functions has to be designed and tuned to control the system, and associated set of rules are generated to govern the membership function of the input output relationship.

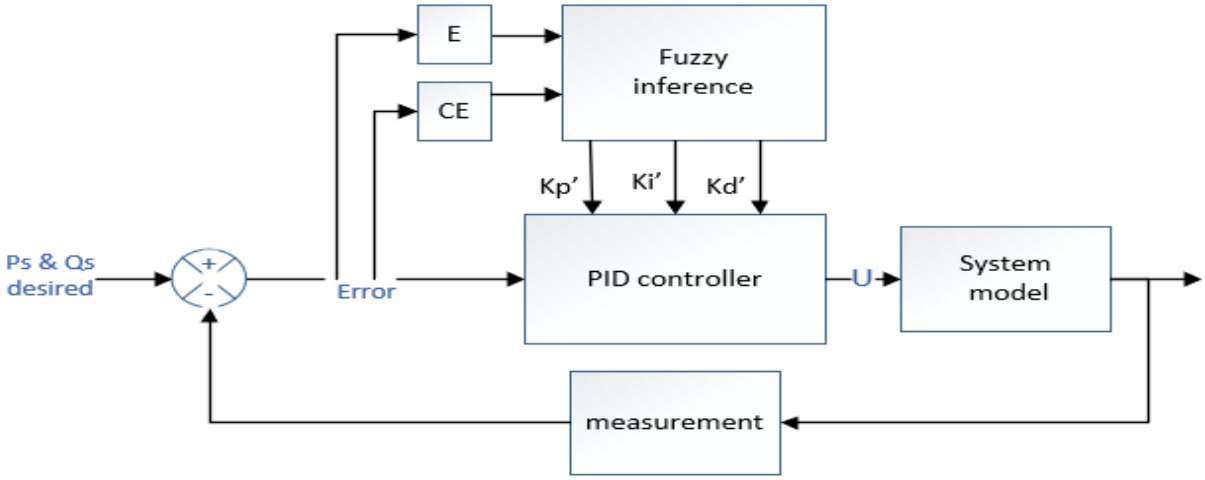

Fig. 3.12Structure of fuzzy PID controller with system model

The mathematical equation of the parameters of PID controller that is online tuned described as:

$$Kp=K_p{}' + K_P o$$
$$Ki=K_i{}' + K_i o \quad \textbf{(3.66)}$$
$$Kd=K_d{}' + K_d o$$

Where K_p', $K_i'$and $K_d'$are outputs of fuzzy logic controller based on the above figure expression. $K_P o, K_i o$ and $K_d o$ are the initial set value of the PID controller. Then also Kp, Ki and Kp are parameters of PID that will be tuned to provide online and self-tuned values in different situation of system variable.

The rules of fuzzy PID control are based on the control of people with long-term understanding of the theory lessons and learned technically artificial. Fuzzy self-tuning PID parameters rule [27]:

- When error is large, should take larger kp and smaller kd in order to speed up the response of the system, and take a smaller ki in order to avoid a greater overshoot restrict the integral action.
- When error is medium, in order to make the system has a smaller overshoot, kp should be made smaller. At this point, kd has greater impact on the system, should get smaller, ki values should be appropriate; □
- When error is small, to make the system has good stability, should take a larger kp and ki, kd should be appropriate in order to avoid oscillation occurs near the equilibrium point.

According to the above rules may draw the following 49 fuzzy relations. The rule tables for PID parameters are shown in Table 3.2 a, b and c respectively.

E	CE						
	NB	NM	NS	Z	PS	PM	PB
NB	PB	PB	PM	PM	PS	Z	Z
NM	PB	PM	PM	PS	Z	Z	PS
NS	PM	PM	PM	PS	Z	NS	NS
Z	PM	PM	PM	Z	NS	NS	NS
PS	PS	PS	Z	NS	NS	NS	NM
PM	PS	Z	NS	NS	NM	NS	NB
PB	Z	Z	Z	Z	Z	NM	Z

a)

E	CE						
	NB	NM	NS	Z	PS	PM	PB
NB	Z	Z	Z	Z	Z	Z	Z
NM	NB	NS	NM	NS	Z	Z	NM
NS	NB	NS	NS	PS	Z	PS	PS
Z	NM	NS	NS	Z	PS	PM	PM
PS	NM	NS	Z	PS	PS	PM	PB
PM	Z	Z	PS	PS	PS	PS	PB
PB	Z	Z	PS	PM	PM	PM	PB

b)

E	CE						
	NB	NM	NS	Z	PS	PM	PB
NB	PS	NS	NB	Z	PS	Z	PM
NM	PS	NS	NB	NB	NM	PS	NB
NS	Z	NS	NM	NM	NM	Z	Z
Z	Z	NS	NS	NS	NS	Z	Z
PS	Z	Z	Z	Z	Z	Z	Z
PM	PB	PB	PS	PS	Z	Z	Z
PB	PB	PB	PS	Z	Z	Z	PS

c)

Table 3-2Rule table for, a). Kp, b). Ki , c) .Kd

3.7 Design of the RSC Controller

The system controller is designed to control the active and reactive power with terminal voltage and frequency to maintain a constant value such that the wind turbine DFIG system can be modeled as a variable wind speed. To achieve this issue, the rotor-side controller the d-axis of the rotating reference frame used for d-q transformation is aligned with air-gap flux in voltage-oriented control schemes. The actual electrical output power, measured at the grid terminals of the wind turbine is compared with the reference power obtained from the tracking characteristic. A Proportional-Integral - Derivative (PID) and F_PID regulator is used to reduce the power error to zero. The output of this regulator is used for rotor current Idqr reference which compared with the currents that is injected to rotor winding from rotor side converter. Iqr is the current component that produces the electromagnetic torque Tem and active power and Iqr component also produces reactive power. The output of this current controller is taken as the voltage Vqr and Vdr generated by rotor side controller. The current regulator is assisted by feed forward terms which predict the d-axis and q-axis of the rotor voltage Vr.

Let's rewrite equation 3.50 And equation 3.51 as follow;

$$V_{dr} = R_r I_{dr} + \sigma L_r \frac{dI_{dr}}{dt} - Vdr'' \tag{3.67}$$

$$V_{qr} = R_r I_{qr} + \sigma L_r \frac{dI_{qr}}{dt} + Vqr'' \tag{3.68}$$

Where, $Vdr'' = g\omega_s \sigma I_{qr}$ and

$$Vqr'' = g\omega_s \sigma I_{dr} + g\frac{L_m V_s}{L_s}$$

The rotor side voltage converter control changes the magnitude and angle of applied rotor voltage. The rotor side converter control schemes consist of two cascaded control loops. The inner current control loops regulate independently the d-axis and q-axis rotor current component, i_{dr} and i_{qr}, according to synchronously rotating reference frame. The stator-flux oriented reference frame is the most commonly used for control of stator active and reactive control. In the stator-flux oriented reference frame, the d-axis is aligned with the stator flux linkage vector. Equation (3.47) and (3.48) indicates that *Ps* and *Qs* can be controlled independently by regulating the rotor current components; i_{qr} and i_{dr} respectively.

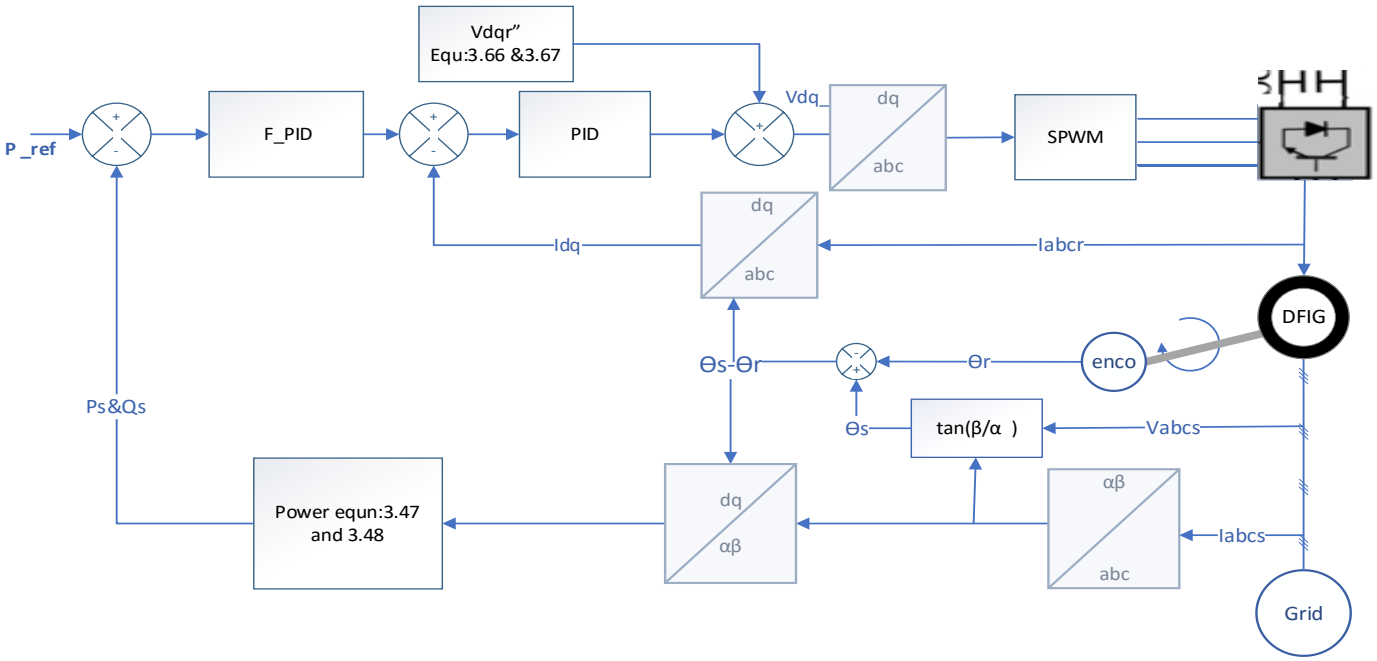

Fig. 3.13, Proposed control scheme of rotor side converter

As shown above figure 3.13, the actual value of active and reactive power compared with the respective reference power then the error signal given as an input to the F_PID controller. Consequently, the reference value of idr and iqr which determined from the output of power control loops compared with the actual currents and minimized the error by controller. Finally, the outputs of current controller used as input for mathematical model of double fed induction generator.

3.7.1 Design of the Current Control Loops

Let;

$$V_{dr\prime} = R_r I_{dr} + \sigma L_r \frac{dI_{dr}}{dt} \quad (3.69)$$

$$V_{qr\prime} = R_r I_{qr} + \sigma L_r \frac{dIqr}{dt} \quad (3.70)$$

Equation (3.66) and (3.67), it can be written as matrix form

$$\frac{d}{dt}\begin{bmatrix} I_{dr} \\ I_{qr} \end{bmatrix} = -\frac{R_r}{\sigma L r_r}\begin{bmatrix} 1 & 0 \\ 0 & 1 \end{bmatrix} \times \begin{bmatrix} I_{dr} \\ I_{qr} \end{bmatrix} + \begin{bmatrix} V_{dr\prime} \\ V_{qr\prime} \end{bmatrix} \quad (3.71)$$

Equation (3.68) indicates that $i_{dr}$and i_{qr}respond to $v_{dr\prime}$ and $v_{qr\prime}$ respectively, through first order transfer function. It is therefore possible to design the following feedback loops with PID controller.

$$\boldsymbol{V_{qr\prime} = (K_p + \frac{k_i}{s}) * (i_{qr} * - i_{qr})} \quad (3.72)$$

$$\mathbf{V_{dr\prime} = (K_p + \frac{k_i}{s})*(i_{dr}*-i_{dr})} \quad (3.73)$$

For the design current controller, it is necessary to know a closed loop transfer function of independent dq axis currents separately. so, the d-axis current control closed loop transfer function from equation (3.50) will be:

$$\frac{idr}{vdr + gwsσiqr} = \frac{1}{Ls + Rr} \tag{3.74}$$

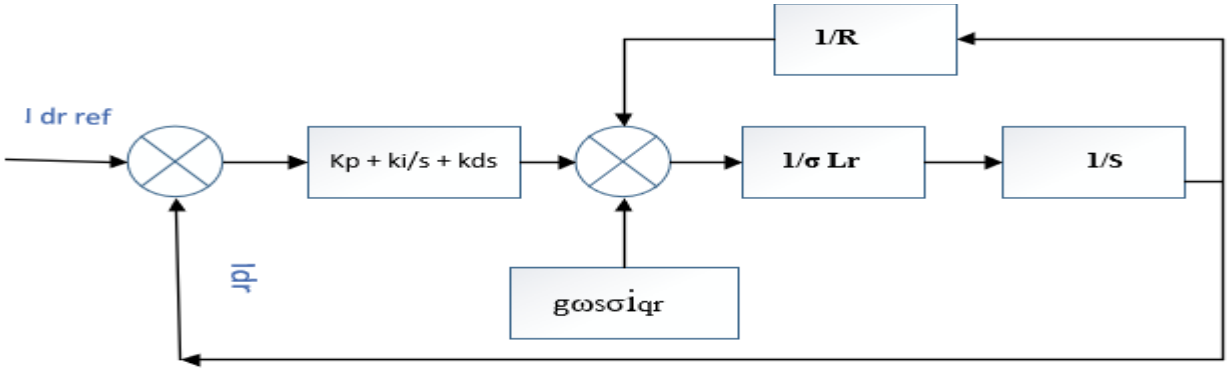

Fig. 3.14, The closed loop transfer function with PID controller of q- axis

The q-axis closed loop current control transfer function from equation (3.51) can be:

$$\frac{iqr}{vqr + gwsσidr - g\,{}^{Lm}/_{Ls}\,Vs} = \frac{1}{Ls + Rr} \tag{3.75}$$

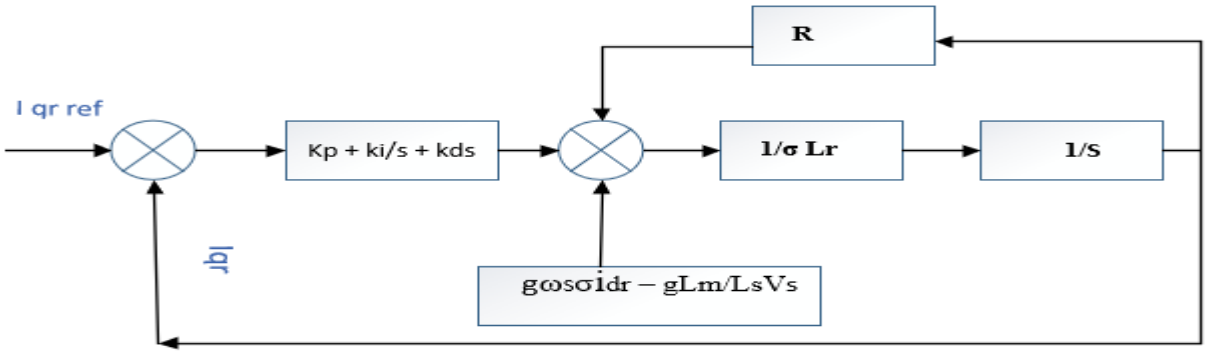

Fig. 3.15, The closed loop transfer function with PID controller of d- axis

Then equation (3.50) and (3.51) can rewritten as

$$V_{dr} = V_{dr'} - g\omega_s\sigma I_{qr} \tag{3.76}$$

$$V_{qr} = V_{qr'} - g\omega_s\sigma I_{dr} + g\frac{L_m V_s}{L_s} \tag{3.77}$$

3.8 Design of GSC with controllers

The main objective of grid side converter is to maintain dc -link voltage constant with various schemes, voltage oriented control techniques is approached to solve this issue. This is based on transformation

between the abc stationary reference frame and synchronous frame. The control algorithm is implemented in the grid voltage synchronous frame where all the variables are DC components in steady state.

The design of grid side controller has two cascade control loops, inner control loop and outer control loops. The outer loops regulate the dc link voltage and reactive power exchange between grid side converter and the grid. Inner control loop regulates independently the d-axis and quadrature axis of grid side converter AC side current components I_{dg} and I_{qg} in the synchronously rotating reference frame

From the above Figs, the ac-side circuit equations of the GSC can be written as

$$\frac{d}{dt}(I_{abcg}) = \frac{R_g}{L_g} I_{abc} + \frac{V_{abcg} - V_{abcs}}{L_g} \quad (3.78)$$

Applying the synchronously rotating reference frame transformation for equation (3.60) and (3.61) with the *d*-axis aligned to the grid voltage vector *vs* (*vs* = *vds*, *vqs*= 0), the following *d-q* vector representation can be obtained for modeling the GSC ac-side and applying the Laplace transforms to the above two equations:

$$V_{qg} = R_g I_{qg} + g L_g I_{qg} + \omega_s L_g I_{dg} + V_q \quad (3.79)$$

$$V_{dg} = R_g I_{dg} + g L_g I_{dg} - \omega_s L_g I_{qg} + V_d \quad (3.80)$$

V_{dg} And V_{qg} can be obtained by the feedback loop and controller output, lets say

$$V_{qg1} = (k_{pg} + \frac{k_{ig}}{s} + s k_{dg})(I_{qg}^* - I_{qg}) \quad (3.81)$$

$$V_{dg1} = (k_{pg} + \frac{k_{ig}}{s} + s k_{dg})(I_{dg}^* - I_{dg}) \quad (3.82)$$

Substituting (3.81), (3.82) in (3.79), (3.80) respectively, and being vq(s) =0, the reference for the voltage's values v_{qg} and v_{dg} can be obtained or written by:

$$V_{qg} = V_{qg1} + \omega s L g I dg \quad (3.83)$$

$$V_{dg} = V_{dg1} - \omega s L g I qg + Vs \quad (3.84)$$

The reactive power exchange between grid side converter and grid is given by

$$Q_g = \frac{3}{2} V_{ds} . I_{qg} = \frac{3}{2} V_s I_{qg} \quad (3.85)$$

The angular position of the supply voltage is calculated as [21].

$$\theta e = \int \omega s dt = \tan^{-1} \frac{v\beta}{v\alpha} \quad (3.86)$$

And also, we can write in terms of α and β of stationary reference frame with the stator and mutual inductance of machine parameters.

$$\theta e = \tan^{-1} \frac{L_s i_{\beta s} + L_m i_{\beta r}}{L_s i_{as} + L_m i_{ar}} \quad (3.87)$$

Where V_α and V_β are the, β (stationary 2-axis) stator voltage components, or by applying phase locked loop (PLL) system which used for determine grid frequency and phase angle.

As shown figure 3.17, the F_PID controller controls the outer control loops which controls dc link voltage and reactive power of the system. Actual value of dc link voltage measured from parallel of capacitor and compared with desired dc link voltage, the error between the two dc-link voltage minimized by fuzzy PID controller. In this case fuzzy logic controller used as to tune the parameter gain of PID controller which described in detail in section 3.6. PID control which controls the error between measured Iqg and reference iqg current. The outputs of dc link controller acts as reference idg current component's and compare with desired stator d-axis current. The last outputs of two controller are added with their respective equation 3.80 and 3.81to give value of v_{qg} and v_{dg}. The value of v_{qg} and v_{dg} voltages converted into v_abc using inverse park transformation and are considered to be the reference input values to the PWM converter by which level of DC voltage and required power factor is achieved.

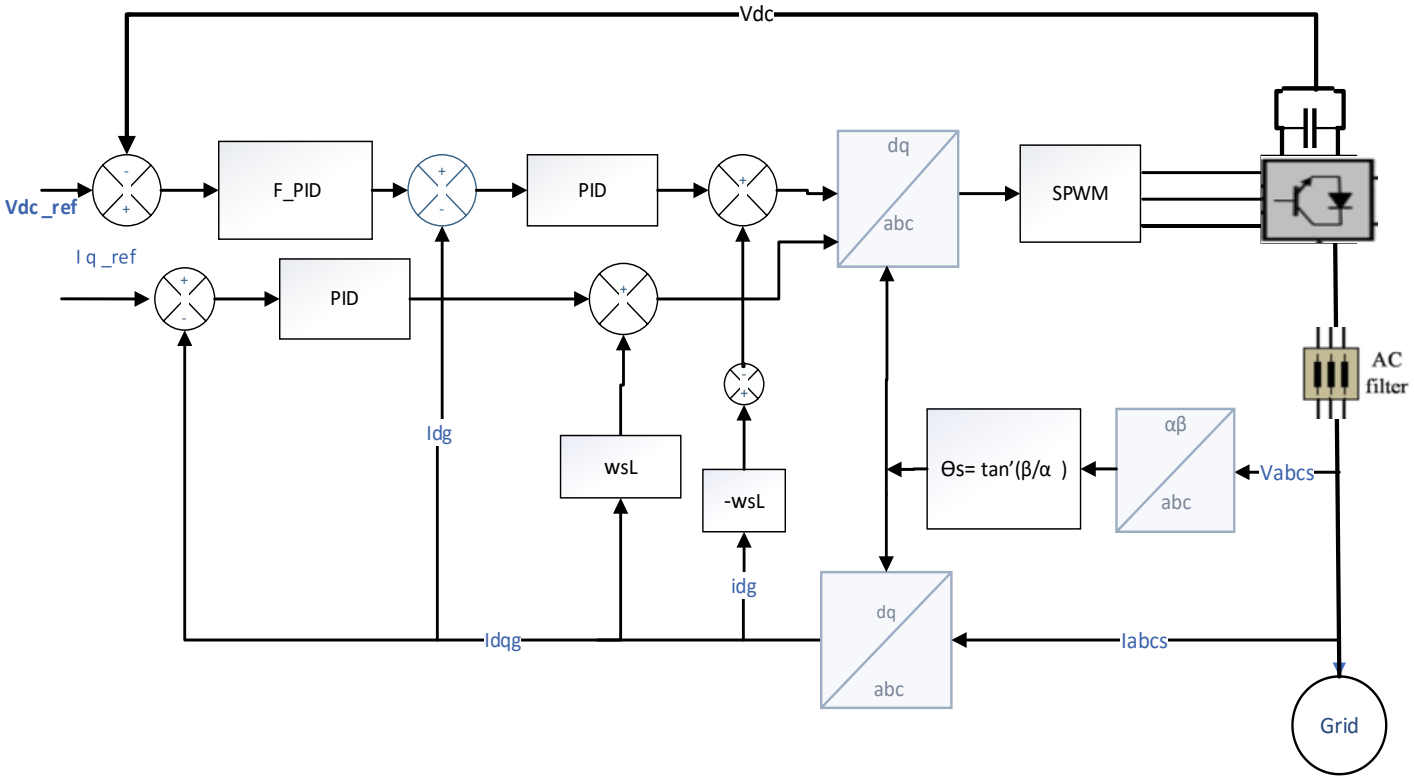

Fig. 3.16, Proposed grid side converter control block

CHAPTER FOUR

4 Result and Discussion

This section presents the simulation results of the designed controller system and discussion on the result obtained from MATLAB/SIMULINK simulation. The objective of this work was control of active and reactive power flow for wind speed variation and comparative analysis of fuzzy PID and conventional PID controller. For comparation, the desired and actual power for both controllers is plotted on same scale and on the time domain specification. The MATLAB/Simulink model for both controllers PID and FPID is shown in the figure (4.1).

4.1 MATLAB SIMULINK model

The active and reactive power control for double field induction generator was modeled, deigned and analyzed in the mathematical model and simscape section of this thesis. It is concerned with the simulation results of the closed loop control of the system using Fuzzy-PID and PID with MATLAB/SIMULINK. The simulation is analyzed by step response and wind speed variation of the closed loop system using dq model. The overall system simulation block includes different sub-functional blocks: fuzzy-PID controller, PID controller, different transformation, and DFIG model are the main sub-functional blocks.

The controllers are designed for 4KW DFIG with its parameter given in a table (4-1). As shown figure (4.1) reference power (active and reactive), DC motor acts as variable turbine speed, are inputs to the system and stator current, rotor current, active power, reactive power and electromagnetic torque are outputs of the system. The three input (Ps_ref, Qs_ref and speed) and output (Ps, Qs) of the DFIG model are given as input to controllers and two outputs from outer power controller are rotor current reference to inner current controller and also the output of the inner controller which is Vdr'and vqr' are used to calculate the reference rotor voltage. Those voltages are an input to the double fed induction generator mathematical system model.

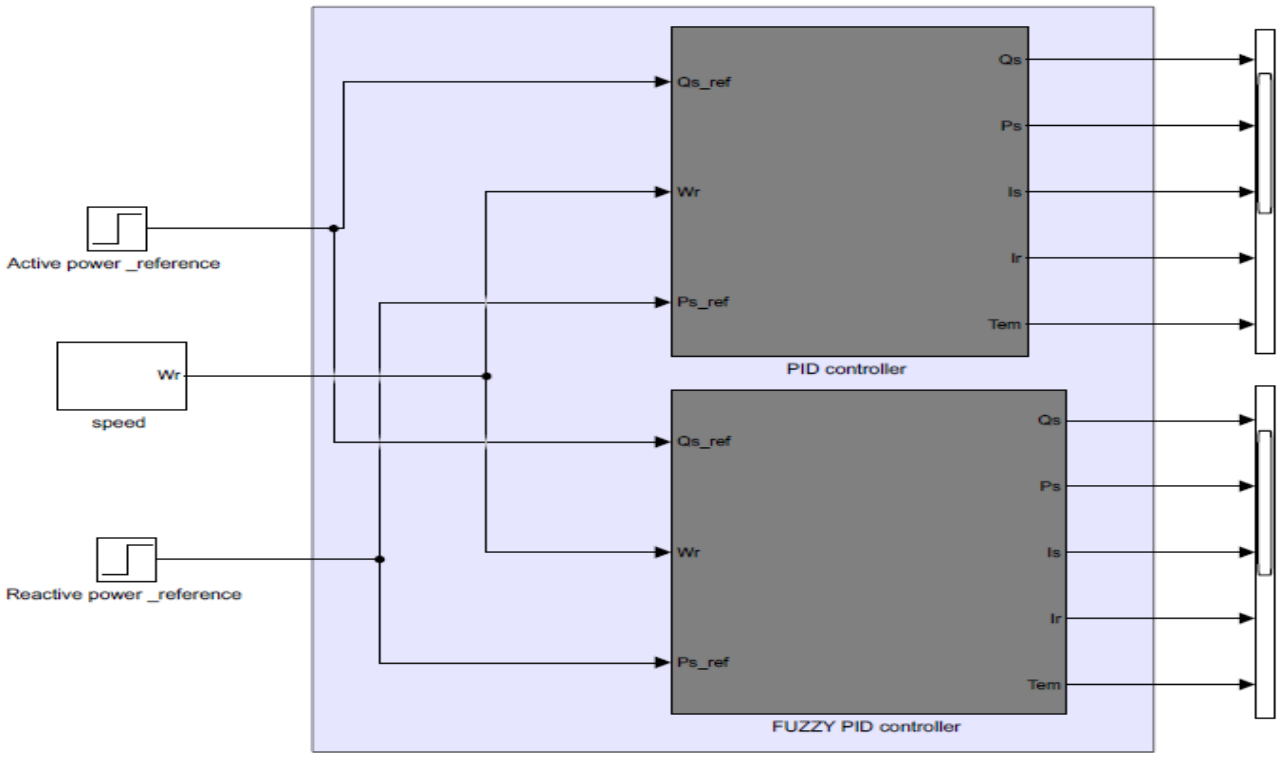

Fig. 4.1,Overall system MATLAB block of DFIG model with both Fuzzy -PID and PID

Two different cases are considered in the simulation study to show the effectiveness of the proposed control strategy for the same wind speed and reference input. First, simulation performed using transfer function or modeled equation in (3.45) and (3.46) which illustrates briefly in figure 4.16 and figure 4.20. Secondly, simulation study is performed by considering using MATLAB/ Simscape shown in figure (4.27) to identify which one is more approaches to reality. For both controllers PID and Fuzzy-PID used for extract the maximum power from variable wind speed at sub- synchronous generator speed.

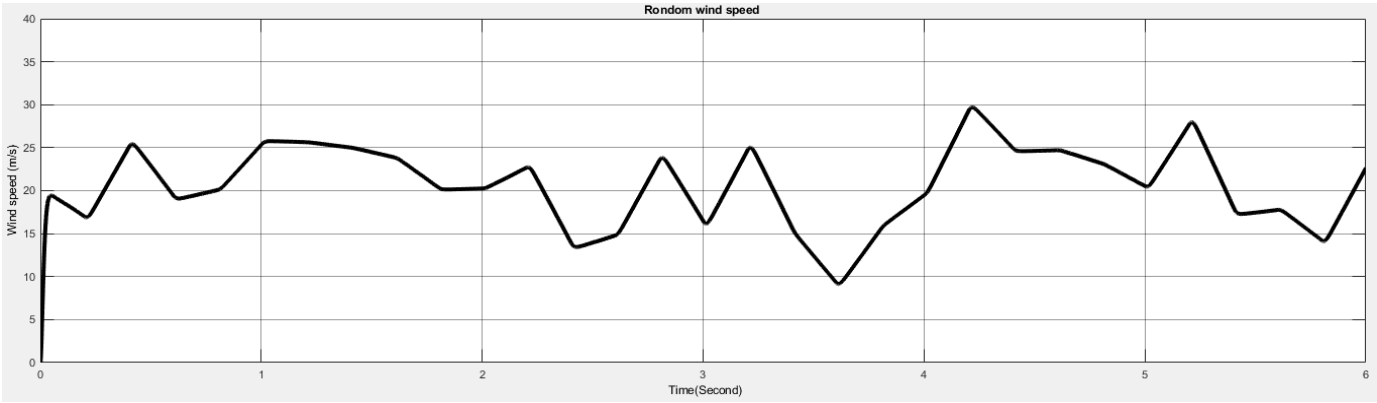

Fig. 4.2, Wind speed profile

A wind speed in reality, it is seasonal and has intermittent property. The wave form of wind speed depends on the topography, different country has different average wind speed annually. The simulation for the proposed system is effective as well as implemented in reality we have used a wind which are varies from time to time as shown in figure (4.2). The wind speed source used for modeled double fed induction generator MATLAB/Simulink simulation block and which is designed by DC motor prime mover as turbine speed variation of wind energy conversion system. The speed values vary randomly for this simulation for 6 seconds. The simulation result shown from figure 4.3 to figure 4.6, the values which varies with respect to wind speed variation.

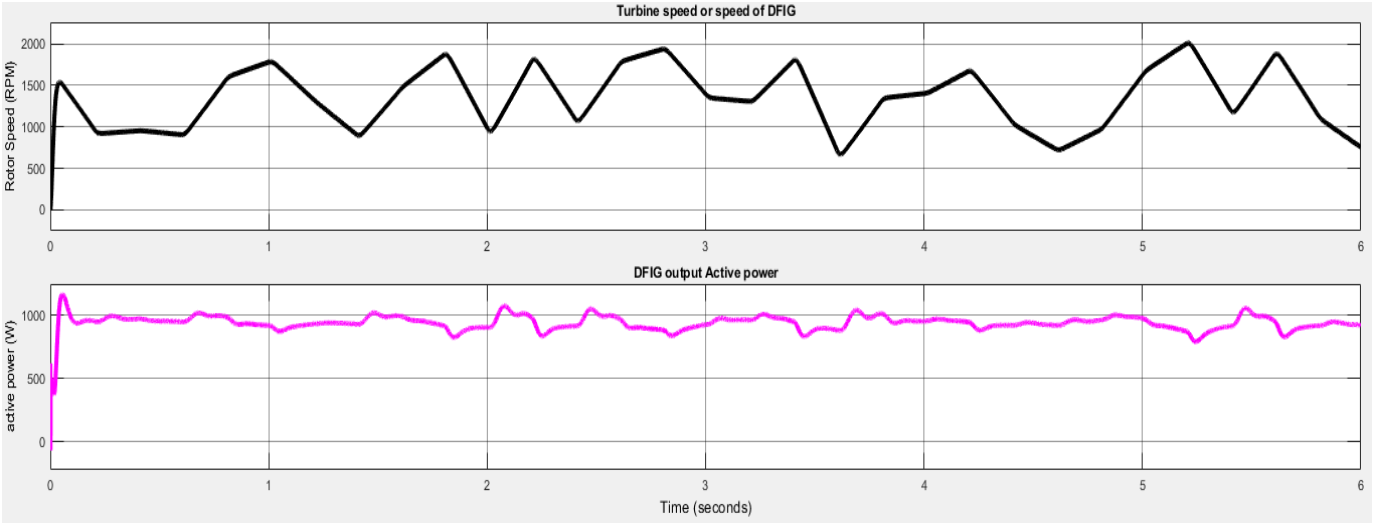

Fig. 4.3,Wind speed with active power without controller

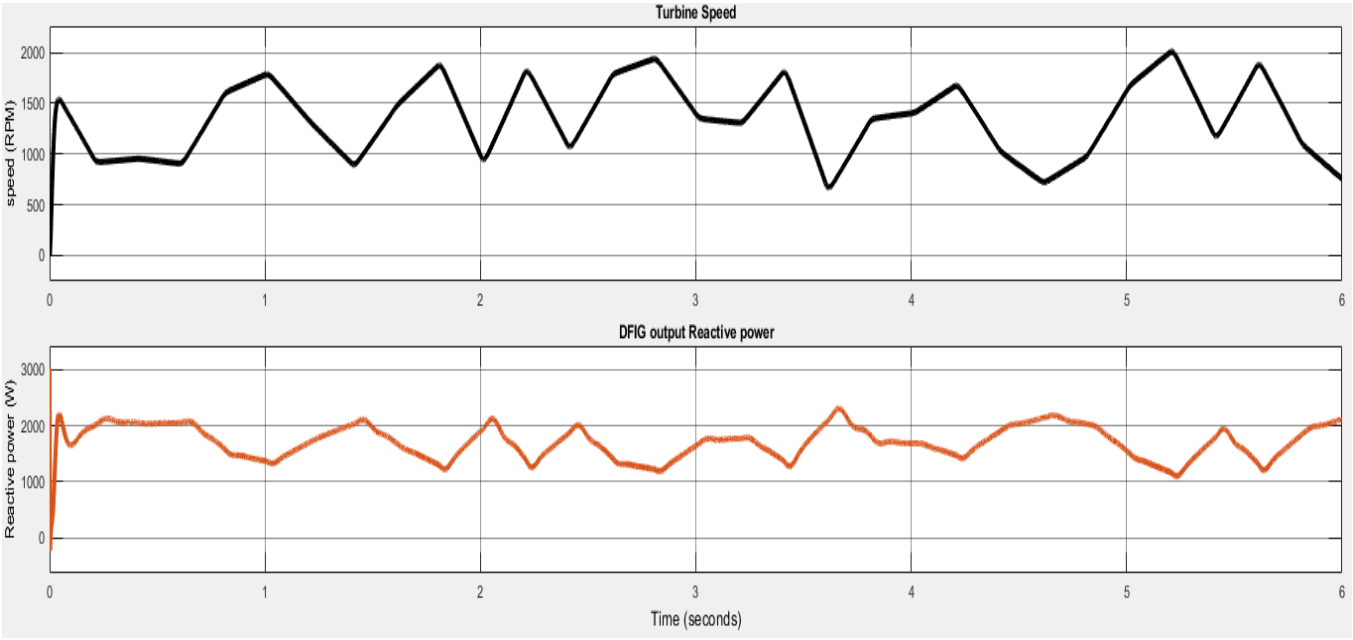

Fig. 4.4,Reactive power without controller

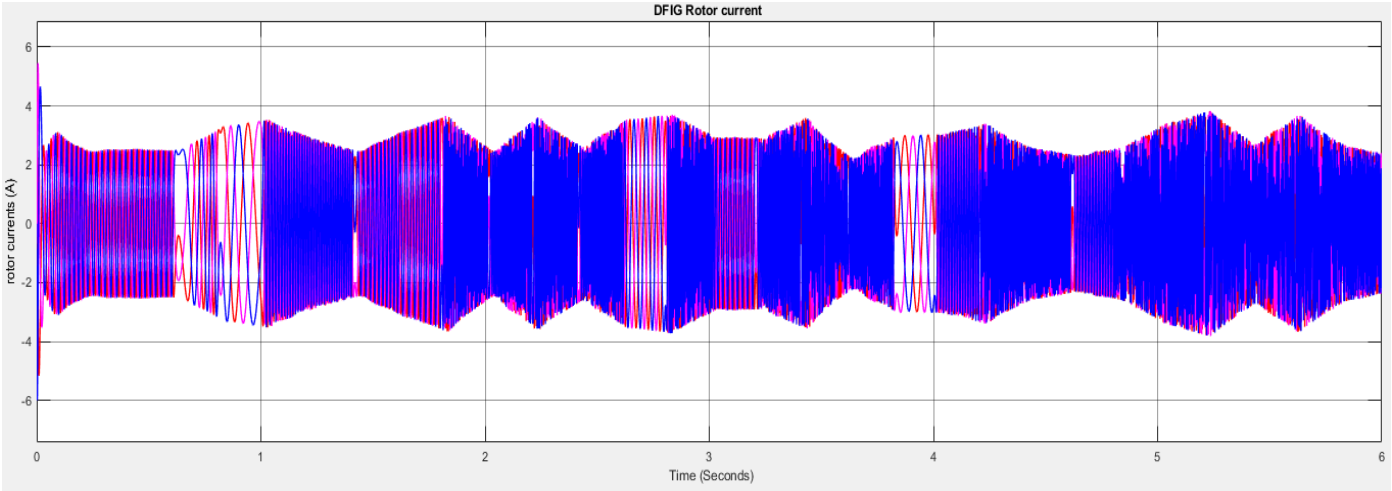

Fig. 4.5,Stator current terminal with varying wind speed

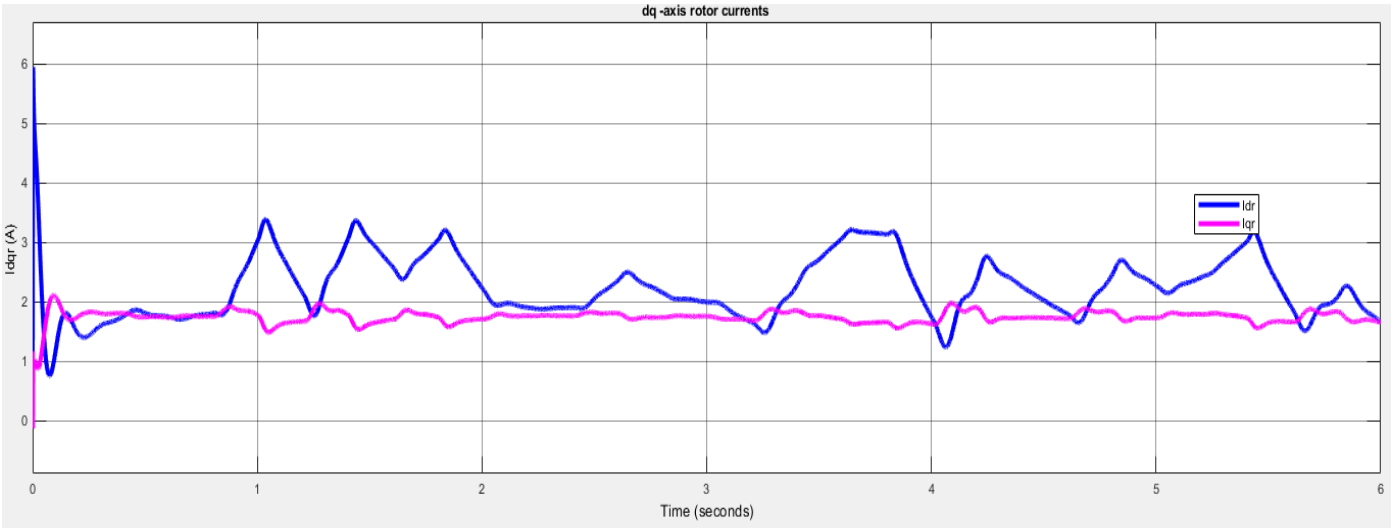

Fig. 4.6, Dq rotor currents without controller

To illustrate the simulations and controller performance clearly, the variation of wind speed that used to for turbine input as shown in the figure (4.2) replaced by steps input. This speed value from 0 sec up to 2 sec is 17 m/sec, 2sec up to 4 sec is12 m/sec and 4sec up to 6sec is 30 m/sec. The result shown in figure (4.8) is dc motor output speed in revolution per minute (RPM)which used as prime mover (turbine with gearbox) or generator rotor speed attached to the shaft.

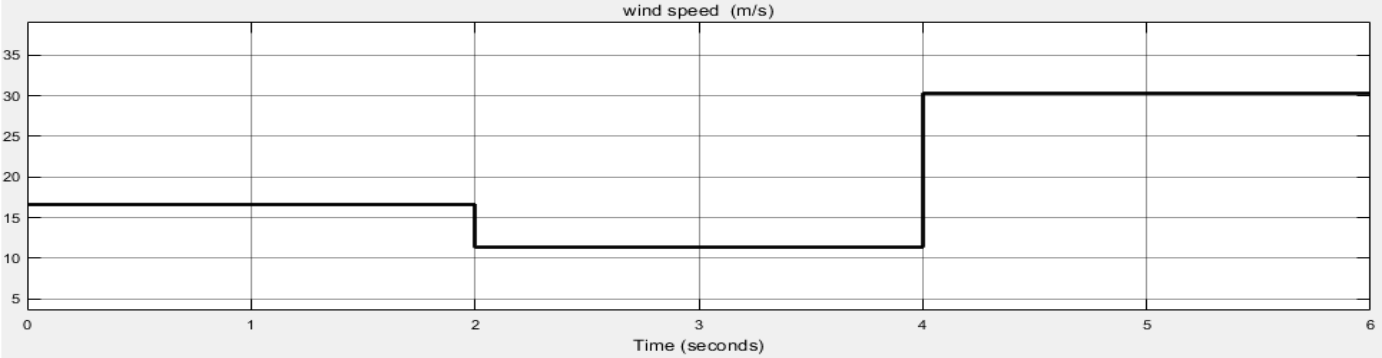

Fig. 4.7,Wind speed (m/s)

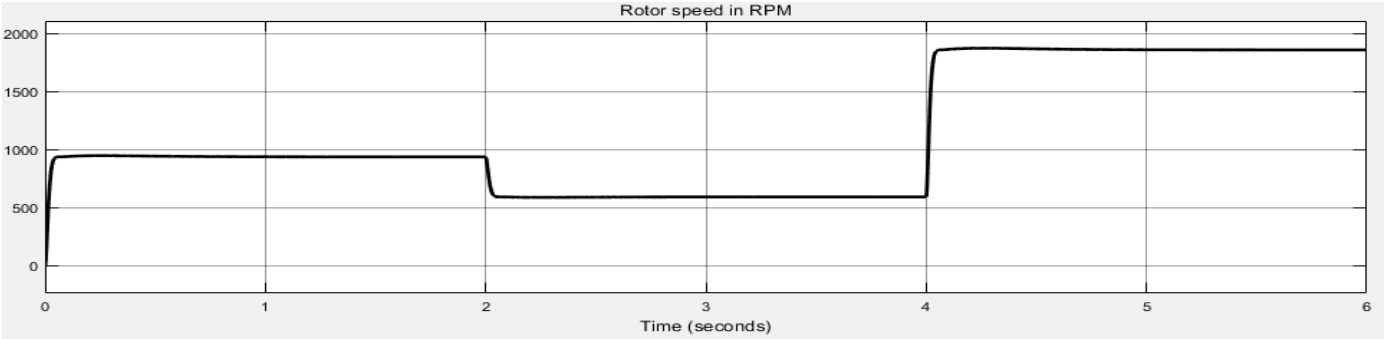

Fig. 4.8,Wind turbine speed in RPM

The power generated by a wind turbine depends on wind speed based on double fed induction generator as shown figure 4.9, the speed of the wind an input to the turbine using gearbox and speed up the wind speed and connected to the shaft of the generator. The model responded as expected form theory of wind variation with power. Increase the power production as speed of rotor or turbine increase and decrease output power as wind speed decrease. But the controller adjusts the output to become constant maximum value by controlling rotor current from Vdc source via rotor side converter. As shown figure 4.9 the relation of power and speed; the wind from zero to 2 sec speed, power starting with some overshoot is constant, 2 to 4 sec wind speed is decreasing and the power is decreasing and wind speed from 4 sec up to 6 sec is increasing and power also increases

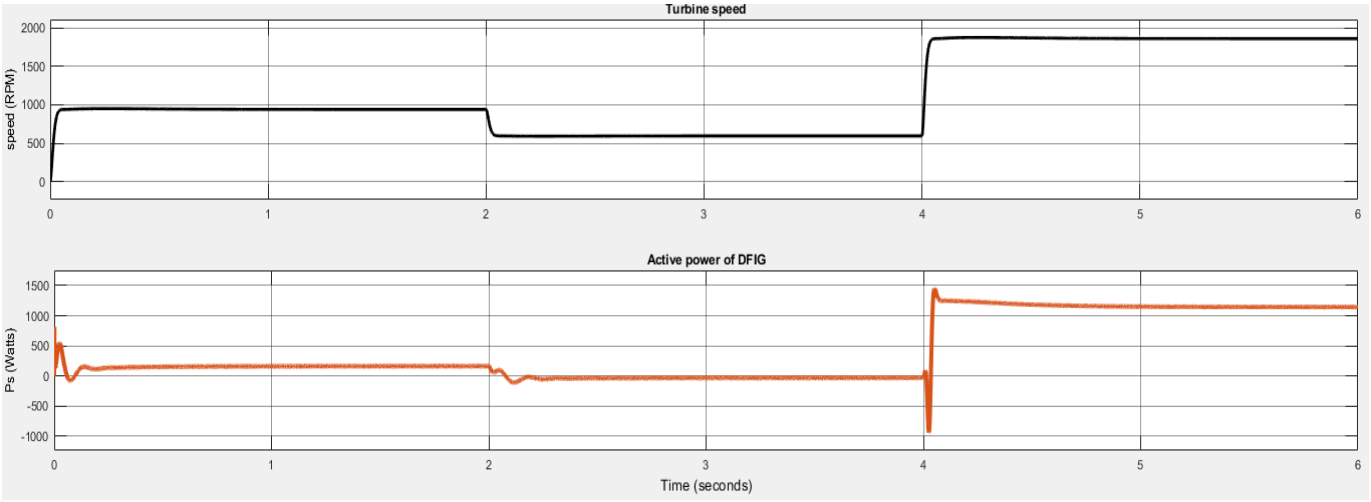

Fig. 4.9,Variation of Active power response with turbine speed

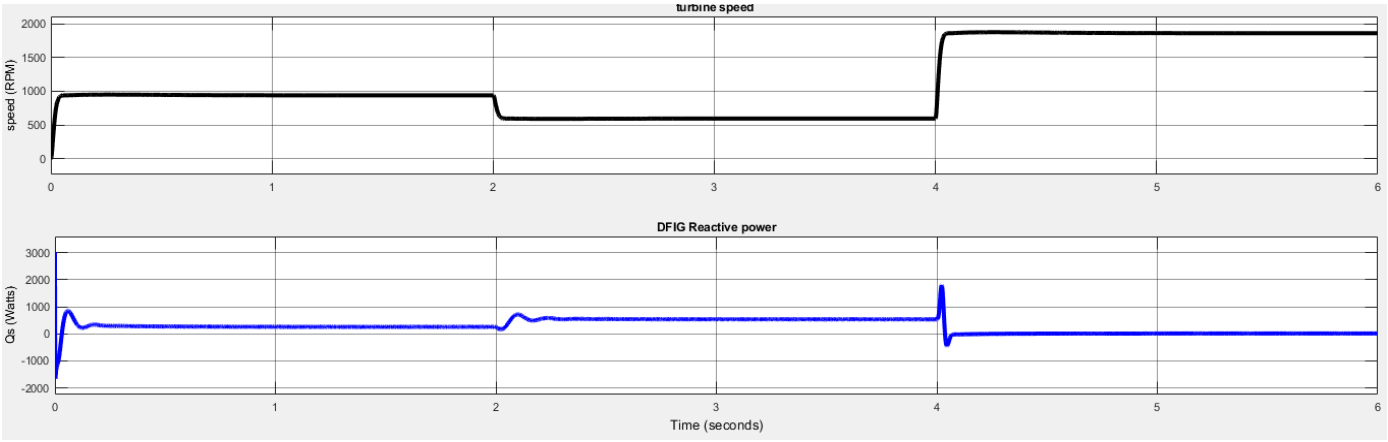

Fig. 4.10,Variation of Reactive power response with turbine speed

The simulation results in figure 4.10 shows that variation reactive power with speed of wind. when speed of the wind increases, the reactive power as function of d_axis rotor current as shown in equation 3.48 decreases because of the injected magnetizing rotor current decreases.

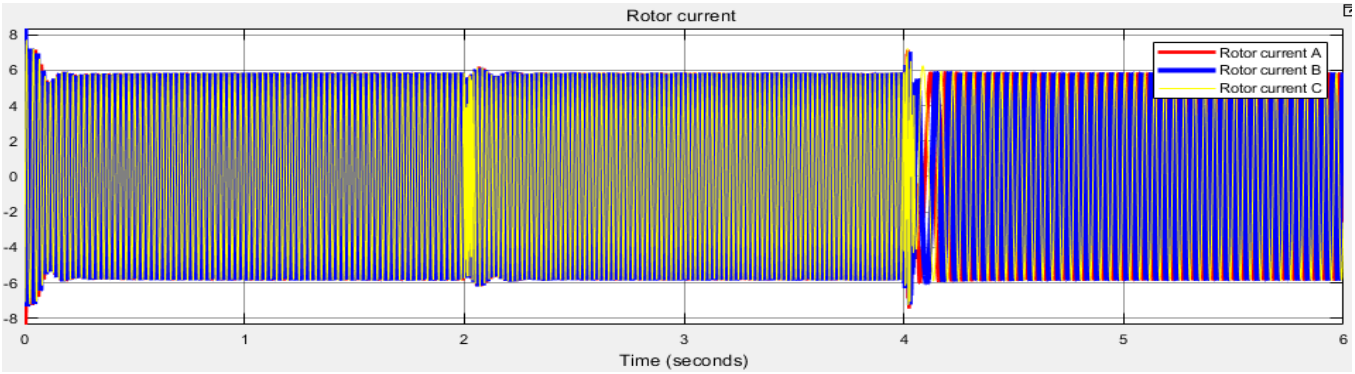

Fig. 4.11, three phase rotor currents in (A)

Rotor currents excited by rotor side converter from DC link voltage to a double fed induction generator based on speed variation as shown below figure (4.11). The rotor current feds to machine depends on slip speed of the generator which generates constant frequency and voltages at the stator terminal. As shown figure below uncontrolled rotor currents with its frequency are varies when speed deflects its value. And, figure (4.12) shows zoom out rotor current response.

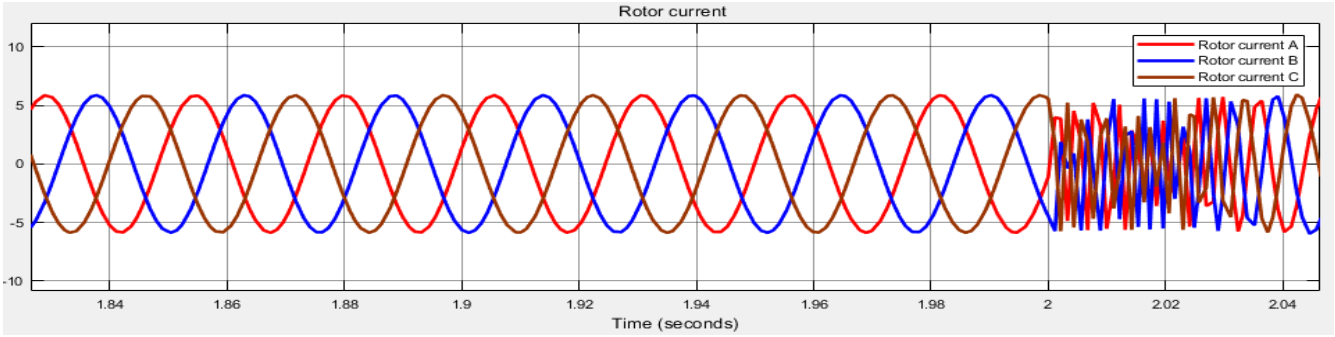

Fig. 4.12, Zoom out rotor current response

Figure 4.13 shown, the generated stator current depends on the variation of turbine speed. The magnitude of currents generated at stator terminal throughout simulation time are the same except at the deflection point of wind speed.

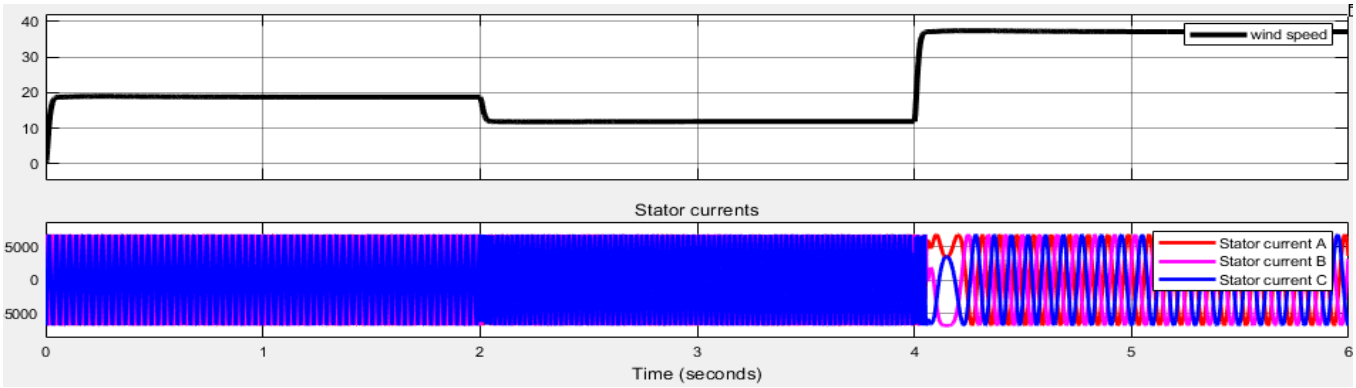

Fig. 4.13, three phase stator current response with wind speed variation (A)

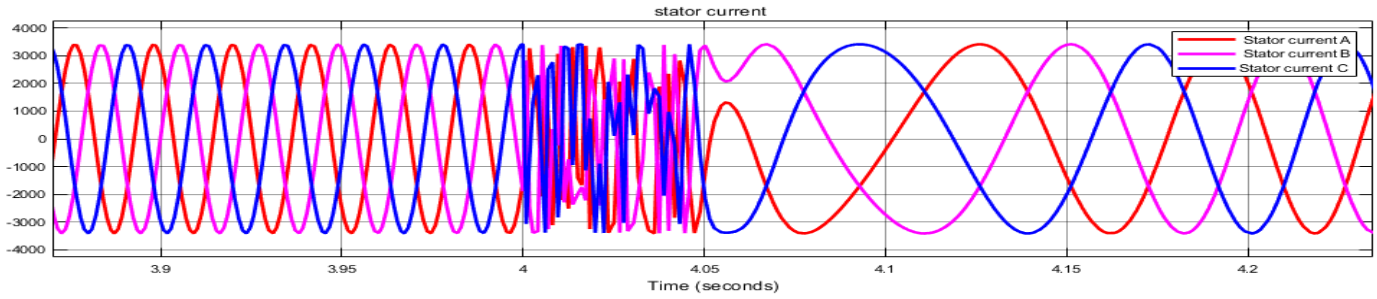

Fig. 4.14, Zoom out stator current response

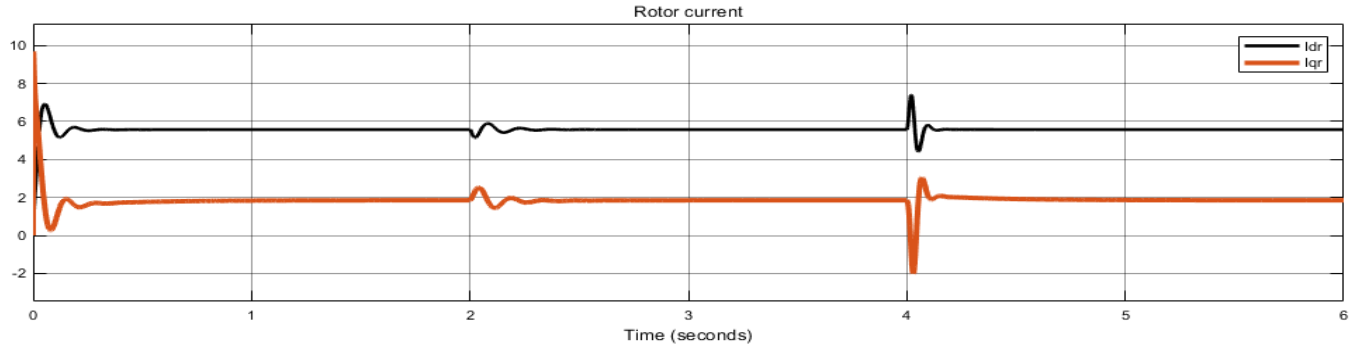

Fig. 4.15, dq rotor currents

Due to the relationship between stator current and rotor current which is generated and fed within system, the power can be easily controlled using rotor dq current. The park transformation as discussed in sections (2.4); rotor currents obtained from MATLAB/Simulink simulation response converted into d- axis and quadrature axis using park transformation. As shown figure (4.15) there is variation of dq value due wind speed changes its value. This dq currents are used to control the generated active and reactive power of double fed induction generator.

4.2 Simulation of DFIG model with PID controller

Power converter are usually controlled utilizing current of rotor control techniques which allow the decoupled control of both active and reactive power flow to the grid. In this investigation, the dynamic DFIG performance is presented for balanced and normal grid conditions. The MATLAB/Simulink block figure (4.16) show's roto side converter PID control of generator power. The reference input power (Ps_ref and Qs_ref) which compares with actual value of double fed induction generator and then the error minimizes by the conventional PID controller.

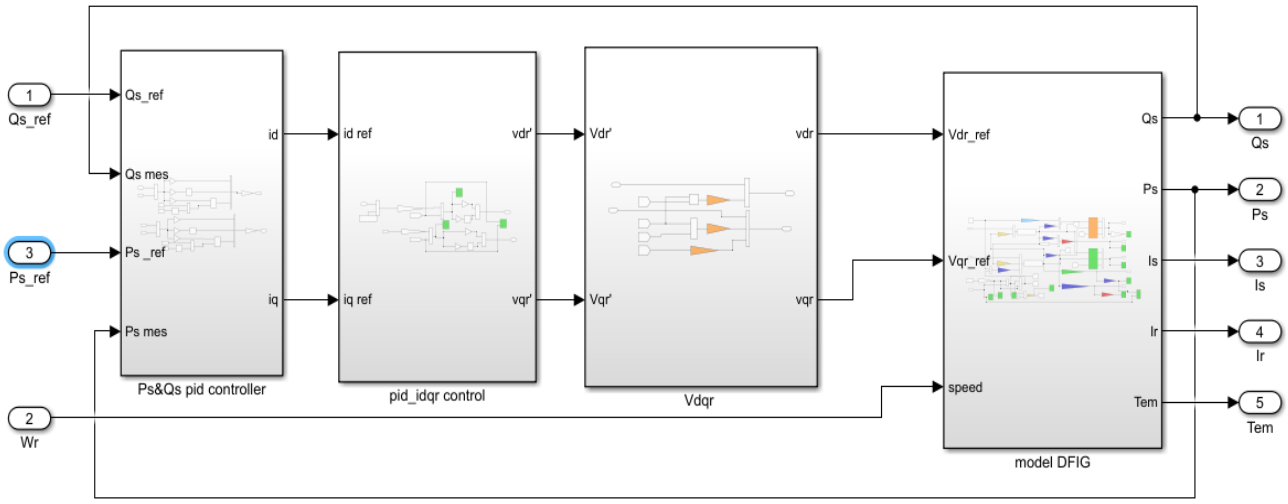

Fig. 4.16, MATLAB/Simulink block of DFIG model with PID controller

This block diagram one sub part of power control of modeled double fed induction generator with conventional PID controller as shown from overall block diagram in figure 4.1. It has two controllers which is inner and outer controller, the outer controller controls the power and gives signal as input to inner controller which acts as reverence currents. The inner controller controls the current by comparing the actual rotor currents and reference currents which takes from the output of outer controller. To achieve a better efficiency of the proposed scheme and to convince the robustness of the system, the parameters of the controllers were adjusted as follows;

PID parameters	Kp	Ki	Kd
Active power	0.012	12.021	0.0012
Reactive power	0.289	30.205	0.0036

Table 4-1:tuned PID controller parameters

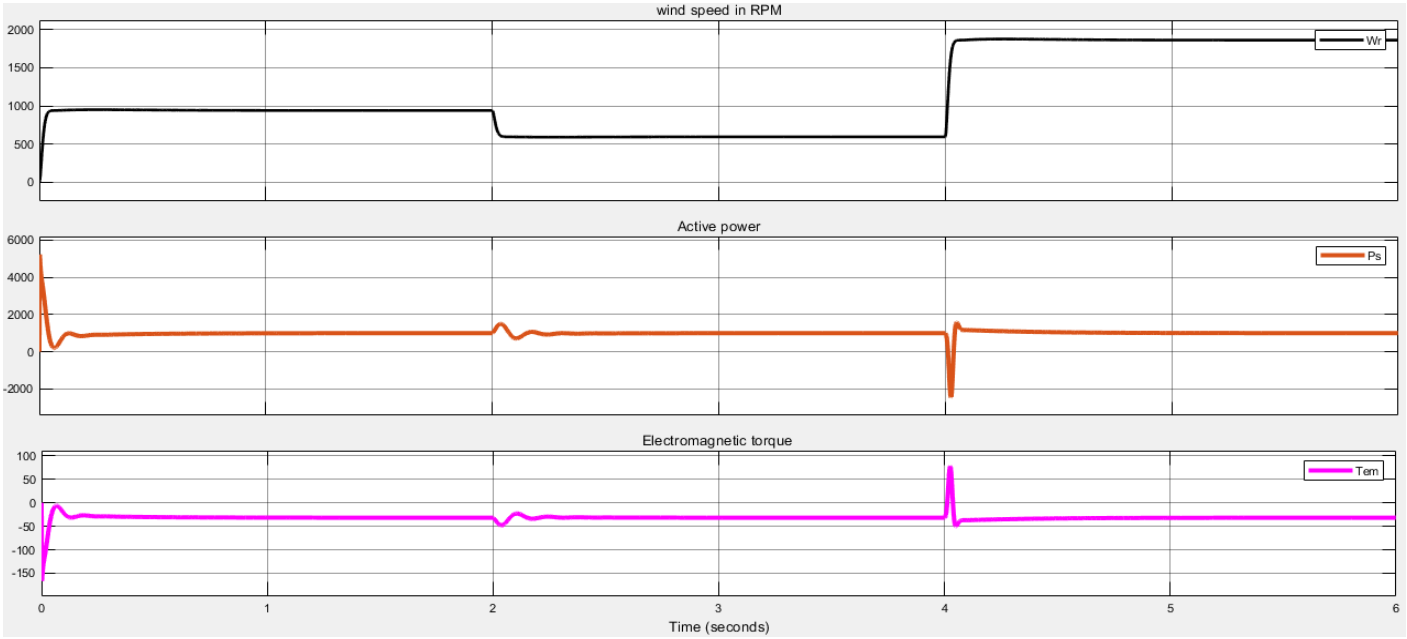

Fig. 4.17, PID control of Active power and electromagnetic response for wind speed variation

The simulation result in figure (4.17) show's controlling of generator active power by PID controller with the parameter obtained in table (4-1). The steady state active power is the same as that of the commanded reference (1KW) power. The system result can follow the reference signal with a rise time of 0.0202 second, settling time of 0.204 second and has 27.3% maximum over shoot value and this indicates that the system has good transient and steady state response. Using model of induction machine, we have got a required active power irrespective of wind speed variation.

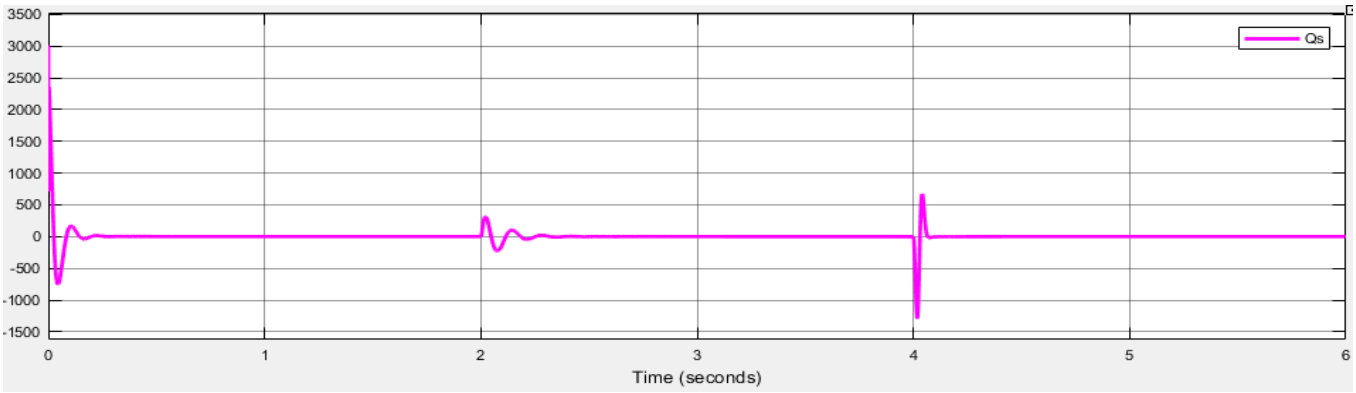

Fig. 4.18, Reactive power response with PID controller

The reactive power PID control shown in the figure (4.18) at the starting of simulation oscillated then stabilize to reference value and also oscillated again at the point of wind speed change its value. It is further

observed that PID self-tuning controller tracks its reference reactive power (0KW) with a settling time of 0.197 sec, rise time of 0.0204 sec, 25% maximum overshot.

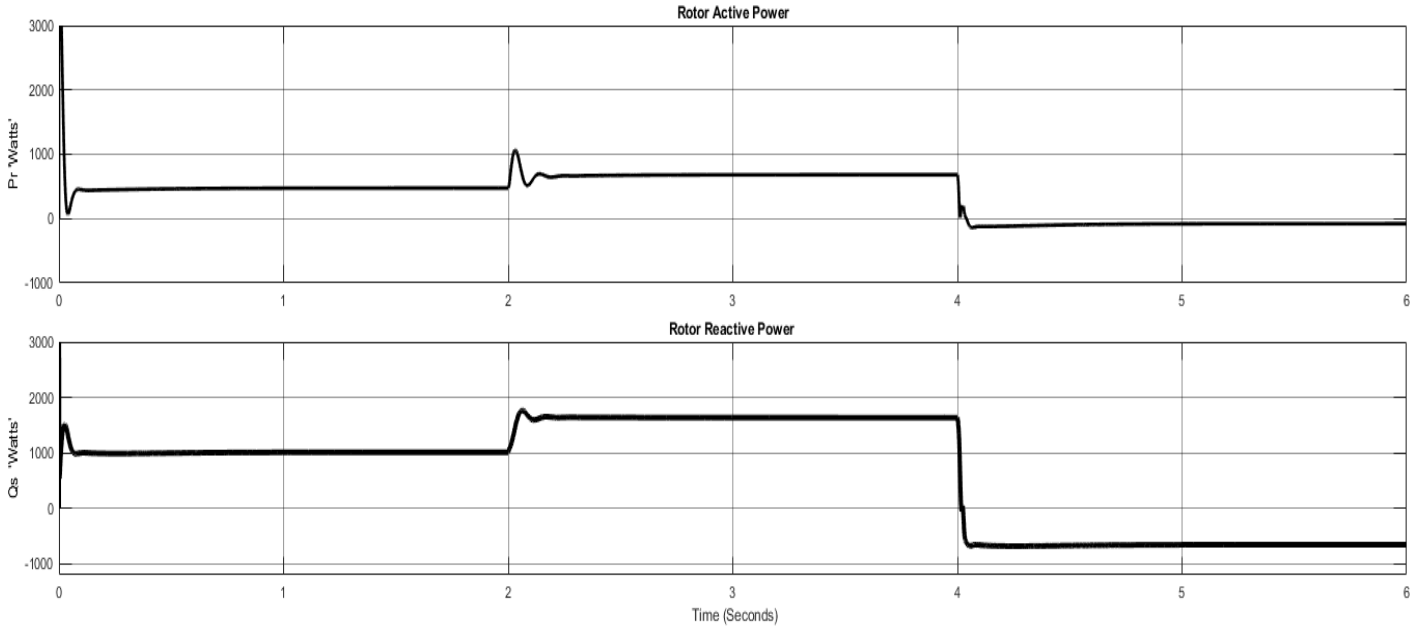

Fig. 4.19,Rotor active and reactive power

DFIG is able to work as a generator in both sub-synchronous or positive slip s and super-synchronous or negative slip operating area. Depending on the operating mode of the drive, the power is fed in or out of the rotor. However, the simulations were done under synchronous speed except this simulation as s illustrates in figure 4.19. The result shows that the active and reactive powers in both conditions, from time 0 to 4.0 seconds, the generator works under synchronous speed and from 4.0 to 6 .0 seconds, DFIG runs above synchronous speed (super synchronous speed). The response of power under speeds are positive values and super speed, power (Pr and Qr) are negative values that indicates the flow of power fed in and fed out from double fed induction generator respectively.

4.3 Simulation of DFIG model with Fuzzy- PID controller

Decoupled controls of active and reactive power flowing between rotor and grid are performed by using vector control. The fuzzy-PID controller and the coordinate transformations block are set to implement the principle of decoupled control of generator power discussed in chapter 3 and the structure of the block as shown in Figure (4.21) and (4.22). Different coordinate transformations (Clarke-park and inverse Park transformation) are vector transformations as discussed in section 3.3.1and taken from MATLAB/ Simulink block. The PID blocks are PID controller in which the Proportional, Integral and Derivative gain parameters are obtained from fuzzy logic controller output. Fuzzy self-tuning PID can tune the PID

parameters for achieving the desired output response in view of speed, overshoot, steady state error. For fuzzy controller, Mamdani controller is used, which has two inputs namely error and rate of change of error, and triple output. Input and output contain seven triangular membership functions as discussed in section 3.5 and figure 3.7

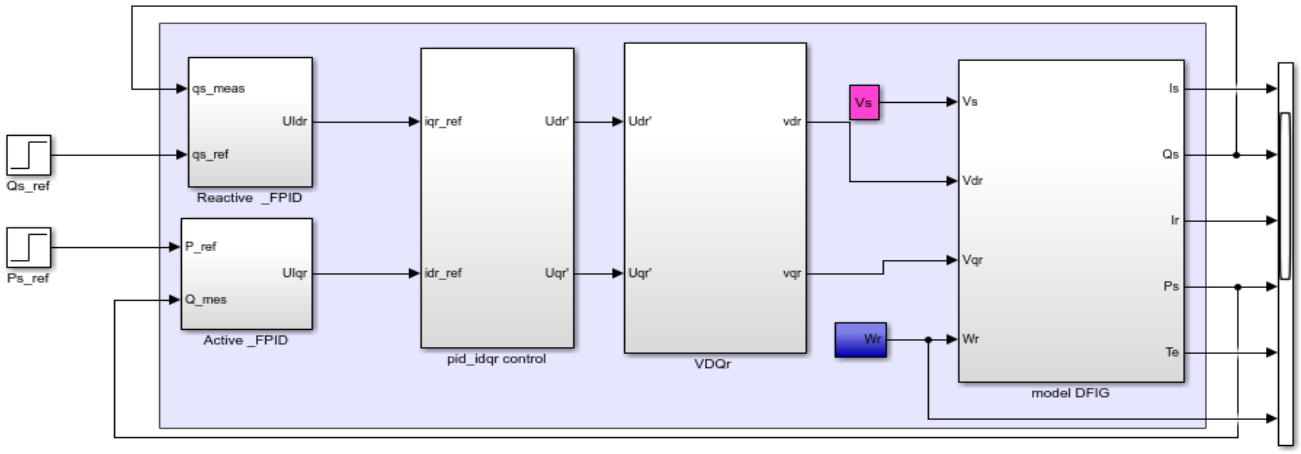

Fig. 4.20, Fuzzy –PID control of active and reactive power DFIG system Simulink block

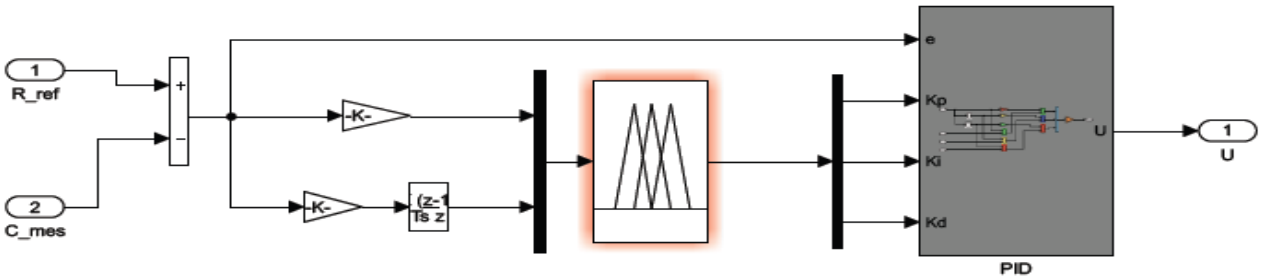

Fig. 4.21, fuzzy tuning PID (F_PID)controller simulation block

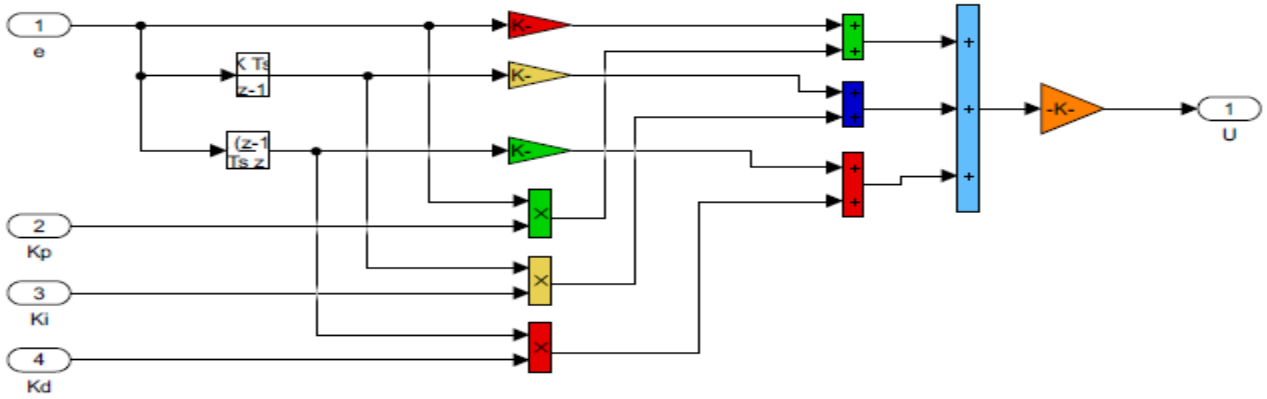

Fig. 4.22, PID controller block components under FPID block and control signal(U)

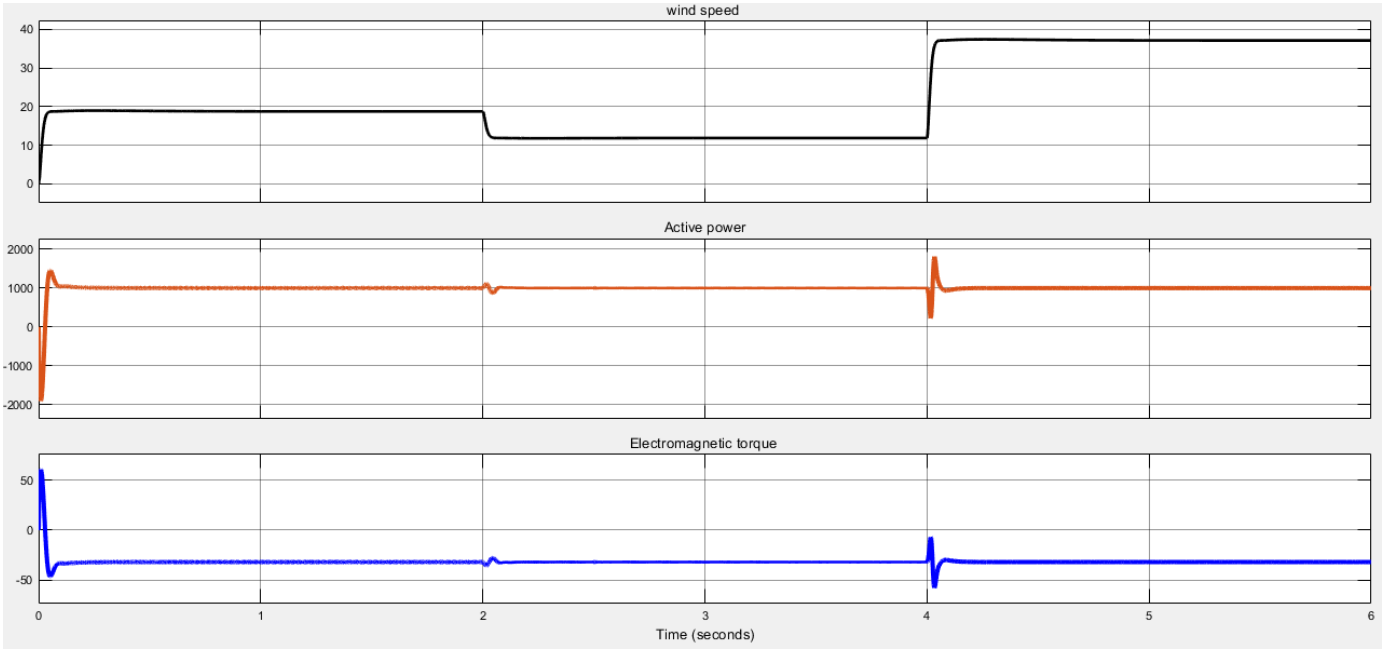

Fig. 4.23, Active power and Electromagnetic response under FPID

DC motor used as wind turbine as shown in figure (4.6) and (4.7) as source of wind speed for double fed induction generator. Figure (4.23) shows the generator active power and electromagnetic torque under varying wind speed. From simulation result, we can see that when wind speed varies the output power become desired constant value due to FPID controller. The performance of the fuzzy PID control response parameters have a settling time less than of 0.167sec, rise time of 0.02 sec, 8.21% maximum overshot.

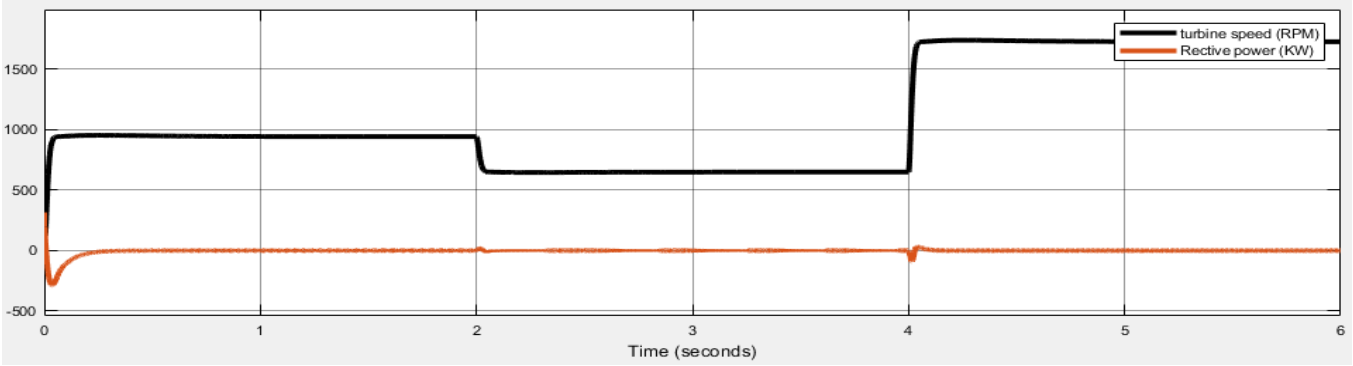

Fig. 4.24, Reactive power response with respect to wind speed under FPID

The reactive power for grid connected wind turbine system need to be zero to get unity power factor. To get unity power factor as the simulation result shown in the figure (4.24) comparing reference input with measured value and minimize error between them by using FPID controller to get desired value. As observed from simulation that fuzzy- PID controller tracks its reference reactive power (0KW) with a settling time of 0.117 sec, rise time of 0.0165 sec, 8.99% maximum overshot.

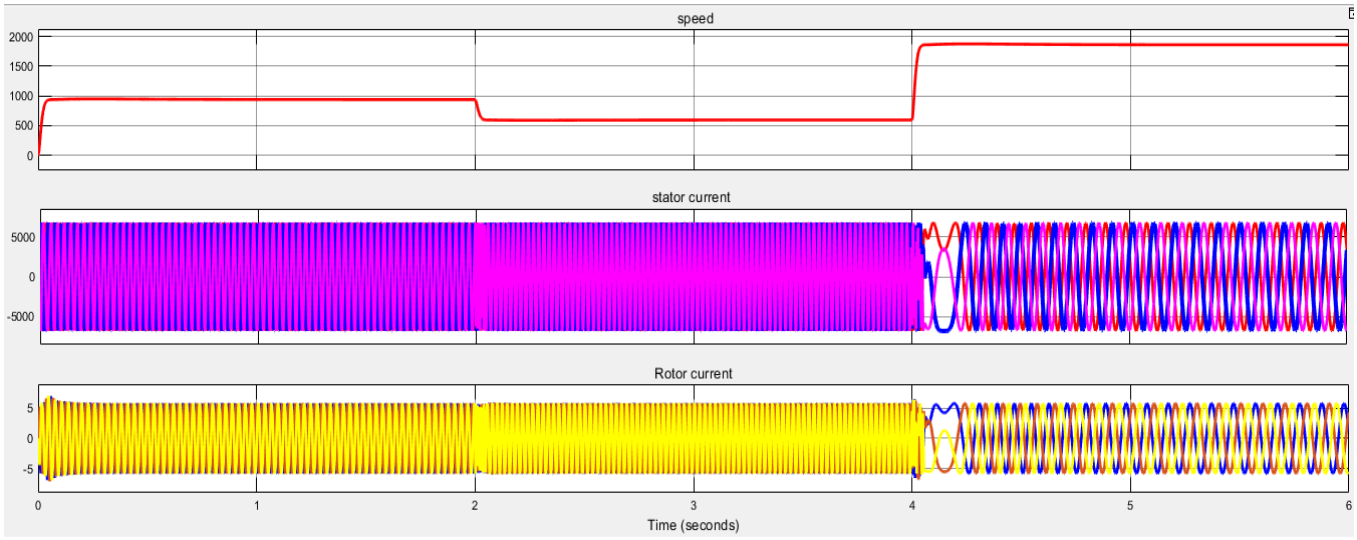

Fig. 4.25, Three phase Stator and Rotor currents in A

Simulation response shown in figure (4.25), the stator and rotor current with respect to variations of wind speed using fuzzy – PID controller. figure (4.26) and figure (4.27) shown below are zoom out response of stator and rotor currents with 120-degree phase shift.

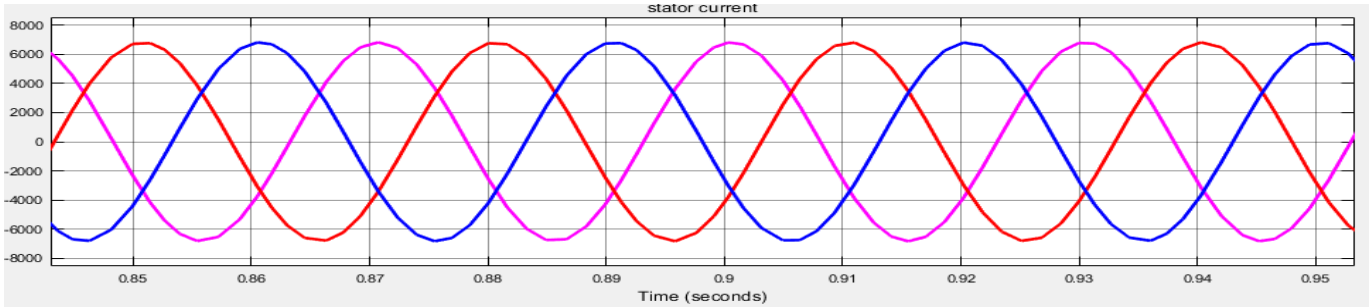

Fig. 4.26, Zoom out stator currents in A

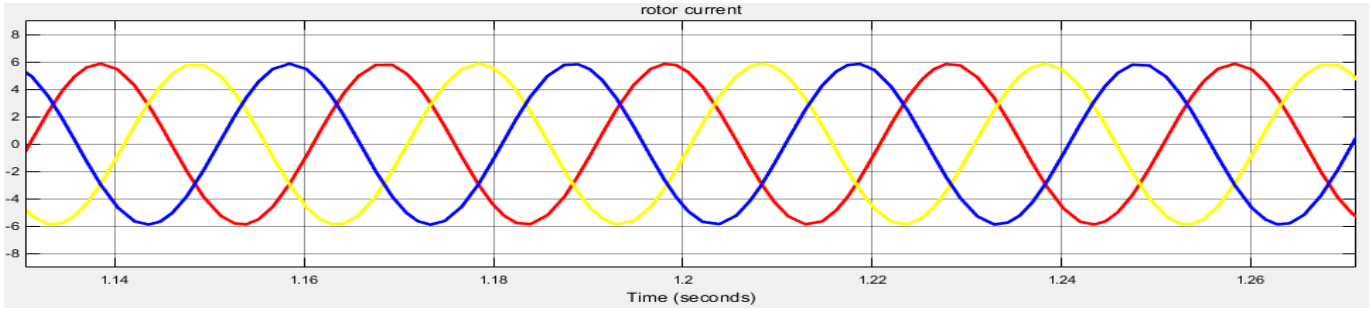

Fig. 4.27, Zoom out rotor currents in A

4.4 Simscape DFIG Simulink model simulation

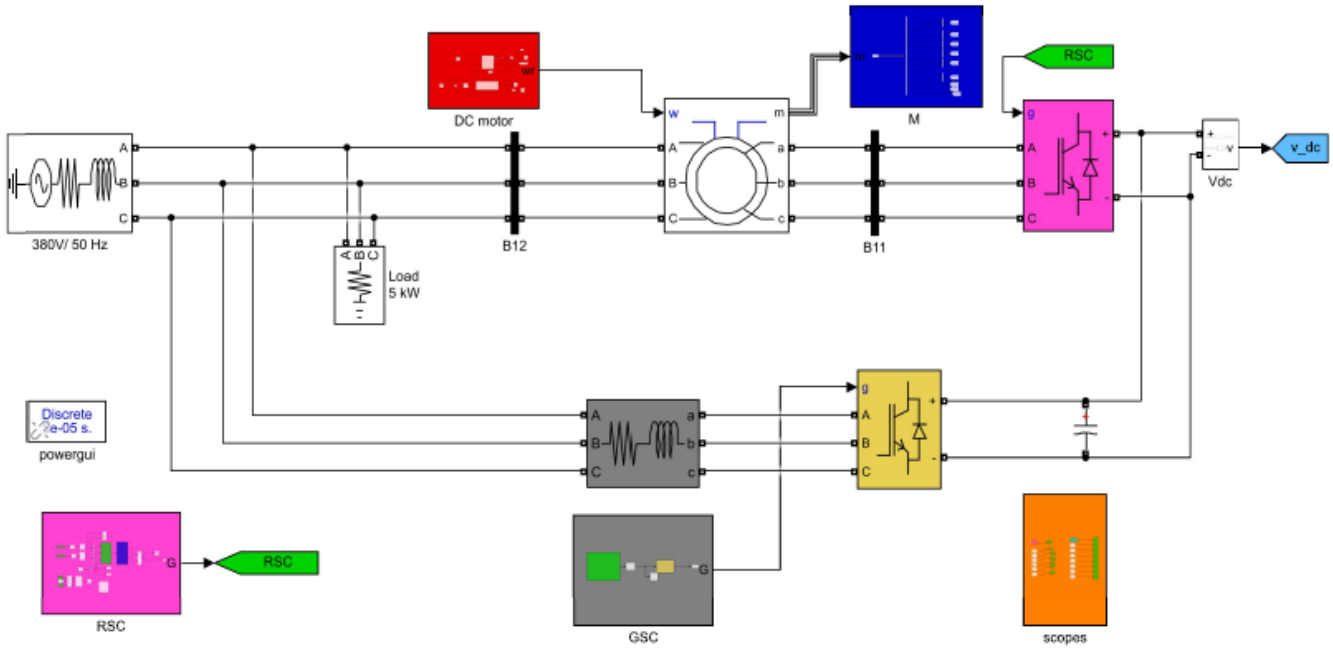

Fig. 4.28, DFIG power control using simscape simulation block

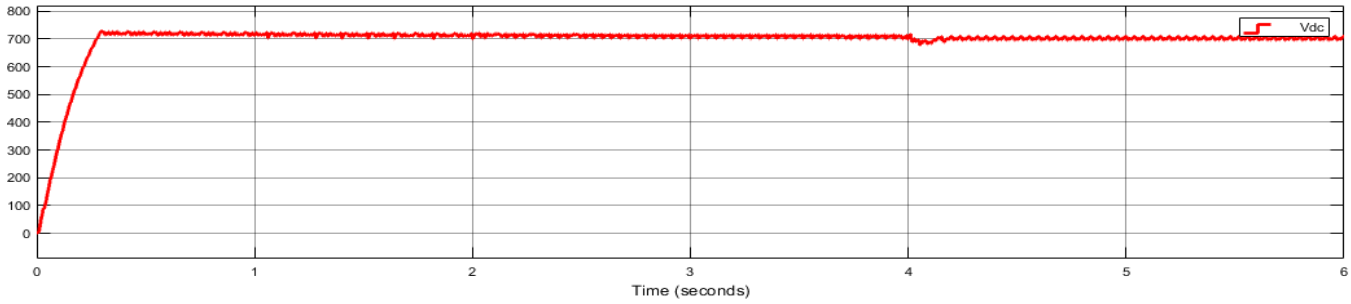

Fig. 4.29, Dc link voltage for grid side converter control

Figure (4.29) shows the response of PID controller when the dc link rectifier or grid side converter control is required to give the desired response i.e., 700 V voltage reference. The outer control loop of dc link voltage has controlled the direction of slip power and maintained a constant value. The PID controller implemented in the grid side converter for controlling of power flow and V_dc by decupled dq axis stator current control to yield dc link voltage maintained constant. MATLAB simulation of grid side converter and controller system block to control dc-link voltage detail shows in appendix A. The performance of the control system is good in control parameters which have a rise time of 0.25 sec, a settling time of 0.95 sec, and maximum over shoot value of 0.89%. when the speed varies, the dc link voltage deflects in the direction of speed value changes and restore after some time or tracks the reference due to the controller.

Figure 4.30 illustrates the response of dc link voltage with fuzzy PID controller as the Simulink block showed in figure at Appendix A.

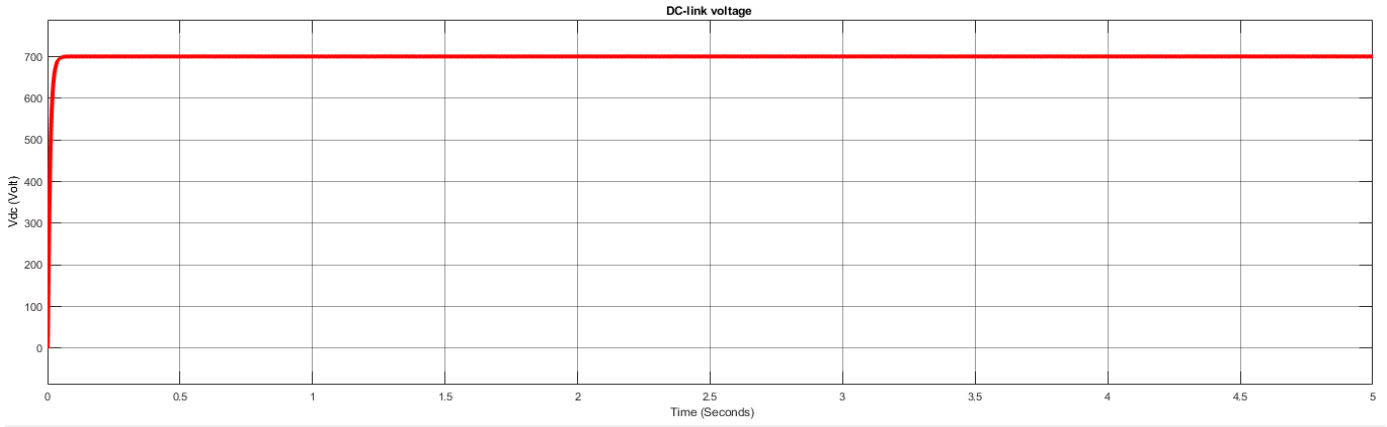

Fig. 4.30, Response of Dc- link voltage with FPID controller

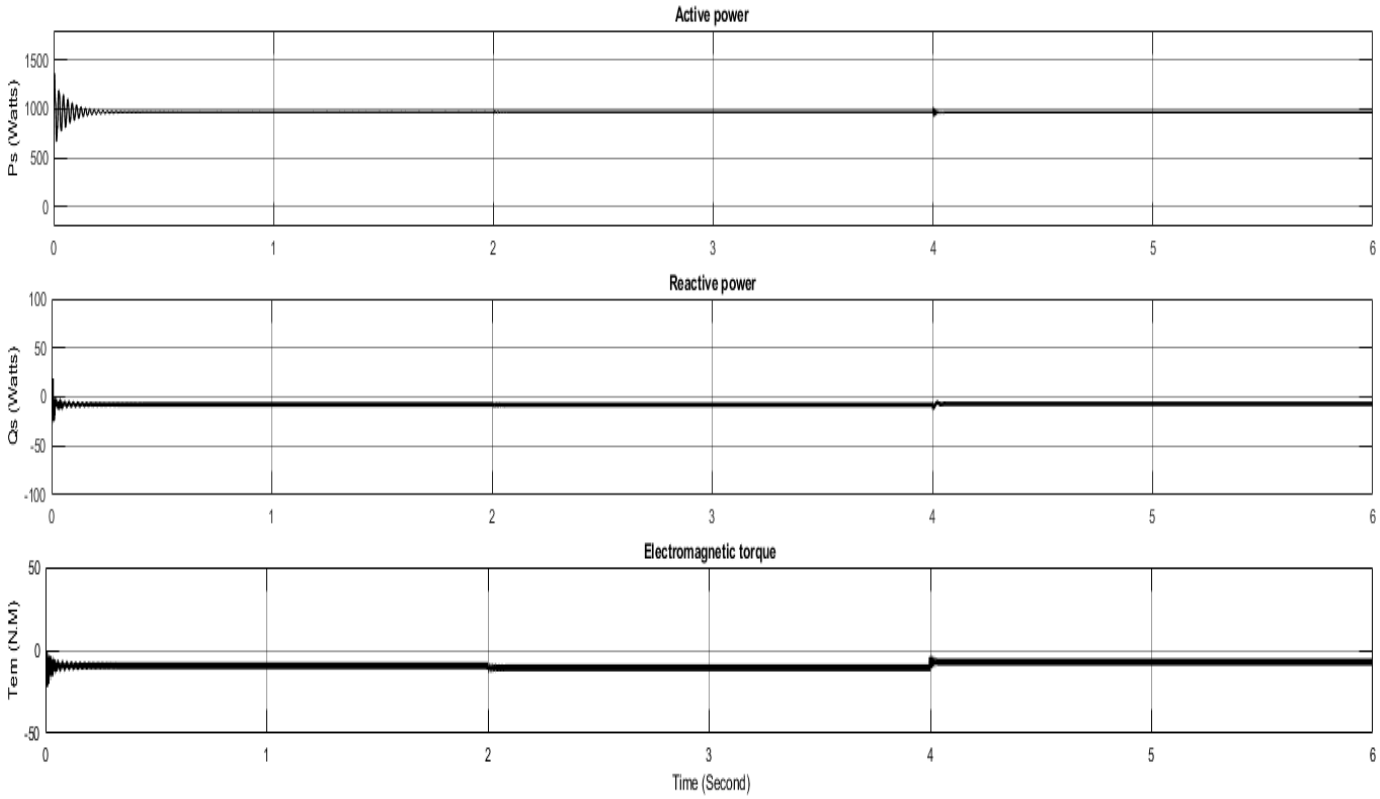

Fig. 4.31, Fuzzy- PID controller response of DFIG

The simulation results show in figure (4.31) parameters which are responses obtained by control the power generated at the stator of the DFIG using direct simscape MATLAB/Simulink toolbox. This control technique allows us to decouple control of active and reactive power of the generator to track the reference power with respect to q- axis and direct- axis current respectively. The PWM converter is current regulated

with the direct axis current is being used to the dc link voltage, where the quadrature axis current component is used to regulate the reactive power in grid side converter control. As the figure shows above, Because of reactive power exists, the power factor of generator cannot be exactly unity. In reality the reactive power cannot make zero due to inductance and capacitance existed in wound induction generator. So, we observed that in the simulation using direct simscape MATLAB/Simulink toolbox the control of active and reactive power of wind turbine control system has the power factor nearly one but not exactly one. This simulation compared with a control system by modeling, the simscape/MATLAB toolbox simulation response approaches to the reality control of double fed induction generator power.

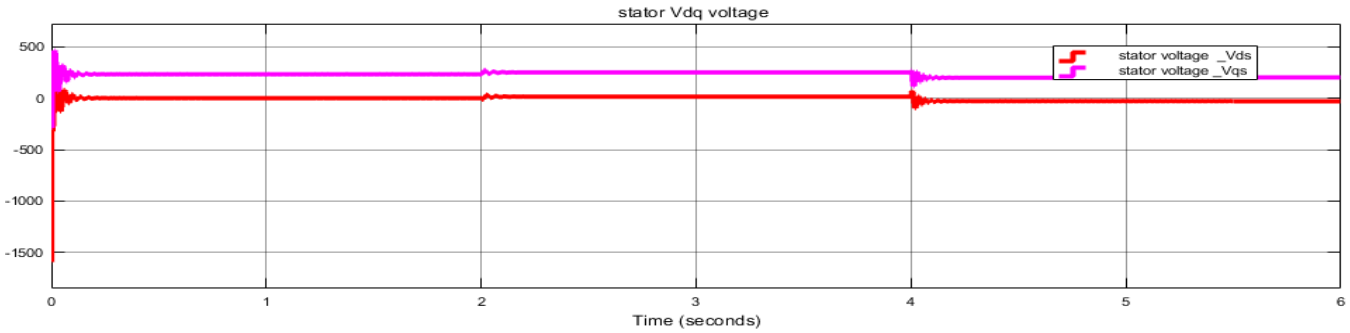

Fig. 4.32, DQ Stator voltage components in V

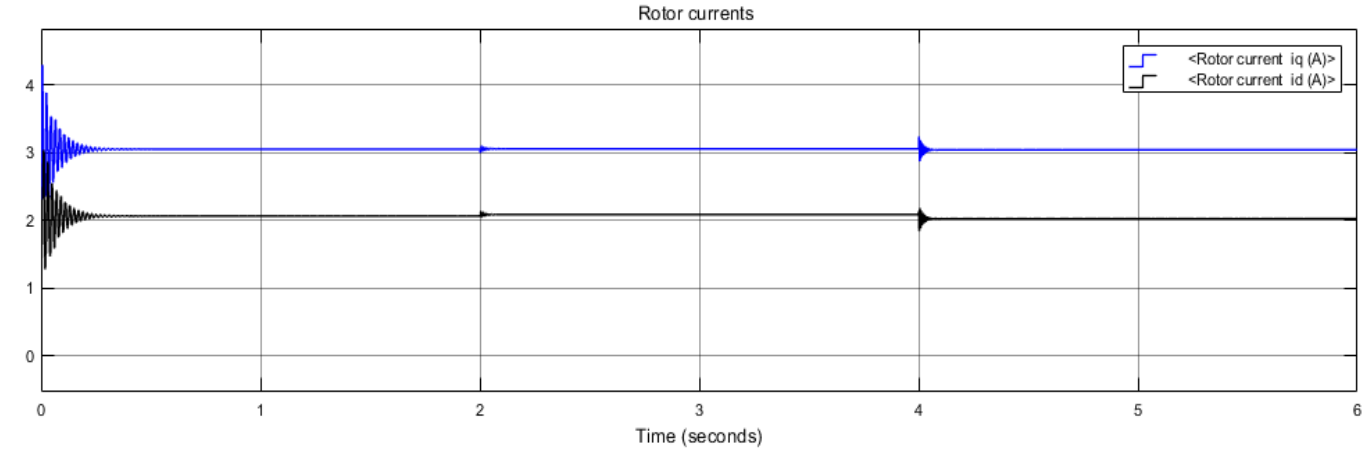

Fig. 4.33, DQ Rotor current components in A

4.5 Comparison of PID and FPID controller mechanisms

The overall MATLAB/Simulink model of the DFIG allows simulating the behavior of the machine using unity feedback and fuzzy-PID controller follow with PID controller for variable wind speed. Thus, the simulation results were carried out to assess its performance DFIG using a controller. The DFIG parameters used in the simulation are found in Table of Appendix A and steady state specification response are shown in table (4-2).

Power	Controller	Overshoot (%)	Rise time	Settling time
Reactive power	PID	25.4	0.0204	0.197
	Fuzzy-PID	8.99	0.0165	0.117
Active power	PID	27.3	0.0202	0.204
	Fuzzy-PID	8.21	0.0204	0.167

Table 4-2:power response of DFIG comparation between PID and Fuzzy -PID controllers

Figure 4-16, 4-20 and 4-28 shows the double fed induction generator modeled system simulated that has to been extracted power from the wind turbine and control of power as function of wind speed varies. The primary goal of wind energy conversion system with double fed induction generator control techniques is to extract maximum power as much as possible from the wind and control as required. For each of the wind speed there is one rotor speed or turbine speed that will result maximum power making the system monotonic. However, for a variable wind speed due to the application of variable wind speed induction generator which directly connected by back to back converter and with importance of DFIG can control power flow to track the desired signal. It is seen that the generator can produce maximum active and almost zero reactive power under variable wind speed which gives unity power factor.

The two simulations which are done with the same wind speed source and reference power inputs to the system as shown figure (4.16) and (4.20). They gave the same response for conventional PID and FPID controller with difference time specification. The Simulink result shows that Fuzzy -PID is better transient response and robust than conventional PID controller for both active and reactive power as shown in the table (4-2).

CHAPTER FIVE

5 Conclusions and Recommendation

5.1 Conclusions

Power converter are usually controlled utilizing variable wind speed techniques which allow the decoupled control of both active and reactive power flow to the grid. In the present investigation, the dynamic DFIG performance is presented for both RSC and GSC. This thesis provides fuzzy- PID controller to tune the parameters of the controller for extracting of power from the WECS using double fed induction generator DFIG. The proposed controller can be used for variable wind speed with DFIG and head by varying DC motor speed as wind turbine speed. A mathematical model of DFIG was developed and tested through Simulation using MATLAB/Simulink. The simulation has been shown that the controller scheme has a great capability of extracting maximum power of wind energy and adapting to wind turbine in fluctuating wind speed the performance of grid side converter was tested for both controller under sub synchronous speed and normal condition (i.e., constant grid, voltage and frequency). Moreover, good transient and steady state response for the different operating point of the system can be achieved by increasing the number of membership functions. As it is observed from the simulation results the average overshoot is 25.4% for active power and 8.99% for reactive power with the proposed fuzzy- PID controller whose overshoot is 27.3 % for active power and 8.21% for reactive power and also rise time and settling time as mentioned above table (4-2) with conventional PID and FPID controller. The proposed controller can adaptively improve the system response by online setting or tuning of PID parameters gain. In conclusion, because of the reason mentioned above, and simulation result with the wind speed changes its value, the proposed fuzzy-PID controller can be recommended as a promising alternative controller to control active and reactive power of DFIG than PID in balanced grid system.

For reality control approach of wind energy conversion system using double fed induction generator, it is better to simulate or test using directly simscape from MATLAB toolbox for simulation instead of a mathematical model of double fed induction generator.

5.2 Recommendation and future work

Although the control of active and reactive power of DFIG was proven by simulation, there are other studies which were done before this technology feasible and apply in industrial application. First, a hardware prototype needs to be constructed in order to implement in reality using a fuzzy-PID controller**.** This can be done using a dc motor as the prime mover and controlling rotor quadrature _axis and d_axis current to control the active and reactive power respectively, produced by the generator. The DC motor

used prime mover or wind turbine which connected to the shaft of a double fed induction machine to run the generator rotor, and the electrical system which is the stator terminal connected to load and power excited by rotor terminal through inverter has to be connected in such a way to implement practically. Secondly, simulation done in this thesis can be taken and simulate using neural network or model adaptive with neutral network control to improve performance of extraction of maximum power and power flow control of double fed induction generator using simscape and DFIG model to get better system performance.

Finally, besides extraction of maximum power in normal condition, the active and reactive power control of generator in an abnormal situation of grid voltage for the extension of the power control system to be built.

References

[1] Jaimala Gambhir, Tilak Thakur and Puneet Chawla, "Modeling and Analysis of DFIG Based Wind Power System Using Instantaneous Power Components," *World Academy of Science, Engineering and Technology International Journal of Electrical and Computer Engineering,* vol. 9, pp. 908-913, 2015.

[2] Selman Kouadria; Youcef Messlem; El Madjid Berkouk, "Sliding mode control of the active and reactive Power of DFIG for variable speed WECS," in *3rd International Renewable and Sustainable Energy Conference (IRSEC)*, Marrakech, Morocco, 2015.

[3] N. RAMESH BABU and P. ARULMOZHIVARMAN, "WIND ENERGY CONVERSION SYSTEMS A TECHNICAL REVIEW," *Journal of Engineering Science and Technology,* vol. 8, pp. 493 - 507, 2013.

[4] J. Hu, H. Nian, B. Hu, Y. He and Z. Zhu, "Direct Active and Reactive Power Regulation of DFIG Using Sliding Mode Control Approach," *IEEE Trans. Energy. Convers.,* vol. 25, pp. 1-4, Dec 2010.

[5] Swagat Pati and Swati Samantray, "Decoupled Control of Active and Reactive Power in A DFIG Based Wind Energy Conversion System with Conventional P-I Controllers," in *International Conference on Circuit, Power and Computing Technologies [ICCPCT)*, SOA University Bhubaneswar, India., 2014.

[6] Rabie Gohar and F. Servati, "Modeling a DFIG-Based Wind Turbine Focusing on DFIG and Aerodynamic Models," *European Online Journal of Natural and Social Sciences,www.european-science.com,* vol. 3, pp. 744-757, 2014.

[7] J. S. Sathiyanarayanan and A. Senthil Kumar, "Doubly Fed Induction Generator Wind Turbines with Fuzzy Controller Survey," *Hindawi Publishing Corporation Scientific World Journal,* vol. 5, pp. 1-8, June 15 2014.

[8] M. K. a. M. Khan, "Wind Power Generation in India: Evolution, Trends and Prospects," *Int. Journal of Renewable Energy Development,* vol. 2 (3), pp. 175-186, 2013.

[9] A. Belay, "Maximum Power Extraction of PMSG Based Variable Speed Wind Turbine Using Self-Tuning Fuzzy Controlle," *masters thesis, http://etd.aau.edu.et/handle/123456789/(online),addis ababa university , ethiopia,* February 2017.

[10] M. Elazzaoui, "Modeling and Control of a Wind System Based Doubly Fed Induction Generator:Optimization of the Power Produced," *Journal of Electrical & Electronic Systems,* vol. 4, no. 1, pp. 141-148, 2015.

[11] M. E. A. a. H. Mahmoudi, "Fuzzy control of a doubly fed induction generator based wind power system," *WSEAS Transactions On Power Systems,* vol. 12, pp. 73-78, 2017.

[12] K. Ouhaddach , H. El Fadil , A. Senhaji Malih , L. Ammeh, "New MPPT Optimizer for Wind Turbine Energy Sources," in *international conference on automation ,control engnering and computer science (ACECS) ,proceeding of engineering and technology*, Morocco, 2017.

[13] Selman Kouadria, Youcef Messlem ,El Madjid Berkouk, "Sliding mode control of the Active and Reactive Power of DFIG for variable-speed wind energy conversion system," in *3rd International Renewable and Sustainable Energy Conference (IRSEC)*, Université Ibn Khaldoun Tiaret, December 2015.

[14] Zerzouri Nora, andLabar Hocine, "Active and Reactive Power Control of a Doubly Fed Induction Generator," *International Journal of Power Electronics and Drive System (IJPEDS),* vol. 5, p. 244~251, October 2014.

[15] r. malik, "EEEB344 ELECTROMECHANICAL DEVICES CHAPTER 7," 2017. [Online]. Available: https://abs,cu.edu.tr. [Accessed 29 sep 2021].

[16] Mr. Subir Datta,Dr. J. P. Mishra and Dr. A. K. Roy, "Modified speed sensor-less grid connected DFIG based wind energy conversion system for decoupled control of active and reactive Power," in *International Conference on Power and Advanced Control Engineering (ICPACE)*, India, 2015.

[17] P. S. Yang Han, "Modeling, control and electromagnetic transient simulation of the doubly fed induction generator-based wind energy generation system," *journal in SAGE,* vol. 3, no. 90, pp. 275-289, March 1, 2014.

[18] Hind Djeghloud, Amar Bentounsi and, "Sub and super-synchronous wind turbine-doubly fed induction generator system implemented as an active power filter," *International Journal of Power Electronics,* vol. 3, no. 2, pp. 189-212, 2011.

[19] Sifat Shah, A. Rashid, MKL Bhatti, "Direct Quadrate (D-Q) Modeling of 3-Phase Induction Motor Using MatLab / Simulink," *Canadian Journal on Electrical and Electronics Engineering,* vol. 3, no. 5, pp. 237-243, may 2012.

[20] Eshaft, Hisham Salem Ali, "Grid and Rotor Sides of Doubly-fed Induction Generator-based Wind Energy Conversion System Using Sliding Mode Control Approach," August 2017.

[21] Mr. Subir Datta,Dr. J. P. Mishra and Dr. A. K. Roy, "Modified speed sensor less grid connected DFIG based wind energy conversion system for decoupled control of active and reactive Power," in *International Conference on Power and Advanced Control Engineering (ICPACE)*, India, 2015.

[22] Mahmoud Zadehbagheri , Rahim Ildarabadi and Majid Baghaei Nejad, "Sliding Mode Control of a Doubly- fed Induction Generator(DFIG) for Wind Energy Conversion System," *International Journal of Scientific & Engineering Research,* vol. 4, p. 1573 1581, November 2013.

[23] X. Jing, "Modeling and Control of a Doubly-Fed Induction Generator for Wind Turbine-Generator Systems," *Master's Theses,http://epublications.marquette.edu/theses_open/167,* p. 167, 2012.

[24] Ooi, Juan W. Dixon , Boon-Teck, "Indirect Current Control of a Unity Power Factor sinusoidal Current Boost Type Three-phase Rectifier," *IEEE Transactions on Industrial Electronics,* vol. 35, pp. 508-515, November 1988.

[25] O. H. A. M. I. J. A. A. Gussay Abdalrahman, "Space Vector Pulse Width Modulation Technique Applied to Two Level Voltage Source Inverter," *SUST Journal of Engineering and Computer Science,* vol. 19, no. 2, pp. 10-17, 2018.

[26] H Hartono, R I Sudjoko, P Iswahyudi, "Speed Control of Three Phase Induction Motor Using Universal Bridge and PID Controller," in *J. Phys: Conf. Ser. 1381 012053*, Indonesia, 2019.

[27] S. Achenef, "Fuzzy PID Based Temperature Control of Electric Furnace for Glass Tempering Process," *masters thesis ,http://etd.aau.edu.et/handle/123456789/(online). addis ababa university ethiopia ,* March 2017.

[28] Y. Getnet, "Design and Simulation of Fuzzy Logy Based Frequency Controller for Standalone Micro Hydro Power Plant," *masters thesis, http://etd.aau.edu.et/handle/123456789/(online),addis ababa university , ethiopia,* 30 May 2017.

[29] Mallala Harshavardhan and K.Rajesh, "Modelling and Simulation of Grid Side Control of DFIG Using Fuzzy and PI," *International Journal of Computer Science and Mobile Computing,* vol. 5, pp. 123 - 130, 8 August 2016.

[30] S. Acharya, "Development of A Fuzzy PI Controller for A Grid Connected Wind Energy Conversion System," in *PIN-769008, ODISHA*, ROURKELA, 2012-2014.

[31] L. X. a. P. Cartwright, "Direct active and reactive power control of DFIG for wind energy generation," *IEEE TRANSACTIONS ON ENERGY CONVERSION,* vol. 21, no. 3, pp. 750- 758, Sep 2006.

[32] Adel Mehdi, Abdellatif Reama and Hocine Benalla, "MRAS Observer for Sensorless Direct Active and Reactive Power Control of DFIG Based WECS with Constant Switching Frequency," in *Eleventh International Conference* , University Paris-Est, 2016.

[33] Ivan Villanueva, Antonio Rosales perdo ponce and Arturo Molina, "Stator –Flux –Oriented Sliding Mode Control for Double Fed Induction Generator," in *DOI: 10.5772/intechopen.70714*, March 7th 2018.

[34] Ganti, V.C., Singh, B, "Quantitative Analysis and Rating Considerations of a Doubly Fed Induction Generator for Wind Energy Conversion Systems," in *IEEE conference on Industry Applications Society Annual Meeting (IAS)*, Oct. 2010.

[35] Azzouz TAMAARAT, Abdelhamid BENAKCHA, "Performance of PI controller for control of active and reactive power in DFIG operating in a grid-connected variable speed wind energy conversion system," *Front. Energy,* vol. 8(3), p. 371–378, 2014.

[36] A. E. Noureddine El mouhi, "active and reactive power control of dfig used in WECS using pi controller and back stepping," in *International Renewable and Sustainable Energy Conference (IRSEC)*, Tangier, Morocco, 2017.

[37] S. D. a. S. BAYHAN, "Active and Reactive Power Control of Doubly Fed Induction Generator Using Direct Power Control," in *4th International Conference on Power Engineering, Energy and Electrical Drives*, Istanbul, Turkey , 13-17 May 2013.

[38] Eltamaly, A.M., Alolah, A.I., Abdel-Rahman, M.H, "Modified DFIG control strategy for wind energy applications," *IEEE International Symposium on Power Electronics Electrical Drives Automation and Motion (SPEEDAM),* pp. 653 - 658, 2010..

[39] Jean Claude Mugisha, Bernard Munyazikwiye and Hamid Reza Karimi, "Design of Temperature Control System Using Conventional PID and Intelligent Fuzzy Logic Controller," in *Proceedings of 2015 International Conference on Fuzzy Theory and Its Applications (iFUZZY)*, Yilan, Taiwan, 2015.

[40] F. Mazouz, S. Belkacem, Y. Harbouche, R. Abdessemed and S. Ouchen, "Active and Reactive Power Control of a DFIG For Variable Speed Wind Energy Conversion," in *Proceedings of the 6th International Conference on Systems and Control*, University of Batna, Algeria, May 7-9, 2015.

[41] Eshaft, Hisham Salem Ali, "Grid and Rotor Sides of Doubly-fed Induction Generator-based Wind Energy Conversion System Using Sliding Mode Control Approach," *masters thesis ,http://epublications.marquette.edu/theses_open/167, Saint Mary's University, Halifax, Nova Scotia,* 8 August 2017.

[42] F.Khalilzadeh Moghaddam, Sh. Farhangi, "Improvement of The Stand - Alone DFIG Performance Feed Nonlinear and Unbalanced Loads Using Active and Reactive Theory," in *IEEE Conference on Energy Conversion (CENCON)*, Johor Bahru, Malaysia, 2015.

[43] W. Qiao, "Dynamic Modeling and Control of Doubly Fed Induction Generators Driven by Wind Turbines," in *IEEE/PES Power Systems Conference and Exposition*, University of Nebraska–Lincoln, 2009.

[44] X. Zheng, "Control Method for The Wind Turbine Driven By DFIG Under The Unbalanced Operating Conditions," *masters thesis,https://engagedscholarship.csuohio.edu/etdarchive/832(online),* June 2013.

[45] S. G. a. R. K. Ahuja, "Speed control of induction motor using vector or field oriented control," *International Journal of Advances in Engineering & Technology,* vol. 4, no. 1, pp. 475-482, 2012.

[46] R.Rajeswari, "Control of Doubly Fed Induction Generator Based Wind Energy Conversion System," *International Journal of Advanced Research in Electrical,Electronics and Instrumentation Engineering,* vol. 3, no. 2, pp. 381-389, April 2014.

[47] D. X. a. L. Ran, " "Control of a doubly fed induction generator in a wind turbine during grid fault ride-through,"," *IEEE Transactions on Energy Conversion,* vol. vol. 21, pp. , pp. 652-662, Sep. 2006..

APPINDEX A

3-Phase Double Fed Induction Generator

Rotor type: wound rotor,

Reference frame: Synchronously rotating frame

Parameters of DFIG [46].

PWM frequency	2KHz
Rated power, pn	4KW
Rated voltage	400V
Grid Frequency	50Hz
Lm	0.1722H
Lr	0.005839H
Ls	0.005839H
Rs	1.405Ω
Rr	1.395 Ω
Inertia	0.0131Kg.m^2
Viscous friction	0.002985 N.m. s^{-1}
Dc link capacitor	0.0368F
Lg (filter inductance)	0.00043H
Rg (filter resistance)	0.005 Ω
Number of pole pair	2

DFIG and filter parameters with dc link capacitor

The Simulink block shown on figure (block of grid side converter control) for grid side converter control has sub blocks; Park transformation & inverse park, Vdc controller, Idq controller, calculation Vdqg_ref, Source or grid, filter block and inverter which controlled by switching gates. This system can control the reactive power due to rotor currents and Dc-link voltage that can maintain constant sources for generator

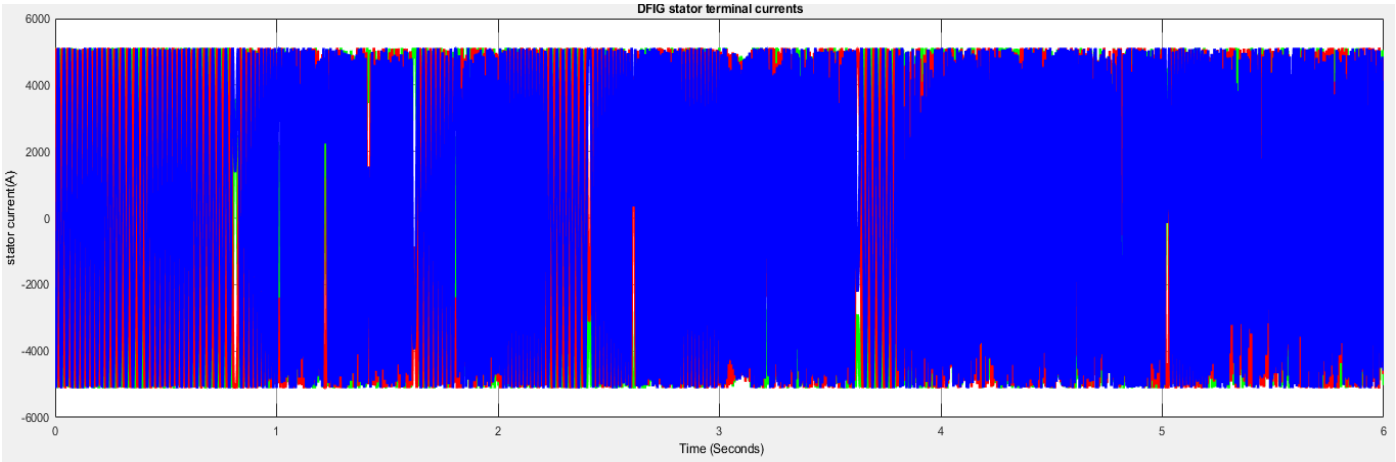

Stator current in A

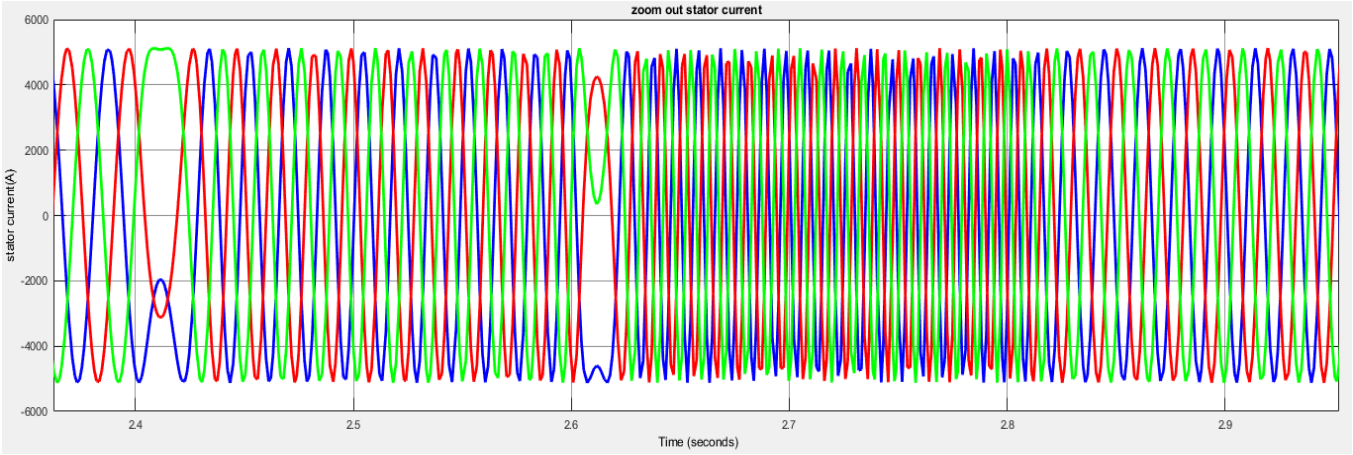

Zoom out stator current

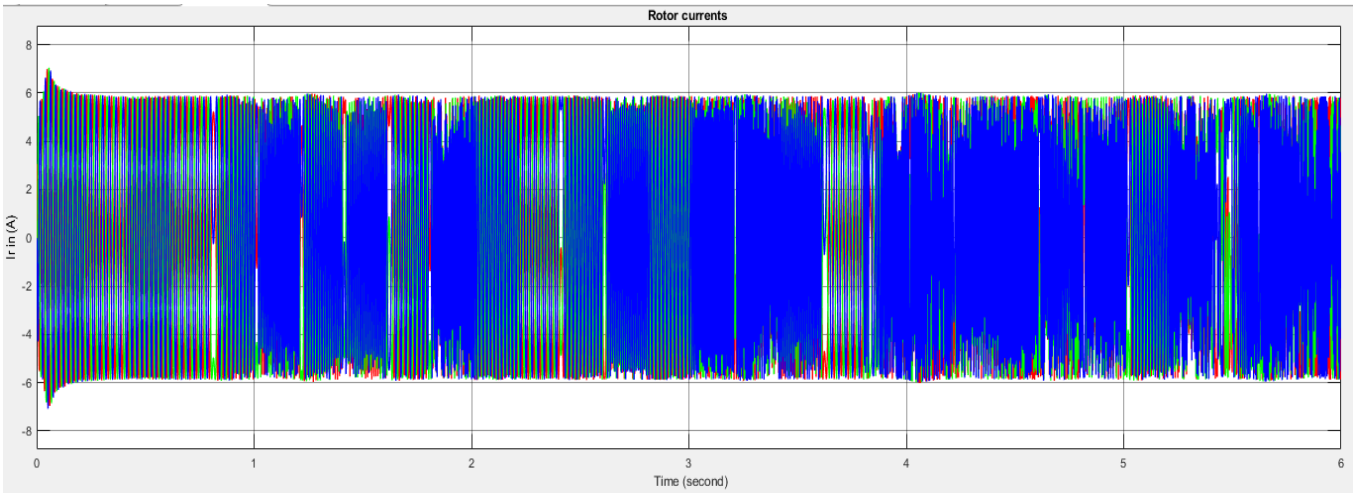

Rotor currents in A

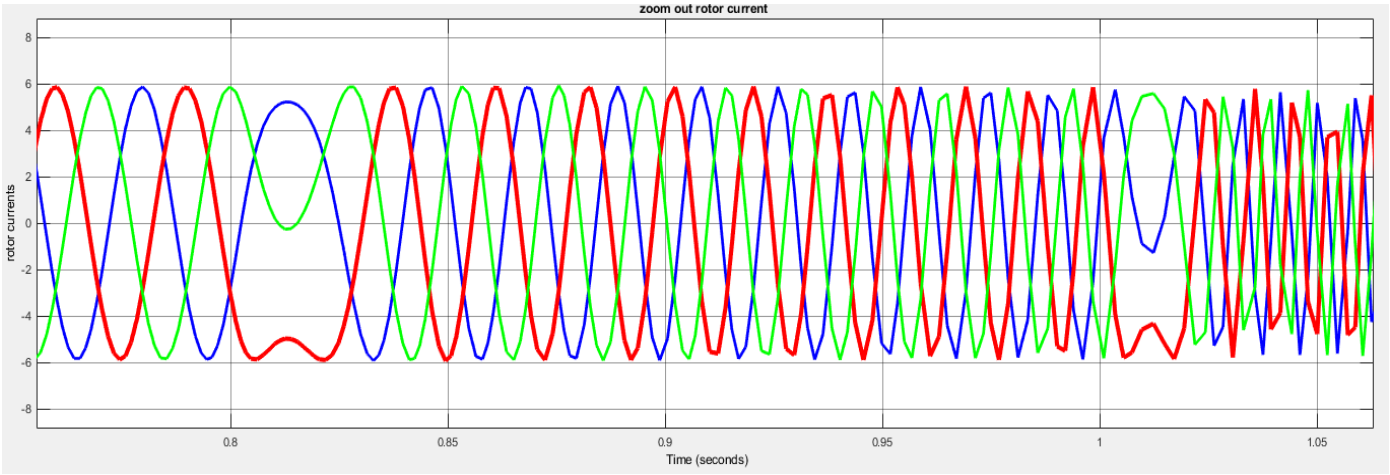

Zoom out rotor currents

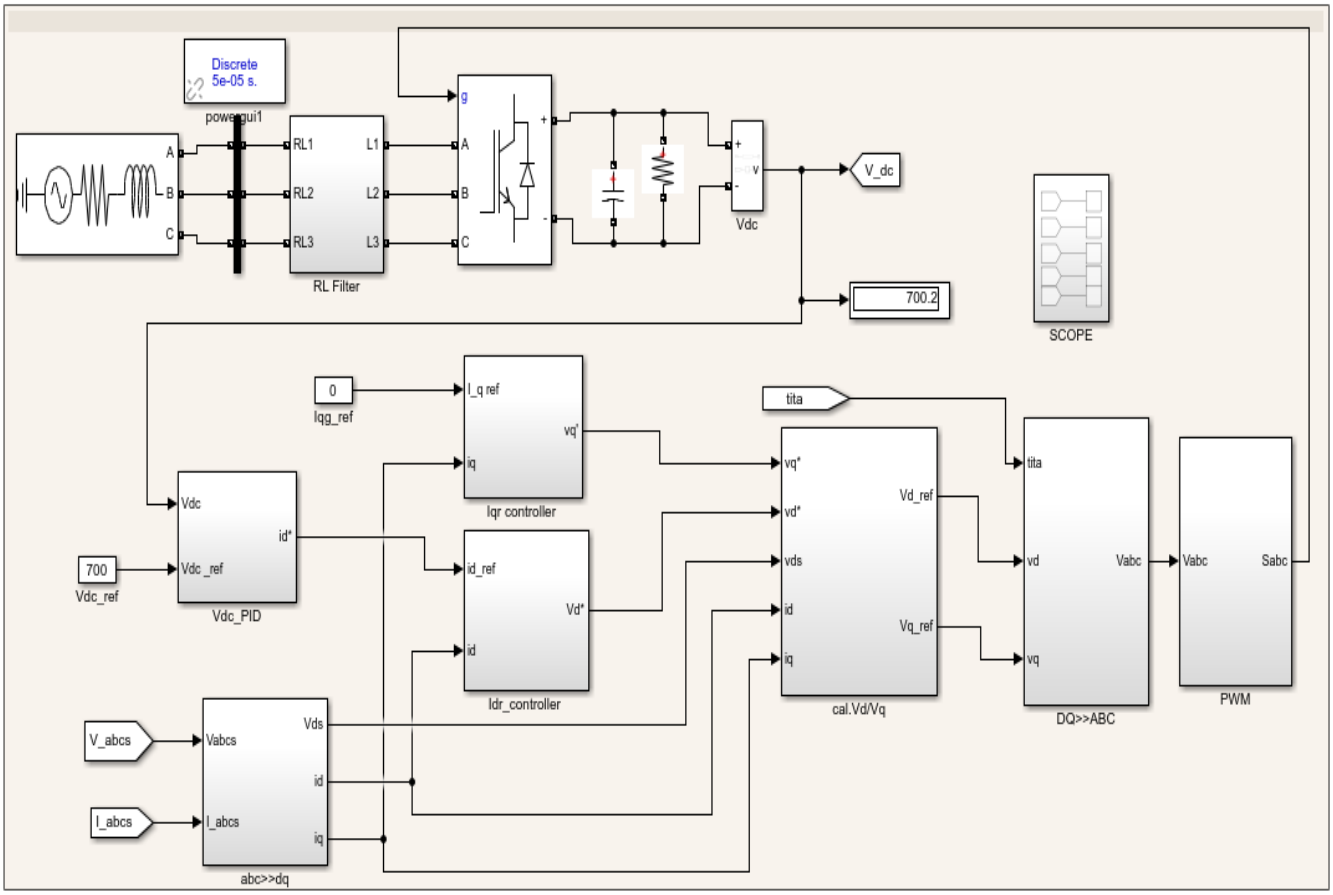

MATLAB/Simulink block of Grid side converter control system

Appendix B

MATLAB code for SVPWM

```
function [sf]=aaa(u)
ts=0.0002;
 Ps=3000;                          %rated power
Rs=1.405 ;                        % stator resistance
Rr=1.39 ;
p=2;                               % pole pair inductance
Lr=0.00584;                        % rotor linkeage inductance
Ls=0.00584;                        % stator linkeage inductance
Vs=400;                            % stator or grid rated rms voltage
Lm=0.1722;                         % mutual linkeage
f=50;                              % stator or grid frequency
Lg=20e-6;
cs=0.006;
Rg=250;
j=0.013;
sigma=(Lr-(Lm*Lm)/(Ls));
Lm/Ls;
Lm/Lr;
Lm*Lm;
ws=2*pi*f;                                %DFIG  slip
 b= 1/sigma;                              % slip speed
L=(Rr*b);
x=0.01*L;
a=exp(-x);
vdc=700;
% space vector
peak_phase_max= vdc/sqrt (3);
 x=u(2);
y=u(3);
mag=(u(1)/peak_phase_max) * ts;

 %sector I                                %sector IV
 if (x>=0) & (x<pi/3)                     if (x>=-pi) & (x<-2*pi/3)
 ta = mag * sin(pi/3-x);                    adv = x  + pi;
 tb = mag * sin(x);                       tb= mag * sin(pi/3 - adv);
  t0 =(ts-ta-tb);                         ta = mag * sin(adv);
 t1=[t0/4 ta/2 tb/2 t0/2 tb/2 ta/2 t0/4];  t0 =(ts-ta-tb);
```

```
t1=cumsum(t1);
 v1=[0 1 1 1 1 1 0];
v2=[0 0 1 1 1 0 0];
v3=[0 0 0 1 0 0 0];
for j=1:7
if(y<t1(j))
break
end
end
sa=v1(j);
sb=v2(j);
sc=v3(j);
end
% sector II
if (x>=pi/3) & (x<2*pi/3)
  adv= x-pi/3;
 tb = mag * sin(pi/3-adv);
ta = mag * sin(adv);
t0 =(ts-ta-tb);
 t1=[t0/4 ta/2 tb/2 t0/2 tb/2 ta/2 t0/4];
t1=cumsum(t1);
v1=[0 0 1 1 1 0 0];
v2=[0 1 1 1 1 1 0];
v3=[0 0 0 1 0 0 0];
for j=1:7
if(y<t1(j))
break
end
end
sa=v1(j);
sb=v2(j);
sc=v3(j);
end
%sector III
if (x>=2*pi/3) & (x<pi)
  adv=x-2*pi/3;
ta = mag * sin(pi/3-adv);
tb = mag * sin(adv);
  t0 =(ts-ta-tb);
t1=[t0/4 ta/2 tb/2 t0/2 tb/2 ta/2 t0/4];
t1=cumsum(t1);
 t1=[t0/4 ta/2 tb/2 t0/2 tb/2 ta/2 t0/4];
t1=cumsum(t1);
 v1=[0 0 0 1 0 0 0];
v2=[0 0 1 1 1 0 0];
v3=[0 1 1 1 1 1 0];
for j=1:7
if(y<t1(j))
break
end
end

sa=v1(j);
sb=v2(j);
sc=v3(j);
end
% sector V
if (x>=-2*pi/3) & (x<-pi/3)
  adv = x+2*pi/3;
 ta = mag * sin(pi/3-adv);
tb = mag * sin(adv);
 t0 =(ts-ta-tb);
t1=[t0/4 ta/2 tb/2 t0/2 tb/2 ta/2 t0/4];
t1=cumsum(t1);
 v1=[0 0 1 1 1 0 0];
v2=[0 0 0 1 0 0 0];
v3=[0 1 1 1 1 1 0];
for j=1:7
if(y<t1(j))
break
end
end
sa=v1(j);
sb=v2(j);
sc=v3(j);
end
%Sector VI
if (x>=-pi/3) & (x<0)
 adv = x+pi/3;
 tb = mag * sin(pi/3-adv);
ta = mag * sin(adv);
 t0 =(ts-ta-tb);
```

```
v1=[0 0 0 1 0 0 0];
v2=[0 1 1 1 1 1 0];
v3=[0 0 1 1 1 0 0];
for j=1:7
if(y<t1(j))
break
end
end
sa=v1(j);
sb=v2(j);
sc=v3(j);
end
```

```
 t1=[t0/4 ta/2 tb/2 t0/2 tb/2 ta/2 t0/4];
t1=cumsum(t1);
 v1=[0 1 1 1 1 1 0];
v2=[0 0 0 1 0 0 0];
v3=[0 0 1 1 1 0 0];
for j=1:7
if(y<t1(j))
break
end
end
sa=v1(j);
sb=v2(j);
sc=v3(j);
end

 sf=[sa, sb, sc];
```